1989

Neurophysiology of Frog Dorsal Root Afferent Fibers and Their Intraspinal Processes

Nancy C. Tkacs
Loyola University Chicago

NEUROPHYSIOLOGY OF FROG DORSAL ROOT AFFERENT FIBERS AND THEIR INTRASPINAL PROCESSES

by

Nancy C. Tkacs

A Dissertation Submitted to the Faculty of the Graduate School of Loyola University of Chicago in Partial Fulfillment of the Requirements for the Degree of

Doctor of Philosophy

April

1989

DEDICATION

To Bill, with deep love and gratitude

ACKNOWLEDGEMENTS

I would like to thank the faculty of the Department of Physiology for the excellent training I have received. I am particularly grateful to Dr. James Filkins for supporting my dissertation research. My thanks also go to Dr. Charles Webber, Dr. David Euler, Dr. David Carpenter, and Dr. Sarah Shefner for serving on my dissertation committee. Their helpful suggestions added much to the research and the dissertation.

My gratitude goes to several individuals who unselfishly shared their time, resources, and expertise. Dr. E.J. Neafsey helped with electrode construction and equipment support. Dr. Robert Schmidt advised me on amphibian care and the experimental model. Ms. Maria Weber provided excellent technical assistance and a cheerful attitude that brightened difficult moments. Mr. Les Plopa maintained my electronics equipment and designed the circuit which was essential to much of this research. Mae and Don Ciancio shared their home with me for several months.

It has been a pleasure as well as a privilege to work with my advisor, Dr. Robert Wurster. His dedication to the principles of scientific training, broad knowledge, insight, and enthusiasm have been an inspiration to me and will surely remain so in the future.

I have appreciated the love and cooperation of my family. My parents, Aunt Catherine, Jessica, and Barbara constituted a great support team. My husband, Bill, contributed in countless ways. My deepest thanks go to him, my partner in turning a difficult goal into reality.

VITA

The author, Nancy C. Tkacs, is the daughter of Margaret and Melvin Feldenheimer and Walter and Marie Camenisch. She was born November 29, 1954 in Philadelphia, Pennsylvania.

Nancy attended public schools in Abington, Pennsylvania until June, 1971. In September, 1971, she entered the University of Pennsylvania in Philadelphia, Pennsylvania. She received a Bachelor of Science in Nursing degree in May, 1975. Nancy married William Tkacs, NC, USN on February 28, 1976. She has two daughters, Jessica and Barbara.

Nancy worked as a staff nurse, intensive care unit at Pennsylvania Hospital in Philadelphia before entering the graduate program in nursing at the University of Pennsylvania in June, 1976. In May, 1977 she received a Master of Science in Nursing degree as a cardiovascular clinical specialist. She worked for the South Carolina Department of Health as a visiting nurse in Beaufort, South Carolina 1978-9.

In October, 1983, Nancy entered the graduate program in the Department of Physiology at Loyola University Stritch School of Medicine. Her dissertation work was completed under the direction of Dr. Robert D. Wurster. Nancy was the recipient of the Schmitt Dissertation Fellowship in 1988.

In May, Nancy will begin post-doctoral studies under the direction of Dr. William F. Ganong, Lange Professor of Physiology at the University of California, San Francisco.

PUBLICATIONS

1. TKACS, N.C., and R.D. Wurster. Innervation patterns to sympathetic ganglia of the bullfrog. Fed. Proc. 45:295, 1986.

2. TKACS, N.C., and R.D. Wurster. Differential effects of four-aminopyridine on synaptic transmission in bullfrog spinal cord in vitro. Soc. Neurosci. Abstr. 13:66, 1987.

3. TKACS, N.C., and R.D. Wurster. Axon vs terminal: Analysis of stimulation parameters exciting single dorsal root fibers. Soc. Neurosci. Abstr. 14:1091, 1988.

4. TKACS, N.C., and R.D. Wurster. Synaptic facilitation and suppression in frog spinal cord, in vitro . In preparation.

5. Plopa, L., N.C. TKACS, and R.D. Wurster. A current monitoring circuit for in vitro applications. In preparation.

6. TKACS, N.C. and R.D. Wurster. Neurophysiology of frog dorsal root fibers and their intraspinal projections. In preparation.

TABLE OF CONTENTS

LIST OF TABLES

LIST OF FIGURES

LIST OF ABBREVIATIONS

AC - alternating current

ADP - afterdepolarization

4-AP - 4-aminopyridine

ARP - absolute refractory period

ARP_i - absolute refractory period - spike initiation

ATX-II - Anemonia sulcata toxin II

CAP - compound action potential

CNS - central nervous system

CR - conditioning response

CS - conditioning stimulus

C-T interval - condition-test interval

DAP - depolarizing afterpotential

DC - direct current

DH - dorsal horn

DH-SNP - dorsal horn supernormal period

DR - dorsal root

DR-DRR - dorsal root - dorsal root reflex

DR-DRP - dorsal root - dorsal root potential

DRP - dorsal root potential

DR-SNP - dorsal root supernormal period

DR-VRR - dorsal root - ventral root response

DTX - dendrotoxin

DW - dorsal white

EPP - endplate potential

EPSP - excitatory postsynaptic potential

GABA - gamma aminobutyric acid

HRP - horseradish peroxidase

I MON - current monitor

LC - lateral column

LC-VRR - lateral column - ventral root response

PAD - primary afferent depolarization

PTH - posttetanic hyperpolarization

PTP - posttetanic potentiation

RRP - relative refractory period

SNP - supernormal period

Solution A - Ringer's + $CdSO_4$ 0.2 mM

Solution B - Ringer's + $CdSO_4$ 0.1 mM + $MgCl_2$ 2.5 mM + $CaCl_2$ 0.5 mM

Stim A - stimulator delivering the conditioning stimulus

Stim B - stimulator delivering the test stimulus

TEA - tetraethylammonium

TR - test response

TS - test stimulus

TTX - tetrodotoxin

VR-DRP - ventral root - dorsal root potential

VRR - ventral root response

CHAPTER I

INTRODUCTION

Synaptic transmission is the predominant form of intercellular communication in the central nervous system. The synapse between two neurons consists of the presynaptic terminal of the transmitting cell, a narrow cleft, and the postsynaptic site on the receiving cell. Electrophysiological properties of presynaptic terminals can be an important factor in this process by influencing transmitter release. The purpose of this dissertation was to develop a profile of physiological and pharmacological characteristics of nerve terminals within the central nervous system. In addition, a parallel profile was developed, characterizing the main axons associated with these terminals. Thus, differences between these two continuous membrane regions could be identified.

Eight chapters make up the dissertation. Chapter II introduces the research question. Chapter III is composed of subsections devoted to nerve terminal studies, electrical stimulation techniques, and pharmacologic modifications of synaptic transmission. In Chapters IV, V, and VI, subsections are assigned to each of the major studies making up the dissertation research.

CHAPTER II

DISSERTATION QUESTION

The functional unit of neural activity, the neuron, has structurally and functionally heterogeneous regions (Fig. 1). The central question of this dissertation is: What are the physiological differences between two of these regions, axons and axon terminals?

The evidence for morphological, physiological and pharmacological differences between axons and their terminal regions has been reviewed (55, 196). Eccles addressed the question of action potential invasion into presynaptic regions. At peripheral synapses such as the neuromuscular junction, numerous factors could combine to make the terminal region electrically inexcitable. These include greater capacitance with loss of myelin, higher threshold, or lack of excitability associated with the membrane specialized for transmitter release. Still, depolarization by passive spread of potential would be effective in causing transmitter release (55).

Waxman also reviewed axonal differentiation (196). Based upon mainly ultrastructural studies, physiologically important morphological changes may occur along the course of axons within the central nervous system. The ratio of internode distance to fiber diameter decreases. Nodes of Ranvier may be longer and may have greater variations in length in central nervous system (CNS) gray matter than in peripheral axons.

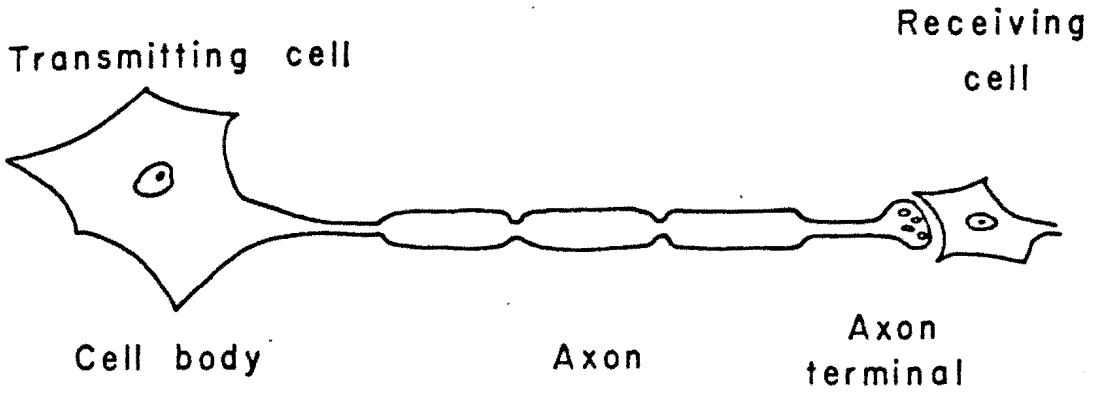

Figure 1. Schematic diagram of neuron and synaptic structure. Morphologically different regions of nerve cells include cell body, myelinated axon, and axon terminal.

He speculates that these morphological changes along central axonal processes may be associated with altered electrophysiological properties, for example, variations in propagation safety factor, nodal conductance changes, or sensitivity to local electrical activity or ion changes. These differences add an additional layer of complexity to models of neuronal processing. Arborizing axon terminal regions could have filtering properties, with some branches unable to conduct all incoming action potentials. This differs from their presumed function of simple transmission lines.

Biochemical evidence for membrane differences between axons and axon terminals has been provided by Hampson and Poduslo (84). Axolemma and synaptic membranes have many proteins of high molecular weight, including several that are probably common to both tissues. However, these membranes have different proteins which bind to lectins, such as Concanavalin A and wheat germ agglutinin. Thus, different membrane proteins are found in the axon and axon terminals.

The aim of this dissertation is to compare physiological properties of sensory axons to properties of terminal regions within frog dorsal roots and spinal cords, respectively (Fig. 2). The use of frog cords in this study was appropriate for several reasons: 1.) The nerve terminals studied are located within the central nervous system, where they make synaptic contacts with other neurons. Previous nerve terminal studies have focused on a specialized peripheral structure, the neuromuscular junction (96, 107, 132). 2.) Activity evoked from sensory afferent terminals or axons can be recorded from dorsal roots and

relative activity quantitated by measuring compound action potential area. 3.) Properties of the axons alone can be evaluated on isolated dorsal roots. 4.) Isolated roots and cords have stable responses for several hours *in vitro* allowing the effects of pharmacological agents to be tested.

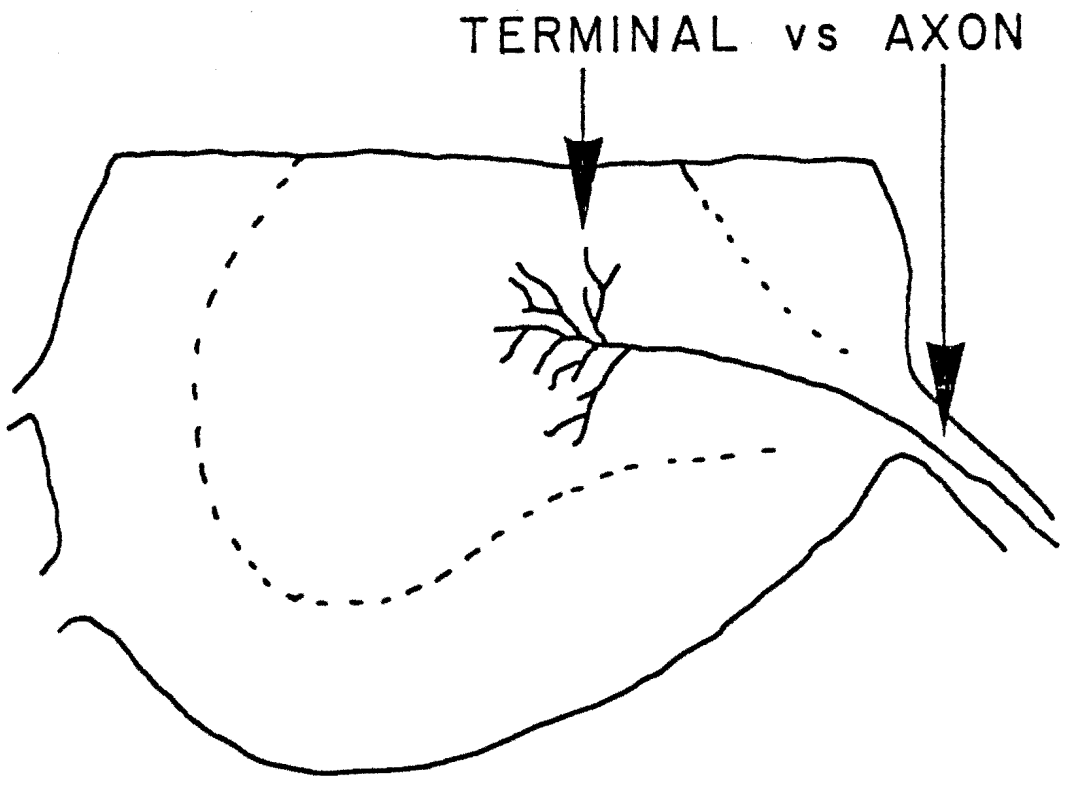

Figure 2. Schematic diagram of frog spinal cord cross-section. A single sensory axon is shown entering the spinal cord in the dorsal root. The terminal arborization of the fiber is located in the dorsal and intermediate gray matter. Dashes indicate the boundary between white and gray matter.

CHAPTER III

LITERATURE REVIEW

The aim of this dissertation is to compare physiological properties of frog sensory axons to properties of spinal axon terminal regions. The literature review covers three broad areas pertinent to the dissertation research. First, sections A through D review major studies characterizing presynaptic terminals involved in chemical transmission. Section E reviews electrical stimulation techniques, focusing on those used in this dissertation. In section F, studies of pharmacologic modifications of synaptic transmission are reviewed. The only studies included here are those in which the major locus of drug action is thought to be presynaptic.

A. Squid Giant Synapse

The properties of axonal membranes have been compared to terminal regions in the squid. Direct intracellular recordings from nerve terminals have been made from the "giant synapse" between neurons in squid stellate ganglia. Early studies on this synapse used current injection to study the effects of presynaptic membrane potential on the postsynaptic response. Depolarizing or hyperpolarizing current injection led to respective small decreases or increases in presynaptic

spike amplitude. These small presynaptic changes were associated with large decreases or increases of postsynaptic potential (82).

Subsequent investigations showed that, after fast sodium channel blockade by tetrodotoxin (TTX), nerve terminals could still show regenerative responses. However, these responses were only observed when presynaptic potassium conductance was blocked by intraaxonal tetraethylammonium (TEA) injection. They were greatly augmented by an increase in calcium concentration in the extracellular fluid. This evidence for a pronounced calcium conductance was only found in the presynaptic terminal region (108).

Further characterization of the presynaptic calcium conductance was carried out by Llinas and coworkers (125, 126). They used voltage clamp methodology to determine the gating characteristics of presynaptic calcium current. In TTX and TEA treated terminals, they were able to inject current reproducing the waveform of the presynaptic action potential. The previously observed relationship between presynaptic spike amplitude and postsynaptic potential was reproduced. This effect could be correlated with the magnitude of presynaptic calcium current.

These studies indicate that one characteristic feature found in terminals but not in axons is the presence of calcium channels. Presynaptic action potential characteristics are important in determining the amount of calcium entering the terminal through these channels. The final intracellular level of presynaptic calcium which is achieved will determine the amount of transmitter released.

B. Neuromuscular Junction

Several investigators have used the techniques of focal extracellular recording and stimulation at peripheral neuromuscular junctions to study motor nerve terminal properties. While synaptic transmission is depressed, usually by elevated magnesium in the bathing medium, the extracellular electrode is moved across the tissue until a location is found from which miniature synaptic potentials may be recorded. In many cases small spikes corresponding to action potentials propagating into the nerve terminal may be recorded by the electrode. The typical configuration of this type of recording, and its correlation to intracellular events, was demonstrated for squid giant synapse in 1962 (186). An electrode is positioned extracellular to the presynaptic axon very close to the synaptic site. This electrode records a biphasic (positive-negative) wave, followed after 1.0 ms by a large negative deflection having a similar time course to the postsynaptic potential. Advancing the electrode further, the tip enters the presynaptic axon at the terminal region and records the usual negative membrane potential and action potential activity.

The experiments on neuromuscular junction were strictly extracellular as these terminals are too small to impale, but the relationship between presynaptic nerve fiber action potentials and postsynaptic potentials is the same. Antidromic activation of the nerve from frog neuromuscular junction revealed that the membrane is electrically excitable throughout its length, which had been a point of controversy up to that time (1965)(107). Calculated conduction velocity

decreased greatly in the terminal region, averaging 0.3 m/s at 20° C. Terminals were able to follow stimulation at frequencies up to 200 Hz.

Studies on rat diaphragm - phrenic nerve preparations also used the technique of antidromic stimulation to characterize properties of nerve terminals at this neuromuscular junction (95, 96). Stimulation of the phrenic nerve consistently resulted in small all-or-nothing spike potentials recorded at the endplate region. These spikes preceded postsynaptic potentials which varied in size. This finding, coupled with the invariable finding that stimulation via the recording electrode at these sites produced an antidromic impulse in the phrenic nerve, supports the view that terminals are electrically excitable. Hubbard and Schmidt extended these observations by assessing the excitability cycle following a suprathreshold conditioning stimulus. They found a supernormal period of 10-20 ms duration, during which threshold was reduced by as much as 13%. This was followed by a period of subnormality with increases in threshold lasting up to 50-90 ms after the conditioning stimulus (96).

C. Spinal Cord Afferent Terminals

Most sensory neurons of the vertebrate peripheral nervous system have cell bodies in sensory ganglia outside of the central nervous system. The peripheral processes of these neurons may lie in any of several somatic or visceral structures including skin, muscle, joint, blood vessel or internal organ. Among the largest diameter, fastest conducting fibers are those sensitive to muscle stretch (group Ia muscle

afferents). Action potentials evoked in these fibers by adequate sensory stimuli travel to the cell body via axons in the peripheral nerves and then to the spinal cord in the dorsal roots. In the frog, the terminals of these neurons within the spinal intermediate gray synapse upon interneurons and motoneuron dendrites. Projections of these fibers in the cat are similar but show additional collaterals to the ventral horn. Ia afferent function has been studied using a variety of anatomical and neurophysiological techniques.

1. Morphology and physiology of Ia intraspinal processes

a. Anatomical studies - Muscle afferents projecting to the frog brachial (103) and lumbar (184) enlargements have been investigated by means of horseradish peroxidase and cobalt chloride tracing, respectively. Muscle afferents terminate exclusively in the base of the dorsal horn and the intermediate gray region. Fine terminations are not readily seen in preparations of this type because of the dense labeling resulting from whole nerve or whole root application of tracer. Szekely described boutons of both the en passant and terminal type (184).

Tracing by means of intraaxonal HRP injections has not been done in frogs, but this method has been applied to the studies of single Ia afferent fibers in cat (31, 158). Ia fibers enter the spinal cord and immediately bifurcate into rostrally and caudally directed axons. These axons may travel in the dorsal columns for many centimeters giving rise to branches at approximately 1.0 mm intervals. Each branch arborizes extensively, giving off many thin fibers in each of three main terminal regions, laminae VI, VII and IX. Terminal branches vary greatly in

length and give rise to one to seven boutons (31, 194).

b. Conduction velocity - Several physiological studies have produced information regarding the conduction velocities of large afferent fibers and their intraspinal projections. The largest diameter myelinated fibers in frog peripheral nerve conduct at 42 m/s at 22° C (62). Given a Q_{10} value of 1.8 (187), it can be calculated that these fibers will conduct at about 29 m/s at 14° C. Frog dorsal root fibers recorded intraaxonally had calculated conduction velocities of >10 m/s at 10° C (148).

Several studies have estimated conduction velocity of the intraspinal courses of primary afferent fibers in the cat using antidromic latency measurements (66, 194) and focal potential recording (56, 140). Both Ia and II fibers (peripheral conduction velocity at 37° C ranging from 102 m/s down to 22 m/s) show large decreases in conduction velocity on reaching the spinal cord. Major axon branches conduct at an average 8-17 m/s for the Ia fibers, terminal branches have calculated conduction velocities from 0.2-1.0 m/s. (140, 194). This is comparable to the value previously mentioned for conduction velocity of terminal fibers of frog neuromuscular junction at 0.3 m/s (107). Polarizing stimuli applied to the cord surface to depolarize or hyperpolarize afferent terminals has no apparent effect on latency of the antidromically conducted action potential (57).

c. Action potential and membrane properties - Intracellular recordings from dorsal root fibers have been made. The difficulty of maintaining stable impalements in these experiments makes it likely that the largest fibers were the sources of most of the data. Eccles and

Krnjevic recorded from dorsal root afferents impaled at the dorsal surface of the spinal cord of anesthetized cats. Action potential heights average 90 mV (muscle afferents) and 82 mV (cutaneous afferents) with durations about 0.5-0.6 ms. A prominent afterdepolarization (ADP) is consistently observed in muscle or cutaneous afferents. This ADP is distinct from the synaptically mediated depolarization (DR-DRP) to be discussed below. It is accentuated by hyperpolarization and depressed by depolarization (58).

Subsequent studies by Eccles and Krnjevic (59) showed that changes occurring after tetanic discharge of these fibers include hyperpolarization, decreased conduction velocity, increased action potential duration and increased magnitude of ADP. Also, they noted that depolarization of dorsal root fibers by external electrodes decreases both action potential amplitude and conduction velocity. Koketsu reported seeing ADP's only rarely in his intracellular recordings of afferent fibers in amphibian and cat spinal cord (115, 116). This may have been due to less stable impalements, for resting potentials were substantially less than those reported by Eccles and Krnjevic (30-70 mV in Koketsu's papers, 50-80 mV in Eccles and Krnjevic). Intracellular recordings from primary afferents of the hamster show ADP's, although this was not mentioned by Bagust, et al. (6).

Using intracellular techniques, Padjen and Hashiguchi focused on passive properties of primary afferents in frog spinal cord (148). Current injection was used to estimate membrane resistance. The authors note a strong rectification at voltages around the resting membrane

potential, with increased membrane resistance on hyperpolarization and decreased membrane resistance on depolarization. The current-voltage data plotted in their Fig. 2 indicate the magnitude of the depolarization-induced resistance decrease. In the hyperpolarizing range R_M is 52 megohms, with depolarization R_M decreases to 10 megohms.

d. Post-tetanic hyperpolarization (PTH) - Tetanization of cat phrenic nerve results in positive afterpotentials (positive on extracellular nerve recordings, therefore reflecting intracellular negativity) (69). The same positive afterpotential is observed following tetanization of cat dorsal roots (198), and the association with intracellular hyperpolarization has been confirmed by intracellular recording (59). This post-tetanic hyperpolarization is also correlated with decreases in excitability and conduction velocity of afferent terminals (193). Similar hyperpolarization following intense activity has been observed in other neuronal systems where it is blocked by such treatments as ouabain, strophanthidin, cooling, and metabolic poisons (15, 175). These findings would indicate a major role of Na-K ATPase in PTH. A similar finding has been obtained for frog spinal cord, in which PTH of the dorsal root potential after dorsal root tetanization is blocked by ouabain (181).

3. Afferent terminals as postsynaptic membranes

a. Dorsal root - dorsal root potential (DR-DRP) - The dorsal root response to stimulation of the homologous or an adjacent dorsal root consists of a prolonged depolarization. The phenomenon of the

DR-DRP has been studied using the following methods: 1) DC recording of root potentials (12, 36, 61, 145); 2) Antidromic activation of terminals with recording of DR evoked potentials (36, 60, 192); 3) Intraaxonal recording from afferent fibers (6, 58, 59, 115, 116, 148).

To summarize the results of these physiological and other pharmacological experiments (8, 9, 46), the prolonged depolarization of the DR-DRP is thought to be synaptically mediated. This primary afferent depolarization (PAD) lasts approximately 100 ms in cat, 250 ms in frog. It is conducted electrotonically out the dorsal root, where it can be recorded close to the spinal cord, but its origin seems to be the terminal region of afferent fibers within the gray matter. Most of the depolarization after a single orthodromic impulse is probably due to the action of the neurotransmitter gamma-aminobutyric acid (GABA) released from axoaxonic synapses of dorsal horn interneurons onto presynaptic terminals of primary afferent neurons (185). Some depolarization, particularly after tetanic stimulation of a dorsal root, may be attributed to an accumulation of extracellular potassium in the dorsal horn (145, 172).

b. Ventral root-dorsal root potential (VR-DRP) - Another interaction found in frog spinal cord is a slow depolarization of a dorsal root in response to ventral root stimulation (12, 36, 78, 116). Grinnell distinguishes between the synaptically mediated "late VR-DRP" (46) and an "early VR-DRP" which was only seen in frog cords treated with gallamine (10^{-3} M) or TEA ($\geq 10^{-4}$ M). His evidence indicates that the early response is mediated through direct electrical contacts between motoneuron dendrites and afferent terminals (78).

c. Spontaneous DRPs - Continuous monitoring of frog dorsal root afferent activity either by DC recordings from whole roots (165, 182) or by intraaxonal recordings from primary afferent fibers (148), reveal spontaneous depolarizations. It should be noted that the control Ringer's solutions used by all three groups did not contain any magnesium ions. The spontaneous depolarizations resembled DR-DRPs in configuration and time course, but were decreased in amplitude (25-40% of evoked DRP's). Spontaneous activity was increased by cooling from 20° to 13° C (182). It was also sometimes seen during recovery from strong electrical or somatosensory stimulation (45).

Pharmacological evaluation of DRP activity (165) allows the following characterizations to be made: 1) DRPs are dependent on synaptic transmission; 2) Enhancing synaptic transmission increases DRPs; 3) GABA antagonism does not decrease DRPs; 4) Excitatory amino acid antagonists reduce DRPs; 5) Interneuron activity may be important in DRP generation. Therefore, a possible mechanism for spontaneous DRPs is rhythmic activity of spinal synaptic networks, including interneurons and primary afferent terminals.

4. Afferent terminals as presynaptic membrane

a. Modifiability of Ia transmission - The Ia-motoneuron synapse has been studied extensively as a model of transmission in the vertebrate central nervous system. Most research reports on the Ia-motoneuron synapse are from in vivo studies of anesthetized cats. In some cases results of these studies have resembled the experiments on other synaptic systems (squid giant synapse, neuromuscular junction), in

other respects this model has unique properties. Many experiments have particularly focused on two maneuvers affecting transmission. These are: post-tetanic potentiation (PTP) and primary afferent depolarization (PAD) associated with presynaptic inhibition (35).

Post-tetanic hyperpolarization of primary afferents has been described above (2d). Transmission at the Ia-motoneuron synapse is potentiated over a time course similar to PTH. The effect of hyperpolarization alone was evaluated using stimulation via surface electrodes on the spinal cord (57). Hyperpolarization of afferent terminals was associated with increases of EPSP's recorded via intracellular electrodes in motoneurons.

Primary afferent depolarization as described above (3a) is associated with decreased effectiveness of synaptic input over a time course correlated with the elevated dorsal root potential. This phenomenon could also be reproduced by extrinsic depolarization of afferent terminals (57). In addition to the decrease in spike height concomitant with the depolarization, membrane conductance is also increased. Padjen and Hashiguchi proposed that a possible mechanism of decreased transmission could be failure of the spike to propagate to all terminals of these branching fibers during the period of decreased resistance (148).

b. Probabilistic transmission - A major recent contribution to research in this field is the substantial evidence that transmission failure occurs frequently at the Ia-motoneuron synapse (86, 99, 158). Experimental manipulations which increase transmission (PTP, paired pulses and frequency facilitation, and decreased temperature) were

effective at decreasing the probability of transmission failures (92, 129).

There are two schools of thought regarding the mechanism of transmission failure. The first is that propagation occurs through all branches and collaterals of Ia fibers and the action potential reaches all terminals. However, due to some limitation of calcium influx or transmitter availability, some boutons do not release transmitter. This explanation has been espoused by Jack, et. al and Redman & Walmsley (99, 157, 158) Based on their correlated morphological and physiological data, it appeared that failure to release transmitter was probably not due to faulty propagation. In these experiments both a single Ia afferent and the motoneuron it excited were identified electrophysiologically, then stained with horseradish peroxidase. Their motoneuron recordings were limited to those located within 2-3 mm of entry of the single Ia fiber. This was designed to maximize the probability of HRP staining all of the Ia terminals at that level. EPSP elements associated with a uniform amplitude occurred with stable latency after a peripheral stimulus. If a single bouton was responsible for that element and propagation was close to a critical level for failure, the element should have appeared with varying latency. HRP labeling identified branches containing boutons which had contributed elements to the Ia-motoneuron EPSP. Even adjacent boutons which could realistically be expected to be isopotential had different probabilites of transmitter release.

The other proposed mechanism is based on the reasoning that Ia fibers entering the spinal cord progress into regions of lowered safety

factor for conduction due to extensive branching and narrowing. Failure of propagation at branch points has been directly observed in invertebrates (79, 130). Differential conduction at branch points is one mechanism proposed to explain transmission failure at the Ia-motoneuron synapse under normal conditions or during primary afferent depolarization (86, 148).

With the restricted segmental location of Redman and Walmsley's study, the possibility of propagation failure at more distant branch points still has not been eliminated. Recent studies of differential conduction at branch points concluded that longer branches were susceptible to propagation failure (178). Perhaps the more rostrally or caudally projecting Ia branches would be subject to this effect. In a recent modeling study, membrane properties of parent and daughter branches were assumed to be homogeneous (177). There is no evidence that this condition is met for Ia axons, branches, and collaterals. One aim of this dissertation is to evaluate whether homogeneity of membrane properties is characteristic of axons and their arborizations.

D. Synaptosomes

When mammalian brain tissue is homogenized and subjected to differential centrifugation under certain conditions, a fraction can be isolated which is enriched in snapped-off nerve terminals called synaptosomes. These synaptosomes retain many morphological and physiological characteristics of central nerve terminals. They contain vesicles of transmitter and mitochondria, they can accumulate and retain

potassium against a concentration gradient, and they may have a potassium-sensitive membrane potential (21).

Experiments using synaptosomes have primarily been flux studies using radiolabeled ions and ion- or potential-sensitive fluorescent dyes. The time resolution of these methods is not comparable to electrophysiological techniques, yet they are particularly useful in characterizing terminal transport processes. The membrane-associated ion pumps and exchange proteins are essential to intraterminal homeostasis, supporting synaptic transmission.

An important issue is terminal handling of calcium, as buffering may be limited by a large surface area to volume ratio (144). There is evidence for two pathways of calcium extrusion from nerve terminals after an action potential: the Na^{+}/Ca^{++} exchanger (141, 142) and Ca^{++}-ATPase (174). The relative role of these systems as well as any contribution by cytosolic calcium binding proteins has not been conclusively determined. The processes restoring calcium to low levels after an action potential may involve two stages with different time courses. First, within milliseconds, $[Ca^{++}]_i$ drops as a consequence of cytosolic buffering proteins and sequestration by intracellular organelles. Second, extrusion of Ca^{++} proceeds over hundreds of milliseconds by means of the membrane-bound systems described above (167).

Pharmacologic sensitivity of potassium efflux from mammalian central nerve terminals has been evaluated in synaptosome studies using ^{86}rubidium. ^{86}Rb was substituted for ^{42}K because it has a longer half-life. Rb accumulates in cells by the action of Na-K ATPase

and passes readily through neuronal potassium channels. The fastest phase of Rb efflux occurred in the first second of wash after a potassium-induced depolarization. This efflux was inhibited by both TEA and 4-AP, with half-maximal inhibition at TEA 0.6 mM or 4-AP 0.1-0.2 mM (14). This indicates a relatively high sensitivity of this process to these potassium channel blocking agents. A component of the fast Rb efflux was also sensitive to decreased calcium or addition of lanthanum to the medium. Therefore, part of the synaptosome potassium conductance may be calcium-mediated (13).

E. Extracellular Electrical Stimulation and Recording in Studies of Neuronal Function

1. Introduction

Extracellular recording of compound nerve and single fiber electrical activity was well developed by Erlanger and Gasser using the cathode ray oscillograph (62). Of particular significance to this investigation is their technique of conduction velocity measurement. They measured changes in the latency to onset of the compound action potential from different stimulation or recording sites and divided the distance between electrodes by this time measurement. This gave a velocity (units of m/s) characteristic of the fastest units contributing to that particular wave. The compound action potential response to strong stimulation showed several distinct waves. This showed that axons making up peripheral nerves do not exhibit a continuum of properties, rather, there are specific subgroups of fibers having

similar properties. In addition they clearly showed that, while configuration and amplitude of the compound action potential change with distance, the area beneath the curve remains the same. The most accurate measure of evoked activity is the area beneath the curve.

Electrical stimulation was used by Adrian (2), Erlanger and Gasser (62), and many others in studies of neuronal function. The fine points of this technique, its usefulness and some associated problems have been reviewed (124, 155). The properties of axons of different diameters in both central and peripheral nervous systems have been studied by these methods, particularly regarding chronaxie, relative refractory, and supernormal periods.

2. Chronaxie

Adequate extracellular electrical stimulation brings an excitable membrane to action potential threshold in a manner dependent on both the intensity and duration of the applied stimulus. Threshold stimulus intensity at very long durations is termed the rheobase. The empirically derived relationship between effective intensity and duration was identified as hyperbolic in appearance by Lapicque in 1926 (reviewed in ref. 72). Lapicque coined the term "chronaxie" corresponding to the duration associated with intensity of 2x rheobase. Ranck states that chronaxie may, in some cases, be equal to 0.7 x membrane time constant, but he indicates that this relationship has not been confirmed for many CNS tissues (155).

Erlanger and Gasser did not find a clear relationship between conduction velocity and chronaxie. This conflicts with Lapicque's

prediction of an inverse relationship between conduction velocity and chronaxie (as cited by Erlanger and Gasser). Their results indicate very little change in chronaxie for fibers with conduction velocities between 10 and 26 m/s, then a rapid increase in chronaxie as conduction velocity becomes slower (62). It can be difficult to interpret results from various investigators and older papers. Many observations were made using whole tissue preparations which differ in representative chronaxie values from single fiber preparations (105). Another confounding factor is that chronaxie can vary with stimulating electrode size, type, and distance from the membrane being stimulated (48, 80).

Two recent studies (16 - 1969, 134 - 1978) did use fairly comparable electrodes and measured chronaxie of central myelinated (16) and unmyelinated fibers (134). Central myelinated fibers had chronaxies of 70-85 μs (mean=76.5). Central unmyelinated fiber chronaxies ranged from 180-310 μs (mean=247.5). The time constant of unmyelinated fibers cannot be determined by intracellular recording because of their small size. The fact that chronaxie is larger in this population may be due to greater membrane capacitance or resistance in this fiber type. Blight has emphasized the functional importance of myelination in decreasing capacitive losses, in addition to its increase of series resistance (22). The observation of longer chronaxie in unmyelinated fibers could be related to their large capacitance as a greater portion of stimulating charge would be needed to discharge C_M. Input resistance will also be greater in unmyelinated fibers due to their small diameter.

3. Early recovery of excitability

After an action potential is evoked in an excitable membrane, there is a delay before a second action potential can be elicited. Paintal has defined three important time periods determining the single fiber response to a second stimulus (151). The first is the absolute refractory period for spike initiation (ARP_i). For the duration of the action potential at the stimulating electrode location, the fiber will be inexcitable at that location. After the action potential at that location is finished, stimulation may produce another action potential. This action potential will not be propagated to a remote recording site because the conducting pathway will still be in its refractory period. Thus, he defines absolute refractory period (ARP) as the time from initiation of the first spike until the first time a second shock results in a propagated action potential. ARP duration is 1.5-2 x spike duration.

The second spike evoked soon after ARP termination is smaller and propagates more slowly than the first spike. The relative refractory period (RRP) is the time from the end of the ARP until the second stimulus produces a spike of normal configuration and latency. This duration is 4 x ARP duration. Spike duration and ARP are inversely related to fiber diameter, conduction velocity and temperature. Changes in spike duration due to different fiber types or temperature are reflected by proportional changes in the recovery (ARP or RRP) to extracellular stimulation (149). Prolonged spike duration due to agents blocking action potential repolarization would be expected to prolong recovery in a similar manner. If the recording site is remote from the

stimulation site, altered recovery could be due to changes at the stimulation site or in the conducting pathway to the recording site.

The author could find no report in the literature of a specific comparison of absolute refractory periods of peripheral axons and their terminals. These values can be calculated from various sources. Absolute refractory period of the largest mammalian myelinated fibers is approximately 0.45 ms at the normal body temperature of 37° C (151). Multiplying by four (see above) estimates RRP duration of these fibers at 1.8 ms. RRP of terminals was longer than this, with reported values of 1.5-4 ms at 34-35° C (95, 96). Smaller peripheral fibers have been studied in cat aortic nerve. Small myelinated and unmyelinated fibers had ARP durations of 10-33 ms at 17° C (150). ARP of frog C fibers (splanchnic nerve) lasts 7.5-8.5 ms at 20° C (70).

ARP has also been measured for central axons of different diameters. RRP of single sensory fibers has been shown to vary with stimulation site. Afferent fiber terminals in cat spinal cord, in vivo, had RRP's of 4-5 ms while the same fibers excited from the dorsal column had refractory periods of 1.5 ms (194). Intracellular recordings of dorsal root fibers of frog spinal cord, in vitro, showed spike durations of 2 ms (15-20° C)(115). Based on Paintal's calculations, this should correspond to an ARP of 3-4 ms. Two types of recovery profiles were observed in lateral Lissauer tract fibers (134). Some, with conduction velocities in the C fiber range, had a short ARP of 1.2 ms followed by a rapid transition to supernormal excitability (see next section). Others, with conduction velocities in the A delta range, had long ARPs of 7 ms followed by a prolonged RRP and no supernormality.

This would seem to indicate that central fibers do not always have recovery processes inversely proportional to conduction velocity as has been proposed for peripheral fibers (149, 150).

4. Supernormal period

a. Introduction - Some excitable membranes show a period of decreased threshold and increased conduction velocity after the passage of a single impulse. This time period has been termed the supernormal period (SNP) (2, 68, 75, 162, 197). The correlation between excitability and conduction velocity during the SNP has not been shown in all studies of the phenomenon and in some cases the magnitude of changes of these two variables can be quite different (76, 114). However, in most studies where both variables have been monitored, there is usually a good correlation between SNP of threshold (decreased threshold to excitation) and of conduction velocity (increased conduction velocity) (34, 197).

Early studies of action potentials and their sequellae used extracellular stimulation and recording techniques. Graham's 1934 study, for example, describes the double-pulse stimulation paradigm most often used to study supernormality in whole nerves (75). The first stimulation, which she termed the conditioning shock, was set to evoke a large A fiber response. The second stimulation, the testing shock, was set to evoke a response less than half of the amplitude of the conditioning response when the test shock was unconditioned. Compound action potential analysis in SNP studies usually involves measurements

of the amplitude (or area) and latency of the conditioned test response, compared to the unconditioned test response. Studies of single fiber SNPs measure threshold changes after single action potentials. The results of both of these methods are comparable (27, 134).

The appearance of a SNP in nerve fibers has been correlated with the appearance of a negative wave, termed the negative afterpotential, following the spike of the compound action potential (62, 75, 77, 81, 162). The intracellular correlate of this extracellularly recorded event is the depolarizing afterpotential (DAP)(11, 23, 27, 58). Two recent studies of supernormality have augmented results obtained with the older method by showing that SNP of the compound action potential is usually associated with a DAP (24, 27). Intracellular recordings from axons which did not show a DAP after the action potential may have been due to depolarization from impalement damage. Passage of hyperpolarizing current through the microelectrode sometimes restored the DAP.

b. Peripheral nerves - The largest diameter fibers (A fibers) of frog or lizard peripheral nerve show a SNP, negative afterpotentials and intracellular depolarizing afterpotentials (3, 11, 27, 34, 75, 128, 156). In double-stimulation experiments, the SNP is evident following the relative refractory period, beginning in 2-5 ms. Maximum supernormality is seen at interstimulus intervals of 10-20 ms. Reported durations of the SNP vary from 30 ms (3, 75) to 200 ms (27, 34), with one report of an extremely long SNP lasting 1-1.5 s (156). Mammalian peripheral A fibers show some supernormality, but to a lesser degree than frog nerves (27, 76). Threshold decreases during the SNP were

3-10% in mammalian preparations, 7-20% in frog nerves (27, 75, 76, 156). SNP of conduction velocity in A fibers was only reported by Graham, with increases of 7% in frog nerve (75). As mentioned above (C), mammalian motor nerve terminals had a SNP lasting 10-20 ms with threshold decreases up to 13% (95, 96).

Supernormality and negative afterpotentials are also characteristic of mammalian C fibers, but they are not always found in frog C fibers (70, 77, 81). The maximum excitability increase in cat C fibers was 10-40% of control (81). This study did not report any conduction velocity changes during the SNP.

c. Mammalian central axons - Large diameter spinal axons have a SNP, negative afterpotentials and depolarizing afterpotentials (23, 58, 162). Large fibers of cat dorsal columns showed increases of excitability of 16% over control during the SNP (162). Supernormality of threshold and/or conduction velocity has also been described in thinly myelinated axons within the central nervous system. Peak changes during supernormality were 7-17% increase in conduction velocity and 7-53% decrease in threshold (114, 179, 197). Central unmyelinated fibers, particularly cerebellar parallel fibers, show supernormality with increases of conduction velocity of 10-20% over control. Increased conduction velocity of parallel fibers during the SNP is even more striking since no mention was made of supernormal conduction in cat C fibers (81). Thresholds can be as much as 40% lower during this period, and amplitude of a test response increases up to 80% over control (68, 112, 134).

d. Proposed mechanisms - The potential recorded inside a squid

giant axon shows two slow phases after action potential repolarization. First, there is an immediate hyperpolarization. This is thought to be due to continuation of the increased potassium permeability responsible for repolarization. This is followed by a slight depolarization to a level just positive to the resting membrane potential. Finally, the potential returns to its resting level (64).

Frankenhaeuser and Hodgkin referred to the brief depolarization as the negative after-potential (64), consistent with the terminology from extracellular recording techniques. Negative after-potentials resulting from successive closely spaced action potentials summate to a continuous low-level depolarization of the membrane potential. These authors were able to account for the negative after-potential by modeling a periaxonal space with restricted diffusion. The potassium leaving the axon during action potential repolarization is trapped in this space causing a local increase of $[K^+]_o$ which depolarizes the axonal membrane. The accumulated K^+ then diffuses away over 30-100 ms (64).

Depolarizing accumulations of potassium have also been proposed to account for the negative afterpotential and supernormal period of mammalian unmyelinated nerve fibers (68, 77, 112). Supernormality of cerebellar parallel fibers is indicated by increased field potential amplitude and decreased latency to the second of two stimuli. The maximum potentiation of the test response was seen at 10 ms condition-test delays. Supernormality persisted for at least 100 ms (68, 112). In this system, conduction velocity is increased when superfusate $[K^+]$ is increased. However, the latency shift

associated with the SNP is decreased by this treatment (112). Gardner-Medwin attributed supernormality to changes in the extracellular environment of these closely packed fibers following activity (68).

The mechanism of supernormality of threshold was also investigated in an invertebrate. Crayfish motor neuron terminals have a pronounced SNP, but relative changes in threshold during the SNP are decreased during superfusion with high K^+ solutions. SNP was decreased by collagenase digestion of surrounding tissue (200), consistent with Gardner-Medwin's hypothesis (68). To summarize, the major mechanism proposed to explain supernormality of unmyelinated fibers is potassium accumulation in the extracellular space. Potassium accumulation depolarizes the membrane, increasing excitability by bringing it closer to action potential threshold.

Supernormality of large myelinated fibers may be due to a different mechanism. Barrett and Barrett found that the depolarizing afterpotential of lizard and frog peripheral axons was increased by hyperpolarization and decreased by depolarization. When they varied $[K^+]_o$ but kept membrane potential steady with current injection, there was no change in the DAP (11). This finding has been confirmed by other investigators (24). Therefore, it is unlikely that the SNP of large myelinated fibers is due to potassium accumulation.

Presently, the DAP of large myelinated axons is thought to be a passive event related to discharge of internodal capacitance. The classical approach assumes that the internode and its associated myelin layers function as a unit with a single resistance and capacitance. More recently proposed models view internode capacitance separately from

myelin capacitance (11, 22). Their models were proposed to explain the long charging time constant during constant current injection, particularly with hyperpolarizing pulses. Discharge of the potential at the internode membrane, after the action potential, occurs through a series resistance consisting of either periaxonal pathways (11) or the myelin sheath itself (22). This process, or passive charging to hyperpolarizing current, has a long time constant because of the large capacitance of the internodal membrane. DAP amplitude and duration will be increased in axons with a higher ratio of internodal membrane resistance to periaxonal leak resistance. Therefore, Barrett and Barrett's model predicts this passive depolarization to be greater in smaller axons with fewer myelin wraps. A DAP of passive origin is also predicted for unmyelinated fibers given the following conditions: 1.) A high specific membrane resistance contributing to a long membrane time constant, and 2.) Axonal K channels which close before complete action potential repolarization (11).

In summary, double-pulse testing of axons shows that many types of axons are more excitable and conduct impulses faster for a period of time after conducting a single action potential. This characteristic is more prominent in smaller myelinated axons and is most evident in central unmyelinated axons. Supernormality is coincident with, and may be the result of, a DAP following the action potential. This DAP may represent a slow time constant of discharge of membrane capacitance. Alternatively, potassium accumulation in the adjacent extracellular space may be the source of this supernormality, particularly in unmyelinated axons.

F. Pharmacologic Alterations of Synaptic Transmission

1. Synaptic pathways in frog spinal cord

In this dissertation pharmacologic modifications of synaptic transmission drawn from literature on central and peripheral synapses were tested on frog spinal cords. The frog spinal cord is a useful model for several reasons. Cords can be taken from adult animals. Mammalian spinal cords show the greatest viability when taken from young animals which may not have the same axonal or reflex activity as adults (113, 118). Frog cord viability can be maintained for several hours, particularly if the preparation is kept cool (188). Two synaptic pathways with different characteristics are present in the frog cord, and the effects of their activation can be compared.

Alpha-motoneurons with cell bodies in the ventral horn have axons projecting out of the spinal cord making up the ventral root. The area beneath the compound action potential recorded from the ventral root can be measured as an index of relative size of the responding population. The motoneurons are brought to action potential threshold by activity in two pathways. Excitation is caused by activity in muscle afferent fibers entering the spinal cord through dorsal roots (DR). In addition, motoneurons are synaptically driven by fibers descending in the lateral column of the cord from the brainstem (LC).

A comprehensive study on frog spinal cords, *in vitro*, characterized the ventral root responses to DR and LC stimulation. Ventral root responses (VRR) to LC stimulation have short onset latency (2.9 ms) and a brief, highly synchronized discharge. DR stimulation

evokes VR responses at longer latency (6.0 ms). The DR-VRR is asynchronous and prolonged, and the area under the curve is 11-12% of the area beneath the LC-VRR (30).

Other investigations used intracellular recordings from frog motoneurons during activation of these pathways (42, 63). Results in both of these studies indicate that the LC input is much more effective in bringing motoneurons to action potential threshold. Although DR stimulation does produce monosynaptic EPSPs in motoneurons, they are small and insufficient to reach threshold (63). These authors concluded that the DR-VRR recorded from whole ventral roots is disynaptically mediated. This information was confirmed by another study (93), in which a monosynaptic response was obtained by facilitation. The latter investigation involved delivering a conditioning DR volley followed by the test DR stimulation. Under these conditions a much larger, presumably monosynaptic response is recorded at interstimulus intervals of 5 to 200 ms. It is important to note that the initial, unfacilitated DR-VRRs appear similar to those recorded by Brookhart, Machne and Fadiga (30).

Czeh examined this question of DR monosynaptic inputs to motoneurons using intracellular recording techniques. He reported that DR monosynaptic inputs are sufficient to reach threshold for action potential initiation (44). Katz and Miledi's results conflict with this finding, as they emphasized the importance of di- and trisynaptic inputs in bringing motoneurons to action potential threshold (106).

2. Agents used to block synaptic transmission

Early studies of synaptic transmission were frequently performed under conditions of partial block of transmitter release. This was particularly important in studies of neuromuscular transmission for two reasons. First, contraction of an impaled muscle fiber could move or break the recording electrode (49, 50, 95, 96). Second, the relative depression of transmitter release in the steady state allows the effect of facilitatory maneuvers to be demonstrated, such as addition of calcium (50) and repetitive stimulation (96).

Many neuromuscular junction studies use high magnesium (12-16 mM) to suppress transmitter release. The actions of Mg^{++} are antagonistic to Ca^{++} in this regard. On the other hand, the effects of these divalent cations on threshold are the same, both causing an increase in threshold (50). Investigators who use solutions with altered divalent cation composition need to consider effects on surface charge. Altered membrane charge distribution changes normal channel gating characteristics (73). In addition, complete withdrawal of calcium should be avoided, as there may be a direct role of calcium ions in gating of certain channels (5).

Cadmium is another divalent cation which has been used to block calcium influx through voltage-sensitive calcium channels (41, 126, 135). Several recent intracellular recording studies on mammalian CNS tissues in vitro used Cd^{++} (0.2 mM) to block calcium influx (38, 122, 160). In studies of the squid giant synapse, calcium currents in the presynaptic terminal were greatly decreased by Cd^{++} 1.0 mM (126). Much lower concentrations were effective at decreasing evoked

transmitter release at the frog neuromuscular junction. In this preparation EPP amplitude was reduced to less than 10% of control in a solution of 5.0 μM Cd^{++} with Ca^{++} 0.5 mM and Mg^{++} 4.0 mM (41).

Recent developments in our understanding of calcium channel heterogeneity have complicated the issue, as more than one type of calcium channel may be responsible for neurotransmitter release. Additionally, the type of channel(s) involved in release may vary in different types of neurons (154). Miller has reviewed the current pharmacology of calcium channels (135). Cd^{++} is listed as a potent blocker (IC_{50} = 10 μM) of "N" and "L" types of channels while being less effective at blocking "T" channels (IC_{50} = 100 μM).

The solutions used to suppress synaptic transmission in this dissertation were developed by modifying divalent cation composition of the superfusing medium. The effectiveness of the modified solutions was indicated by suppression of stimulation-evoked responses in several synaptic pathways.

3. Potentiation of synaptic transmission

a. Introduction - Experiments designed to evaluate the mechanisms of synaptic transmission have frequently used pharmacologic interventions to enhance this process. Prolonging action potential duration at the presynaptic terminal is one way to enhance transmitter release, as shown directly in the study of squid giant synapse by Llinas, Sugimori and Simon (126). Even small increases (1 ms or less) in presynaptic spike duration can substantially enhance transmitter release (152). Although there is reasonable indirect evidence to

implicate a similar mechanism in vertebrate nerve terminals (17), direct evidence of presynaptic action potential prolongation has been lacking.

Classical studies of action potential mechanisms of neuronal membranes attribute repolarization to increased potassium efflux through voltage-gated channels (91). There are several known potassium channels with heterogeneous pharmacology, gating characteristics, distribution and hypothetical contributions to neuronal function (1, 40, 91). Recent reviews have discussed properties of A channels (159), calcium-activated potassium channels (20), and M channels (32). Due to the inaccessibility of presynaptic terminals, it is not possible to adequately characterize the population of potassium channels responsible for action potential repolarization at this locus. Pharmacological studies in several neuronal systems have primarily used two potassium channel blocking agents, tetraethylammonium (TEA) and 4-aminopyridine (4-AP) to enhance synaptic transmission. Brief summaries of effects of these potassium channel blocking agents on selected neuronal tissues and synaptic transmission are presented in Tables I and II.

b. 4-AP - In studies of squid giant synapse, aminopyridine compounds (3-AP, 4-AP) have been used to block potassium currents of the presynaptic terminal membrane (127). The concentrations used in this study varied from 1-20 mM. At these concentrations, the aminopyridines block the delayed rectifier, I_K, very effectively (87). Much lower concentrations of 4-AP have been demonstrated to enhance synaptic transmission in vertebrate neuronal systems. Injected intravenously or intraarterially into anesthetized cats, it increases the

TABLE I. ACTIONS OF 4-AMINOPYRIDINE ON NEURONAL TISSUES

A. Neuronal Membranes - blocks potassium currents

System	Current (if known)	Range of [] or K_d	Reference
Hippocampus	I_A	0.5-2.0 mM	199
Cultured neurons (spinal and hippocampal)	I_A	K_d=2.0 mM	171
Molluscan	I_K	K_d=0.8 mM	87
	Transient K	K_d=1.5 mM	189
Rat nodose ganglion		1-30 µM	176
Frog - Ranvier node	Fast I_K	K_d=20 µM	53

B. Axons - spike broadening, late activity or bursting

System	Range of []	Reference
Rat spinal roots - unmyelinated axons	5.0 mM	25
Rat spinal roots - young or demyelinated	1.0 mM	26
Rat (young) sciatic	0.1-5.0 mM	113

C. Synaptic transmission potentiation

System	Range of []	Reference
Squid (blocks presynaptic I_K)	1-30 mM	127
Neuromuscular junction - frog	5-20 µM	74
mouse	1-30 µM	136
	0.1-0.8 mM	166§
Bullfrog sympathetic ganglion	0.6-5.0 µM	119
Frog spinal cord	10-100 µM	67
Hippocampus	5-10 µM	33, 164

§ This study was carried out under acidotic conditions which decrease the effectiveness of 4-AP (133).

TABLE II. ACTIONS OF TETRAETHYLAMMONIUM ON NEURONAL TISSUES

A. Neuronal membranes - blocks potassium currents

System	Current	K_d	Reference
Molluscan neurons	I_K	6.0-8.0 mM	88
Frog - Ranvier node	I_K	0.3-0.5 mM	53, 89, 168

B. Axons - spike broadening

System	[]	Reference
Rat spinal roots - unmyelinated fibers	50 mM	25

C. Synaptic transmission potentiation

System	Range of []	Reference
Neuromuscular junction - frog	0.1-1.0 mM	17, 74, 117
mouse	0.1-1.0 mM	166
Bullfrog sympathetic ganglion	25-500 μM	119

D. Synaptosome rubidium efflux (via K conductance pathway)

Type of efflux	K_d	Reference
Fast	0.6 mM	14
Calcium-dependent	0.2 mM	13

DR-VRR (101, 123) and potentiates intracellularly recorded Ia-motoneuron EPSPs (98, 101). Doses in these studies were 0.1-1.0 mg/kg. Reflex transmission in frog spinal cord is enhanced at concentrations 10^{-5}-10^{-4}M in a solution with Ca^{++} 1.8 mM/Mg^{++} 5.0 mM (67). Reported effective doses at frog and mouse neuromuscular junction are expected to depend on the experimental pH (136) and vary from 10^{-6}M to 10^{-4}M (100, 166). In frog sympathetic ganglion (119) and in rat hippocampus (33, 164), synaptic potentiation is achieved with doses of 10^{-6}-10^{-5}M. In general, these doses are well below the effective dose of 4-AP to block the delayed rectifier. In addition, they are lower than the doses used to block the transient potassium current, I_A. In molluscan neurons 4-AP blocks I_A with a dissociation constant of $1.5x10^{-3}$M (189). In mammalian neurons, one type of transient potassium conductance is blocked by 4-AP $0.5\text{-}2x10^{-3}$M (171, 199).

Several of the reports on 4-AP effects on transmission included, as a discussion point, the proposal that synaptic potentiation by low-dose 4-AP is achieved by direct enhancement of calcium influx (67, 101, 136). This notion is particularly attractive since none of the intracellular studies included in the above group described action potential prolongation of the postsynaptic neurons at these low doses of 4-AP (33, 98, 119). One report supports this proposal, based on results from intracellular recordings. Rogawski and Barker have reported enhancement of calcium current in cultured mouse spinal cord neurons by 4-AP 0.5-1.0 mM (161). However, this concentration range is still up to 100 times greater than the effective doses in most synaptic transmission

studies.

In summary, the mechanism of synaptic facilitation by 4-AP is still unclear despite the number of studies substantiating its efficacy. None of the well-characterized potassium channels involved in action potential repolarization are sensitive to these low 4-AP concentrations (1) (however, see section 3b). The mechanism at neuromuscular junction appears to involve increases in quantal content. This mechanism is apparently less important at the Ia-motoneuron synapse, where there is a decrease in transmission failures due to an increase in the number of boutons releasing transmitter (98). Prolonged action potential duration has not been reported at a vertebrate central nerve terminal after 4-AP treatment.

c. TEA - This ion has been used to block potassium channels in a variety of preparations, including nodes of Ranvier of large frog axons. In this preparation the dissociation constant is 0.3-0.5 mM (53, 89, 168). This blocking agent is not specific to the delayed rectifier potassium channel; it can also block calcium activated potassium conductance (88, 121).

TEA enhances chemical transmission by increasing quantal content as demonstrated in numerous studies on peripheral synapses (17, 109, 117, 119, 166). A large range of doses were used in these studies, from 25 μM (119) to 20 mM. Koketsu found the threshold dose for effectiveness at augmenting transmission to be 0.2 mM (117). This dose was also effective in Benoit and Mambrini's study (17). Katz and Miledi used the highest doses, 5-20 mM, to produce maximal effects (109). Saint, et. al , found TEA 0.8 mM produced near-maximal synaptic

potentiation (166). Although one study used TEA at concentrations from 25 to 500 μM, the responses did not reach a plateau, and a dissociation constant was not calculated (119). TEA also has postsynaptic effects at cholinergic synapses, seen at both the neuromuscular junction and the sympathetic ganglion. It blocks the postsynaptic receptor site, particularly at the higher doses used in experiments designed to evaluate maximal presynaptic effects (109, 117, 119).

The mechanism of presynaptic facilitation by TEA is assumed to be via prolongation of the presynaptic action potential. This hypothesis was not confirmed in a study using extracellular recording of nerve terminals (17). Koketsu observed no action potential prolongation by TEA 1-6 mM on impalements of motor axons near their terminals (117). The effect of TEA on refractory period of vertebrate central nerve terminals is not known.

d. Neurotoxins - There are a few reports on naturally occurring toxins which seem to alter synaptic transmission through presynaptic mechanisms. One example is dendrotoxin (DTX) from green mamba venom. This is classified as a facilitatory neurotoxin because of its reported action of enhancing synaptic transmission at peripheral (85) and central (83) synapses. Similarities between the action of DTX and 4-AP have been noted by Dolly (51).

The effectiveness of 4-AP and DTX to facilitate synaptic transmission may implicate a novel type of potassium channel contributing to action potential repolarization at nerve terminals. Physiological and biochemical evidence supporting this was found in some recent studies (18, 19, 176).

A novel potassium current has been identified in a subpopulation of neurons in rat nodose ganglion. This current is characterized by its extreme sensitivity to 4-AP (1-30 μM) and DTX (3-10 nM). DTX block is irreversible. The current can be distinguished from the A current of rat hippocampal neurons. The nodose cell current is more sensitive to 4-AP and DTX, activates more slowly, and exhibits only partial inactivation. It is not sensitive to calcium block, therefore, it is not likely to be a calcium-dependent potassium current (176). In guinea pig dorsal root ganglion neurons, DTX greatly reduces a non-inactivating outward current at 1.4 nM without affecting the fast transient outward current (homologous to A current). In the presence of 3,4-diaminopyridine, DTX does not have any effect. This supports other work which indicates that at least a portion of aminopyridine-sensitive potassium currents are also blocked by DTX (52, 153).

Highly sensitive binding of dendrotoxin has been demonstrated by rat cerebrocortical synaptosomes with a calculated K_d of 0.3 nM (18). Synaptosomes from chick cortex have two populations of dendrotoxin binding sites. K_d's are 0.5 nM and 15 nM (19). Dolly has proposed that these sites may correspond to the potassium channels of nodose cells described above. The relatively rare occurrence of this current in neuronal somas may be due to a specific distribution on presynaptic membranes, thus explaining the binding found in synaptosome studies (51). This would be consistent with the interpretation of 4-AP experiments on synaptic transmission. If the 4-AP sensitive current slowly inactivates, it could be involved in terminal action potential repolarization. That is a role that would not be expected of rapidly

inactivating currents like the A current.

Facilitation of transmission is also seen after treatment with toxin from the sea anemone Anemonia sulcata . Toxin II from this organism (ATX-II) prolongs action potential duration of many neuronal membranes by suppressing sodium channel inactivation (4). Maximal enhancement of quantal content indicates a 2- to 4-fold increase in transmitter release (137). Although this indicates a facilitating action, it has been emphasized that this effect is far less than the effect of potassium channel blockade to enhance transmission (hundreds-fold observed by Katz and Miledi (109)).

CHAPTER IV

METHODS

A. Tissue Preparation

1. General animal preparation and surgery

The experiments were done on bullfrogs (Rana catesbeiana) of either sex. Their body lengths ranged from 10-15 cm exclusive of legs. They were obtained from one supplier and held for at least two days prior to experimentation. These frogs were housed in large sinks with continuously running water controlled at 22° C and received a diet of live crickets dusted with vitamins three times weekly.

Removal of the spinal cord was performed in the manner of Tebecis and Phillis (188). Anesthesia was induced by immersion in ice water for approximately one hour. While maintaining the frog unresponsive to painful stimuli by surrounding it with ice, a laminectomy was performed from the level of the second or third vertebra to the urostyle, exposing most of the spinal cord including the filum terminale and lumbar roots. The cord was transected rostrally, and roots were cut from caudal to rostral. Care was taken to preserve the greatest possible length of lumbar dorsal roots. When free, the cord was removed to a dissection bath containing modified Ringer's solution at 4° C ("cold" solution; see Table III). The cord was pinned to the

Sylgard base of the dish, dorsal side up. In some experiments two dorsal roots (usually both D9 roots) were excised at this time. The dorsal columns were gently separated along the midline using fine forceps. The cord was then hemisected midsagitally using a microscalpel fashioned from a wedge of straight razor blade held by a small curved hemostat.

Preparation time was approximately 20 minutes. Optimum exposure of the vertebral column and rib processes was achieved after 5 minutes of skin and muscle dissection. The laminectomy lasted 10 minutes. Rhizotomy and cord removal was brief, usual duration of 1 minute. The remaining 4 minutes elapsed during trimming and hemisection. Preparation time was not a criteria for inclusion in the studies. All preparations were included except those showing dorsal root damage after the dissection.

One half of the cord, and both of the free roots were placed in beakers of "cold" solution, briefly bubbled with 97% O_2/3% CO_2, covered and placed in the refrigerator at 4-5° C. This treatment was reported to maintain optimum viability of frog dorsal root ganglia for up to several days (54). The other half was placed in 200 mL of "recovery" solution at 4° C, and bubbled continuously with the same gas mixture until this system reached 14° C. This change of temperature took about one hour. Following this equilibration period, the hemicord was transferred to the superfusion chamber (Fig. 3).

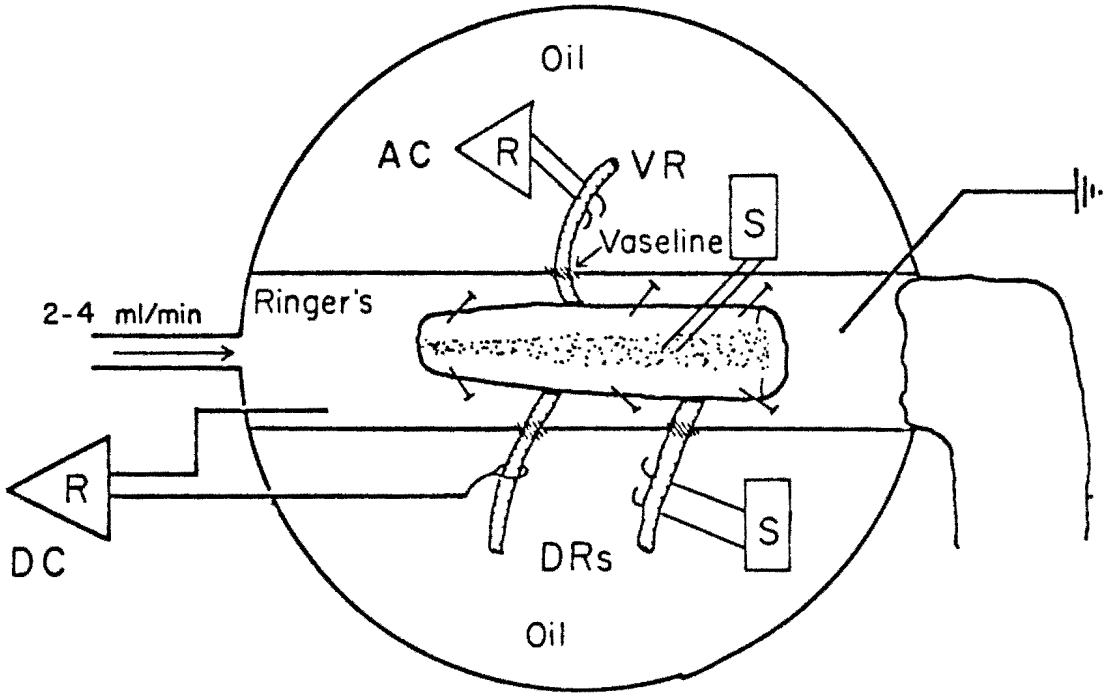

Figure 3. Diagram of frog hemicord in superfusion chamber, instrumented for measurement of reflexes as described in Methods section B.

2. Superfusion bath design

The bath is constructed with a hollow base for circulation of cold ethylene glycol. Continuously bubbled "standard" solution feeds by gravity at a rate controlled by a roller clamp. It flows through stainless steel tubing embedded in the base, and is thereby cooled to 14° C. Fluid removal is accomplished by a cotton wick to a drain tube. The superfusion rate is 2-4 mL/min. The volume of the central chamber which receives the superfusion fluid is 0.25 mL. The central portion is separated from the adjacent pools by Plexiglass dams firmly embedded in the Sylgard base. Once the tissue had been transferred to this chamber, further dissection was done to free a large dorsal root from the dura that remains on the cord. This root (usually D8) was led into an adjacent pool of mineral oil, also at 14-15° C. At the point of exit from the chamber, the root was coated with silicone vacuum grease to prevent desiccation and saline leakage into the oil. The cord was well secured against movement by insect pins etched to a fine tip. In the experiments on dorsal roots alone, a dorsal root was placed in the chamber and pinned through the most proximal portion. The distal end was led through the silicone gap into the adjacent mineral oil (Fig. 4).

3. Composition of electrolyte solutions (Table III)

The solutions listed were kept isotonic by adjusting NaCl and $NaHCO_3$ content to keep total Na^+ at 110 mM. The calculated osmololality is close to plasma values of frogs held in fresh water (39). The use of different temperatures in the early stages of tissue preparation leads to a complication in pH control of the bicarbonate

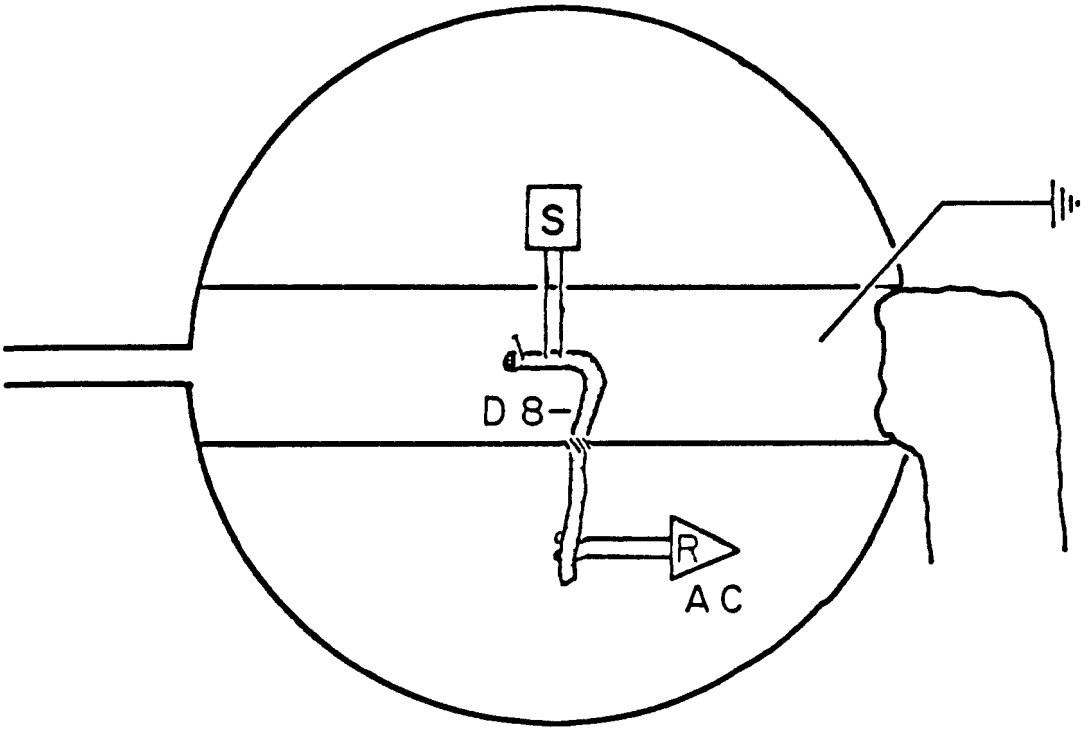

Figure 4. Diagram of single dorsal root in superfusion chamber, instrumented for experiments on recovery of excitability as described in Methods - section D - 3a.

TABLE III

Composition of electrolyte solutions
(Values in mM)

Solution	NaCl	$NaHCO_3$	KCl	$CaCl_2$	$MgCl_2$	$CdSO_4$	Glucose	mOsm
cold	84	26	2.0	1.5	1.5		5.0	238.0
recovery	87	23	2.0	1.5	1.5		5.0	238.0
standard	92	18	2.0	1.5	1.5		5.0	238.0
Cd 0.1 mM	92	18	2.0	1.5	1.5	0.1	5.0	238.2
A	92	18	2.0	1.5	1.5	0.2	5.0	238.4
B	92	18	2.0	0.5	2.5	0.1	5.0	238.2

buffered solution. Carbon dioxide is more soluble in cold solutions, requiring more sodium bicarbonate to maintain the same pH as warmer solution. All of the solutions were bubbled with gas of the same composition: 97% O_2/3% CO_2.

Howell and coworkers have discussed the variations of pH with temperature in frog, in vivo . At 15° C they reported 7.96 to be the mean pH of Rana catesbeiana (94). Previous studies of frog spinal cord in vitro have used Ringer's solutions at pH 7.0-7.5 (45, 47, 145). The solutions used in my experiments were developed empirically, modifying solutions reported by several laboratories. The greatest tissue viability was observed when different solutions were used at different temperatures, keeping pH in the range 7.35-7.45. Although this range is acidotic relative to the in vivo value reported above, I observed no evidence of physiological deterioration of function in impulse propagation or synaptic transmission during experiments lasting up to twelve hours.

Tetraethylammonium (TEA) and 4-aminopyridine (4-AP) were dissolved in < 1 mL of isotonic saline (120 mM NaCl) and added to the standard solution or solution A as indicated in the various protocols. $CdSO_4$, 4-AP, $MgCl_2$, and TEA were obtained from Sigma; all other chemicals are Mallinckrodt "Analytical Reagent" grade obtained through Scientific Products.

B. Assessment of Agents Affecting Synaptic Transmission

1. Stimulating and recording procedures (Fig. 3)

a. Dorsal root - ventral root reflex (DR-VRR) - After preparation of the cord in the usual manner, the cord was placed in the superfusion chamber with a lumbar dorsal root led into an adjoining mineral oil pool and placed over a bipolar stainless steel stimulating electrode. The ventral root of the same segment was placed in another mineral oil pool over a bipolar silver wire electrode. The ventral root was crushed between the electrode poles to obtain a monophasic recording of the evoked compound action potential. The recording electrode was led to the high impedance probe of a Grass P9b or P511 AC amplifier. Filter settings were adjusted for minimum filtering with rise time constant 0.01 ms, fall time constant 600 ms. The amplifier output was displayed on a Tektronix storage oscilloscope and photographed on Polaroid film for subsequent analysis.

Stimulation of the dorsal root was accomplished using a Grass S44 stimulator and SIU5 stimulus isolation unit. Stimulating voltage was set to a level which was supramaximal for the evoked VRR. After control values were obtained, superfusion with the test solution started, during which time the response to a single supramaximal stimulus was monitored every 30-60 seconds until a steady state was reached.

b. Lateral column - ventral root reflex (LC-VRR) - The monosynaptic excitatory pathway to the motoneuron pool is via axons descending in the lateral column of the spinal cord (42). In these experiments this pathway was stimulated by lowering two stimulating electrodes into the lateral column, positioning them to give a maximal response from the ventral root, which was recorded using the methods

described in section 1a. Stimulating electrodes were glass-insulated tungsten wires with sharp tips formed by holding the bare wire in the flame of an acetylene torch (28). Capillary glass was then pulled down over the wire leaving a 50 μm exposed tip (143). These electrodes had 150-200 K ohm impedances measured at 1000 Hz. In these experiments the Grass S44 was used to drive a Grass PSIU6 photoelectric stimulus isolation unit with constant current output. As in measurements of the DR-VRR, the stimulus intensity was set to supramaximal, control recordings were made, then the response to a single supramaximal stimulus was monitored every 30-60 seconds during superfusion with the test solution until a steady-state response was reached.

c. Dorsal root - dorsal root reflex (DR-DRR) - In these experiments the stimulation methods were the same as described in section 1a above (DR-VRR). Two lumbar dorsal roots were led into the mineral oil pool, and one was used for stimulation. For DC recording experiments the cord was positioned to place the dorsal roots as close as possible to the neighboring chamber, exposing very little root to the Ringer's solution. Saline-soaked cotton wicks were placed in saline-filled glass capillary tubes inserted into WPI electrode holders with embedded silver-silver chloride pellets. One wick electrode was placed in contact with the bath, the other was looped around the root in the mineral oil. The potential difference between these electrodes was amplified by a Grass P16 DC amplifier and recorded on a Grass polygraph and Tektronix storage oscilloscope. The filter setting on the P16 amplifier in the DC output mode was set for minimum filtering (rise time switch on minimum, <3 μs). The bath was grounded to amplifier ground.

In some of these experiments, the DR DC response was monitored during direct stimulation of the dorsal gray matter of that spinal segment.

2. Pharmacologic modifications of synaptic transmission.

a. Four-Aminopyridine (4-AP) - This potassium channel blocking agent has been used to enhance synaptic transmission in numerous studies of neuromuscular junction (136) and squid giant synapse (127), as well as in vitro mammalian CNS preparations (33, 164). Concentrations used in these studies range from millimolar values (used on squid giant synapse, where the drug blocks the delayed rectifier potassium channel) to micromolar concentrations used in vertebrate studies. Alterations in the DR-VRR and DR-DRR due to 4-AP application were used as a guide to an effective dose to be used in a subsequent study.

b. Tetraethylammonium (TEA) - This potassium channel-blocking agent has also been reported to enhance synaptic transmission at peripheral synapses at concentrations as low as 25 μM (119). As with 4-AP, the DR-VRR was used as a rough indication of synaptic efficacy in this preparation, to find an effective dose of TEA to be used in a subsequent study.

c. Cadmium (Cd^{++}) - All three synaptically mediated responses were monitored in different experiments using solution A to block synaptic transmission. In some experiments 4-AP, TEA, or 4-AP + TEA were added to solution A. It was apparent after these experiments that the LC-VRR was the most robust response, as it failed only after 15 minutes of superfusion with synaptic blocking solution, whereas the DR-DRR failed in 12 minutes, and the DR-VRR was blocked even

more rapidly. Evaluation of the synaptic blocking efficacy of solution B was only performed using the LC-VRR. In some of these experiments, TEA and/or 4-AP were added to solution B to determine whether they could overcome the block.

C. Chronaxie Study

1. Stimulation procedures

a. Electrode placement - Stimulation near the terminals of large diameter afferent fibers was achieved by advancing one glass-insulated tungsten electrode into the gray matter visible at the cut surface of the hemicord. The electrode was positioned just dorsal to a point midway between dorsal and ventral and lowered into the tissue until a dorsal root compound action potential was seen in response to stimulation at this point (184). This is referred to as dorsal horn (DH) stimulation (Fig. 5).

Stimulation of axons of afferent fibers was accomplished by an electrode advanced into the dorsal white matter to reach the dorsal root entry zone. The latency to stimulation at this site was clearly shorter than the DH response. This will be referred to as dorsal white (DW) stimulation. The path for current return from either cathode was a similar electrode constructed with a 200 μm exposed tip advanced into the ventral gray or white matter at the same spinal level.

b. Stimulating equipment - Isolated constant current square wave stimulation was delivered by a Haer 6i stimulator via a Grass PSIU6 constant current unit. The signal was led to the preparation by way of

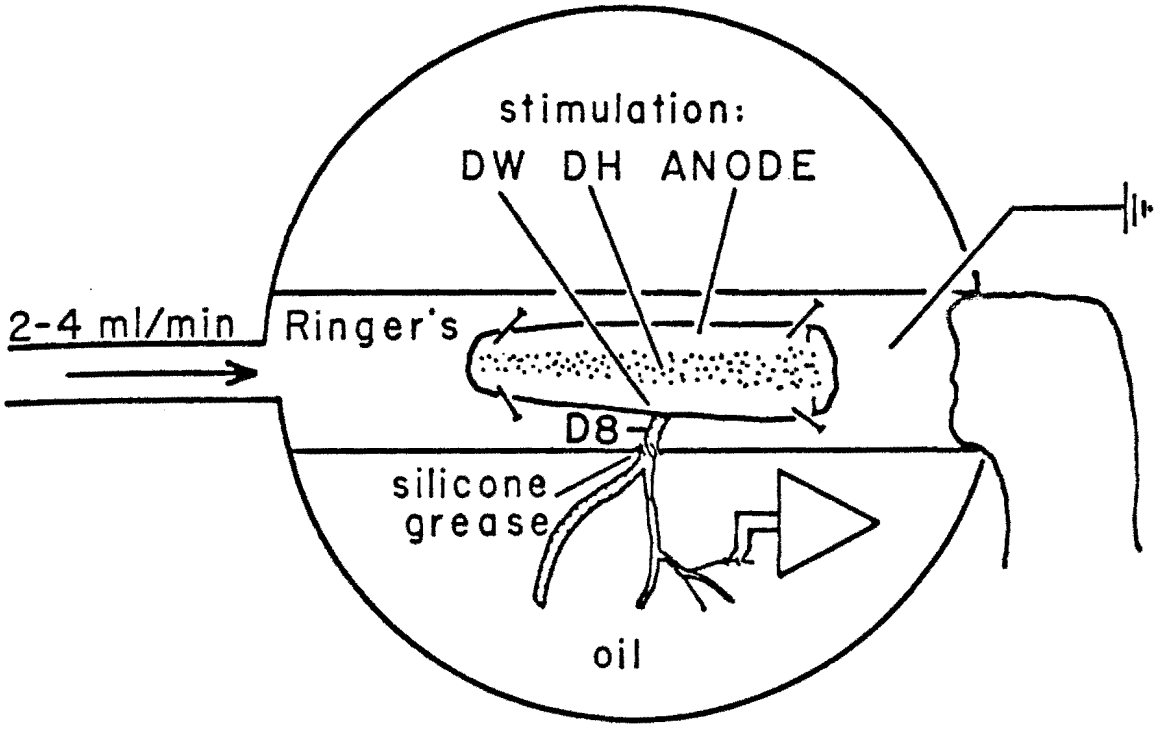

Figure 5. Diagram of frog hemicord in superfusion chamber, instrumented for measurement of chronaxie of single dorsal root fibers tested at two different stimulation sites.

a switch box (Fig. 6) which sent stimulating current through the DH or DW cathode, and a circuit (Fig. 7) which monitored stimulating current as the drop across a 2K ohm resistor in series with the anode.

The current monitoring circuit was developed because of the importance of accurately measuring stimulating current in the present studies. Initial attempts to monitor current followed the usual guidelines of measuring potential difference across a 100 ohm resistor using a differential oscilloscope. This procedure was inadequate because of the small potential developed by the low stimulating currents (as low as 1.0 μA). The square wave current signal appeared to be altered by this monitoring arrangement, and large artifacts developed in the dorsal root recording.

This current monitor incorporates high impedance unity gain operational amplifiers with shielded inputs, taking the output signals to a differential amplifier with a simple common mode rejection adjustment to reduce noise. A DC offset was incorporated to reduce any DC output to zero (for example, due to amplifier drift). The differential amplifier is set for 10X gain, therefore, the usual output signal ranged from 20 to 400 mV in these experiments (stimulating current 1.0-20.0 μA). Finally, a single-ended output line is provided via a BNC type connector for convenience in monitoring the circuit output.

c. Stimulation parameters - Rheobasic current in this setting was defined as the threshold for action potential generation using 500 μsec duration pulses. After the rheobase determination, current amplitude was increased to twice this value and the duration of the

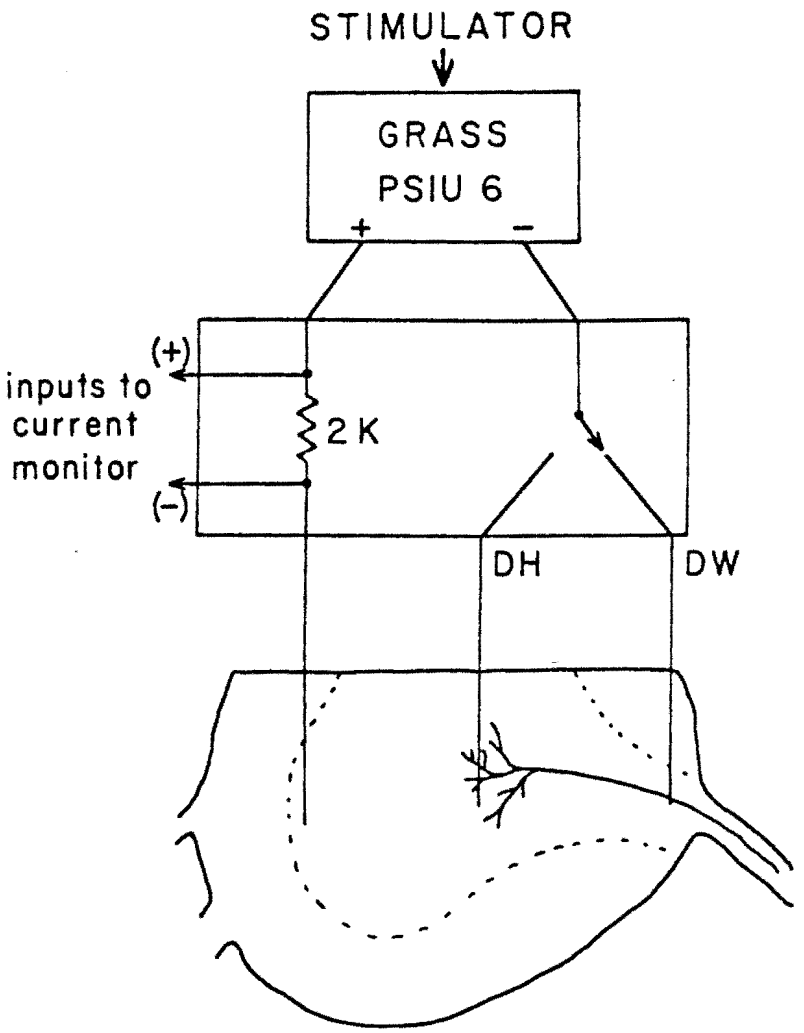

Figure 6. Schematic of hemicord preparation used in the chronaxie study. The stimulating current flows to the preparation via a switch box selecting between the two possible cathodes. The series resistor is located here as well with shielded leads to the current monitoring circuit (Fig. 7).

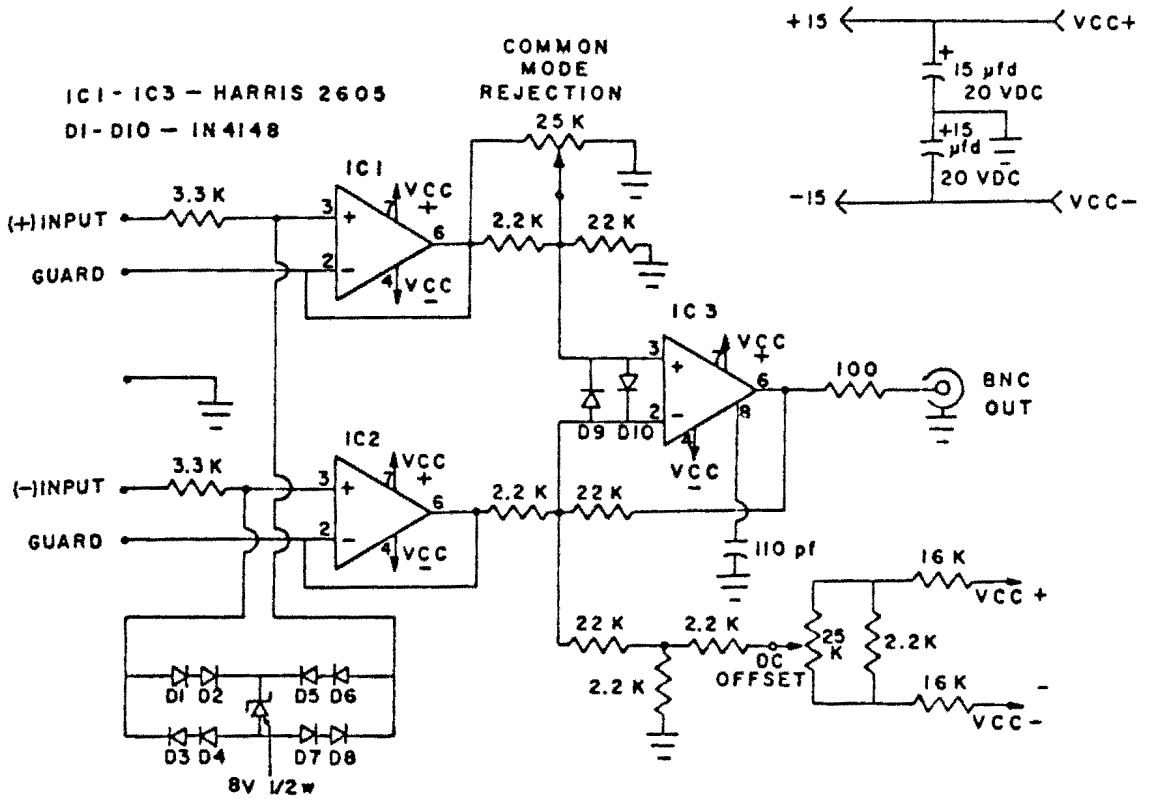

CURRENT MONITORING CIRCUIT

Figure 7. Circuit which receives two guarded inputs and differentially amplifies the signal. This circuit incorporates isolation from ground, common mode rejection, 10X gain, and a single-ended output.

current pulse was varied on the digital dial of the Haer stimulator. The pulse duration was varied by increments of 10 μsec, and chronaxie was recorded as the first duration which produced an action potential if duration was being increased, or the last duration before the action potential failed if duration was being decreased. In some experiments, over several trials, these numbers differed slightly. In these cases the average of the two was recorded as the chronaxie.

2. Recording procedures

Correct placement of the DH and DW stimulating electrodes was verified by a compound action potential response of the dorsal root in the mineral oil pool. The compound action potential was recorded by placing the root across a bipolar silver wire electrode led to the high impedance probe of a Grass P511 AC amplifier. Amplifier filtering was minimal, as stated in section B1a. The amplifier output was displayed on a Tektronix storage oscilloscope and photographed on Polaroid film.

The root was stripped down to progressively smaller bundles of fibers using fine-tipped forceps. After each division viability of the smaller bundles was determined by testing for a compound action potential response to DH or DW stimulation. As this process was continued, the bundles decreased in diameter, and the final divisions were made using insect pins etched to a fine point.

A fiber obtained in this manner was defined as a single unit if it met most of the following criteria: 1) The fiber had a clear threshold to fire an all-or-none action potential to dorsal root stimulation; 2) Increasing stimulating current to supramaximal did not

result in a change in action potential configuration; 3) The isolated fiber could be antidromically activated by stimulation from both DH and DW electrodes with no variation in action potential configuration; 4) The fiber had the ability to follow stimulation at high frequency; 5) The fiber had a rheobase < 20 uA.

3. Data analysis

Values of latency to onset, rheobase and chronaxie were measured during DH or DW stimulation. Results from fibers excited from only one stimulation site (DH or DW) were compared to results from fibers excited from both sites. A one-way analysis of variance showed no difference between the sets of data, therefore they were pooled. Differences between responses elicited at the two stimulation sites were compared using unpaired Student's t-tests.

D. Recovery of Excitability of Isolated Dorsal Roots or the Intraspinal Processes of Dorsal Roots.

The approach described below to evaluate recovery of excitability was implemented in numerous studies on axons (2, 3, 27, 62, 75, 162). A comparable technique has been applied to study dorsal root afferent terminals (36, 60, 192).

1. Recording procedures

The dorsal root compound action potential was recorded by placing the root across a bipolar silver wire electrode led to the high

impedance probe of a Grass P511 AC amplifier. Rise time constant was 0.01 ms, fall time constant was 600 ms. The root was crushed between the electrode poles to obtain a monophasic recording. The amplifier output was displayed on a Tektronix storage oscilloscope and photographed on Polaroid film.

2. Stimulation procedures

a. Dorsal root (DR) - The proximal portion of the excised dorsal root could be identified by the presence of adhering meninges, and by its color, which is paler than the rest of the root. After pinning the extreme proximal part of the root in place in the chamber, the uppermost surface was split slightly by grasping the top with fine forceps and pulling perpendicular to the long axis of the root. This facilitated insertion of two glass-insulated tungsten electrodes (exposed tip of cathode: 75-150 μm, impedance 20-100 K ohms at 1000 Hz; anode: 300 μm exposed tip) which were advanced into this split portion, oriented parallel to the fiber. The distal end of the root in the pool of mineral oil was placed over a silver bipolar recording electrode in a crushed-end mode (Fig. 4).

Two Grass S44 stimulators were used via two Grass PSIU6 constant current units, with one stimulator (Stim A) triggering the second (Stim B) to deliver its stimulus after a variable delay. Stim A delivered square wave pulses of 0.2 ms duration with current intensity set at a level which evoked a large A fiber response (approximately 1 ms to peak) (62) without evoking longer latency responses. The pulse delivered by Stim A is referred to as the conditioning stimulus (CS).

Stim B also delivered 0.2 ms pulses at a current intensity set to evoke a compound action potential (CAP) response of 15-25% the amplitude of the Stim A-evoked response (Fig. 8). The response to Stim B is referred to as the test response (TR). The test responses recorded were either unconditioned or conditioned by a prior CS at interstimulus intervals indicated below.

b. Dorsal horn (DH) - The dorsal horn stimulating electrode was placed in a manner which should have maximized the probability of stimulating the fine terminal branches of the dorsal root axons, rather than peripheral segments. This was accomplished in two ways. First, the cathode and anode were positioned with tips no less than 300 μm apart. This assembly was advanced into the cord about 300 μm with the cathode positioned to enter at the midpoint of the gray matter at the level of the dorsal root being recorded from (Fig. 9). The anode entered the cord at the ventral gray or straight into the ventral funiculus, at the same rostrocaudal level (Refer to DH electrode placement in Fig. 6). This orientation should have maximized the current flow through the ventral and central regions of the gray matter, and decreased spread through the dorsal horn. Maximum effective stimulation by extracellular bipolar electrodes occurs along lines parallel to the electrode orientation (163), so this configuration should preferentially stimulate axon processes staying at this segmental level and projecting towards the ventral horn.

At the conclusion of two experiments, lesions were made by passing a DC current for 10 or 15 seconds, and the tissue was pinned to a chip of Sylgard and fixed by immersion in 10% formaldehyde. The cords

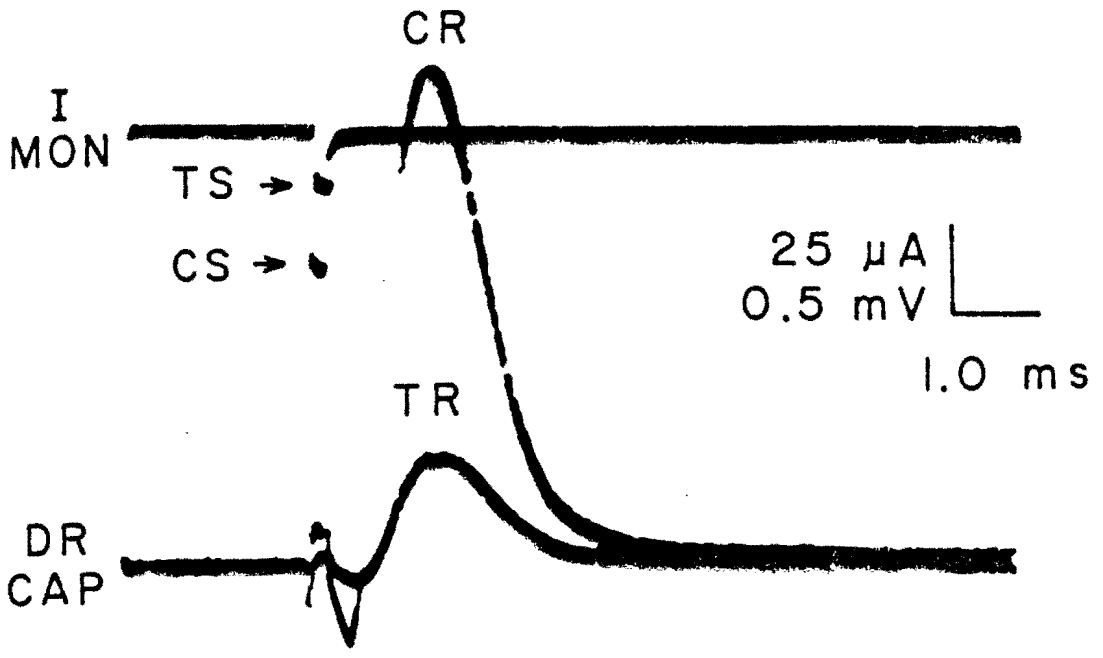

Figure 8. Representative dorsal root compound action potential (DR CAP) responses to conditioning (CS) and test (TS) stimulations of the dorsal root. Area of test response (TR) = 21% of conditioning response (CR) area. The top trace is the output of the current monitoring circuit (I MON).

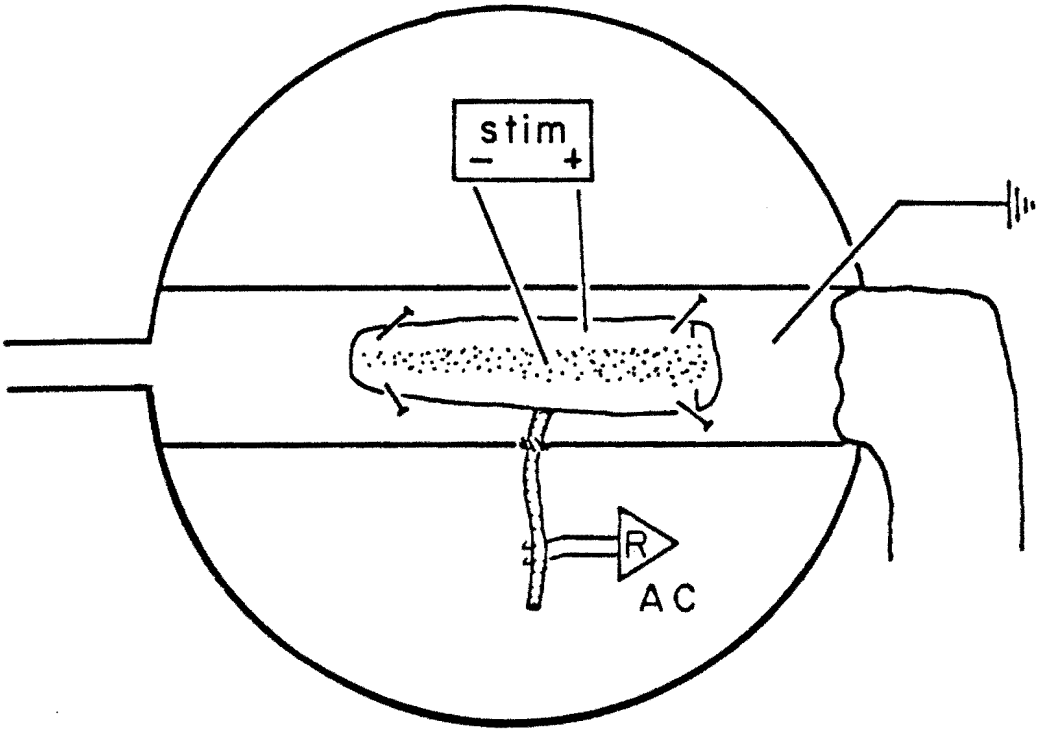

Figure 9. Diagram of frog hemicord in superfusion chamber, instrumented for experiments on recovery of excitability to dorsal horn stimulation as described in Methods section D - 3b.

were subsequently dehydrated, embedded in paraffin, cut in 10 μm serial cross-sections, and stained by the Klüver-Barrera method to aid verification of correct stimulating electrode placement (111).

The second method of optimizing electrode placement near the terminals was physiological. Several studies of nerve terminal excitability have indicated a prominent supernormal period of dorsal root afferent terminals. In my experiments preliminary placement of the electrode under visual inspection was followed by paired-pulse testing. Two stimulators were set up in the same manner as described above, with the stimulus duration set for 0.3 ms. Stim A was set to evoke a nearly maximal response. Stim B was set to evoke a response of 15-25% the amplitude of the conditioning response (Fig. 10). The interstimulus intervals were 10, 20 and 30 ms. Conditioned test responses were compared with the unconditioned test response by visual inspection of the oscilloscope trace of the CAPs. If the conditioned response did not appear to be larger, the stimulating electrode was moved and the new position tested. This protocol was most successful when there was a 5 - 10 minute delay between electrode insertion and paired-pulse testing.

The stimulus duration used depended on the tissue. DR stimulus duration was 0.2 ms, DH stimulus duration was 0.3 ms. These values were chosen based on results of the chronaxie study, to compensate for the longer chronaxie at the DH stimulation site (72).

3. Data analysis

Compound action potential area was measured using a Houston

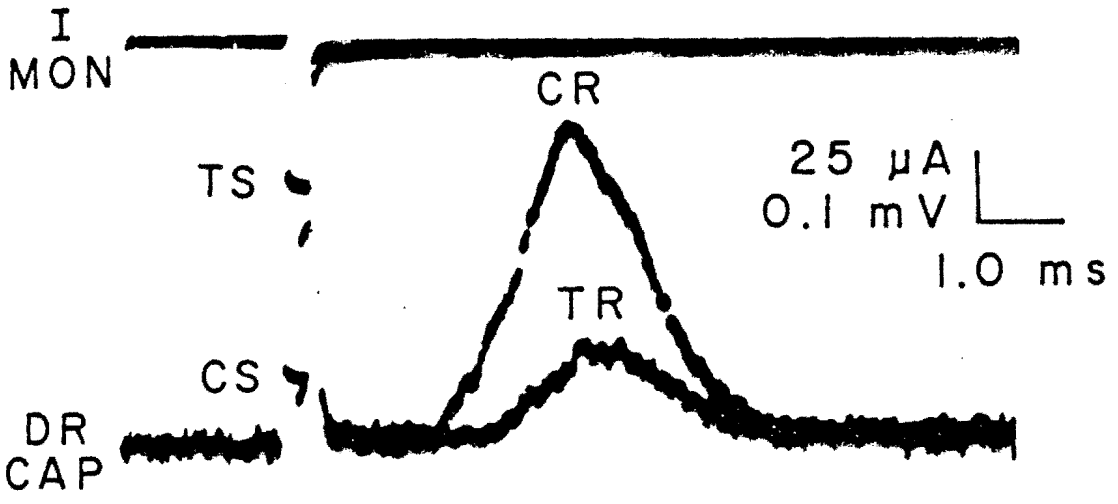

Figure 10. Representative dorsal root compound action potential (DR CAP) responses to conditioning (CS) and test (TS) stimulations of the dorsal horn. Area of test response (TR) = 26% of conditioning response (CR) area. The top trace is the output of the current monitoring circuit (I MON).

Instruments graphics tablet connected to an Apple II+ computer. A straightedge was held at the level of the isoelectric line for each trace, and the area of the first negative deviation from the line was measured by tracing around the outline of the curve and back along the straight baseline.

The results for recovery are expressed as percent of area of unconditioned test stimulus. The area of the CAP to an unconditioned test stimulus was measured two times during each experimental period, and the two values were averaged.

Statistical tests applied depended on the design of each study and will be discussed individually.

4. Alterations in early recovery period with TEA and 4-AP

a. Tissue preparation - This study used hemicords with dorsal horn stimulation and isolated roots to compare the sensitivity of terminals and axons, respectively, to potassium channel blocking agents. The early recovery process was monitored at interstimulus intervals of 3, 4, 5, 6, 7 and 8 ms. The area of the conditioned CAP is expressed as percent of area of the unconditioned test response.

b. Experimental protocol (Fig. 11) - After equilibration in the bath, the superfusion medium was changed to solution A. Control values for recovery were measured during the final 8 minutes of this 20 minute cadmium treatment period.

Protocol: The effect of K-channel blockers on relative refractory period to dorsal horn (DH) or dorsal root (DR) stimulation.

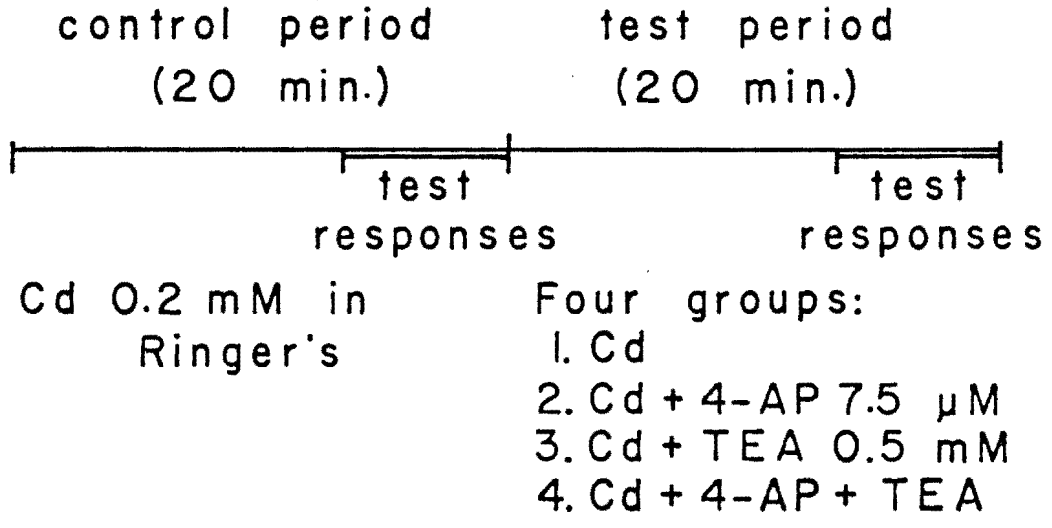

Figure 11. Experimental design used to study dorsal horn and dorsal root recovery of excitability during potassium channel block.

The superfusion solution was then changed to consist of one of the following:

Cd:	continue solution A
4-AP:	solution A + 4-AP 7.5 μM
TEA:	solution A + TEA 0.5 mM
TEA-4-AP:	solution A + TEA 0.5 mM + 4-AP 7.5 μM

Recovery measurements for the test period were made during the last 10 minutes of a 20 minute superfusion with one of these test solutions.

c. Data analysis - Linear regression analysis, plotting % recovery vs delay (interstimulus interval) was performed on the recovery data for each experimental period (Fig. 12). The analysis included only those time points where recovery was < 100%. The time to 50% recovery, or t_{50} is calculated from this analysis. For each experiment, Δt_{50} = test t_{50} - control t_{50}. A positive value is interpreted as an indication that recovery is prolonged by the drug, relative to the cadmium control.

The statistical test performed was a 2-way analysis of variance for factorial design, with two groups (DH and DR) subjected to one of four drug treatments (listed above). Post hoc analysis was performed using a Newman-Keuls test.

Figure 12. Data analysis procedures used in the potassium channel block study. Representative traces of unconditioned and conditioned compound action potentials to dorsal horn stimulation are shown with the analysis of these responses. Δt_{50} = +0.47 ms for this experiment.

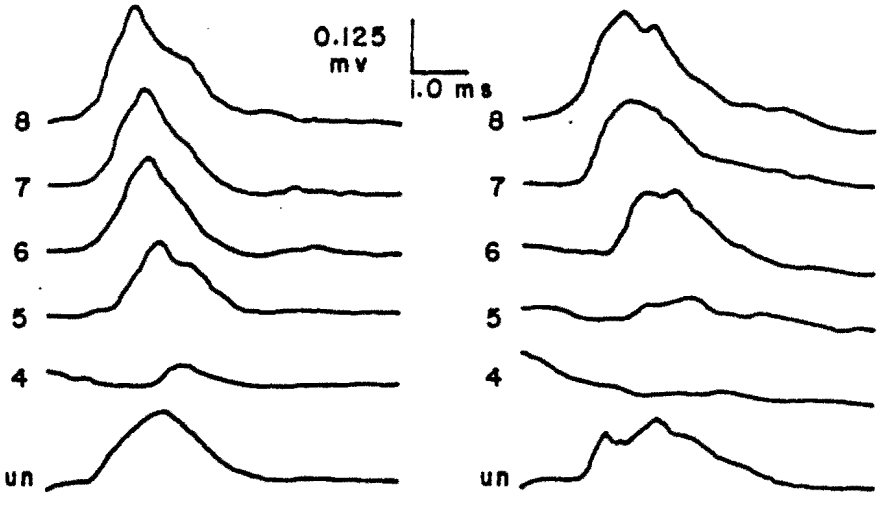

Data analysis:

- Measure area of unconditioned and conditioned responses
- Linear regression on points
- Calculate $\Delta t_{50} = t_{50(test)} - t_{50(control)}$

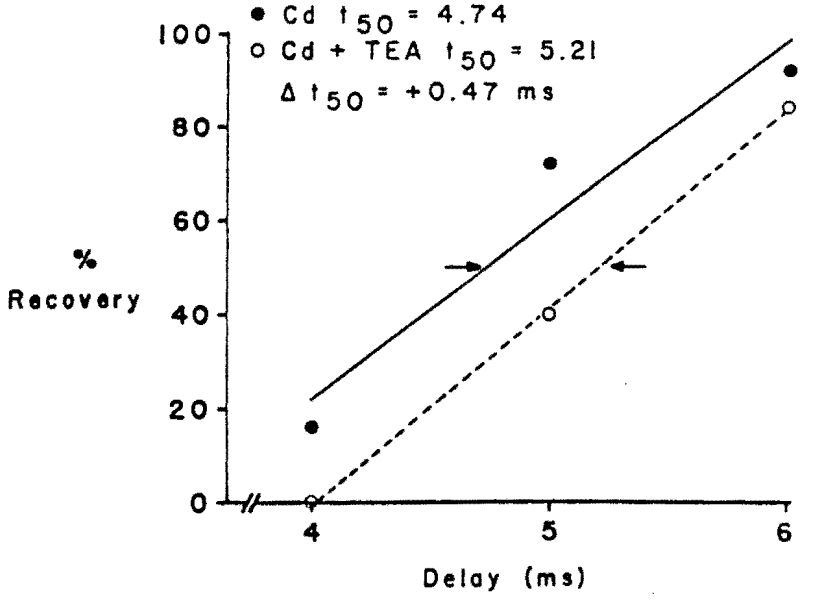

5. The effect of cadmium on early recovery to dorsal horn stimulation

The contribution of calcium activated potassium conductances to afferent terminal recovery of excitability was studied in 4 hemicord preparations. In these experiments the early recovery process to dorsal horn stimulation was measured at interstimulus intervals of 4, 4.5, 5, 5.5, 6, 6.5, 7, 8, 9 and 10 ms. A t_{50} value was calculated for the control period and for measurements made after 15 minutes of superfusion with solution B. Control and experimental t_{50} values were compared with a paired t-test. An additional group of 14 cords were included from the study of section D5. Interstimulus intervals used were 4, 5, 6, 7, and 8 ms. Recovery was tested in the control condition and during the final 5 minutes of the 20 minute superfusion with solution A. Control and test t_{50} values were compared with a paired t-test.

6. Supernormal period

This study addressed quantitatively the presence and magnitude of a supernormal period of dorsal root afferent terminals, via DH stimulation, and axons, in the isolated DRs. Persistence of supernormality after synaptic transmission was blocked by cadmium was also evaluated.

In the dorsal horn experiments included in this study, the conditioning stimulus was delivered peripherally, to the dorsal root in the mineral oil. This was done to be consistent with the methods Wall used in his study of primary afferent depolarization in cat spinal cord (192). Additionally, the supernormal period in some fiber systems is thought to be due to potassium accumulation (112). Delivering a large

conditioning pulse to the dorsal gray matter would evoke potassium release from a large population of interneurons in the dorsal horn, confounding the interpretation of a supernormal finding of the terminals alone.

Interstimulus intervals used in this study were 10, 20, 30, 40, 60, 80, 100, 150 ms. After the tissue (hemicord or isolated root) was placed in the superfusion chamber, positioned for recording, and the stimulating electrodes had been inserted, there was a pause of about 15 minutes for further stabilization. Then stimulation parameters were adjusted according to the guidelines above and data collection began. Stimulation rate was slow (0.06-0.08 Hz) to decrease cumulative effects. The unconditioned test response was recorded twice and the responses to stimulus pairs at delays listed above were each recorded once, randomly varying the order of presentation. When the first series was finished, superfusion with solution B began. The next series of stimulations was performed after 15 - 20 minutes of superfusion with the new solution, after which the experiment was terminated.

In these experiments both area and latency to onset of CAP responses to unconditioned and conditioned test stimuli were measured. Data from these experiments were analyzed for overall effects of conditioning. The area (% of unconditioned test response area) or change in latency (μs) was measured at each interstimulus interval. Then these values were averaged, giving a single number reflecting average supernormality for that tissue. The same process was repeated during solution B. The results from 10 experiments (5 on each tissue) were compared by two way analysis of variance with repeated measures.

The presence of a linear trend in the values over the 8 interstimulus intervals was evaluated with linear regression analysis for each set of recovery curves (195).

Chapter V

RESULTS

A. Synaptic Transmission

The experiments on synaptic transmission were performed to verify the efficacy of various agents reported to facilitate or suppress synaptic transmission. The purpose of these preliminary experiments was to develop appropriate solutions to be used in more direct studies of nerve terminal properties (sections C, D, and E). In each case frog cord synaptic transmission appeared to be altered by drug concentrations reported to affect transmission in other neuronal systems (17, 33, 41, 67, 98, 100, 101, 109, 117, 119, 123, 136, 164, 166).

The dorsal root response to stimulation of the homologous or an adjacent root (DRP), was elicited in three ways. Stimulation of an adjacent root is one way, shown in Fig. 13C. Stimulation of the dorsal gray matter in the region of afferent terminals evokes an antidromic compound action potential, followed by a prolonged depolarization. An example is shown in Fig. 23 (DH). Responses elicited at this site in later experiments (sections C, D, and E), were recorded on a much faster time scale with AC amplification to focus on the early antidromic spike activity. Stimulation was also given to the dorsal root which was recorded from (homologous root). This was accomplished by stimulation at the dorsal root entry zone (Figs. 19 and 20), or at the end of the

root, distal to the recording electrode (Fig. 23).

Facilitation of synaptic transmission by 4-AP and TEA was shown by increased amplitude and area of DR-VRR's. 4-AP also increased DR-DRP amplitude and spontaneous DRP's. Cadmium suppressed synaptic transmission in all pathways including the LC-VRR.

With the exception of 4-AP experiments, the drugs were only tested in one or a few preparations. The rationale for this is that the drugs have already been shown to be effective in other systems at concentrations used in this dissertation. The brief series of experiments discussed here were carried out to confirm drug effectiveness at altering transmission in the isolated frog cord. Statistical tests were not employed because of the small number of experiments in each group.

1. Four-aminopyridine

a. Alterations in DR-VRR and LC-VRR - The effectiveness of 4-AP to potentiate the DR-VRR and LC-VRR were compared. Traces from representative experiments are shown in Fig. 13. The form of the DR-VRR and LC-VRR control traces is consistent with the observations of other investigators (30, 42, 93). Comparing DR- to LC-evoked responses, there are differences in configuration, latency and amplitude (note differences in calibration). DR stimulation elicited a VRR with onset latency 9.7 ms, duration of the first spike was 7.5 ms, with amplitude 3.9 mV. The LC-VRR onset latency was 4.0 ms, duration was 4.0 ms, with

Figure 13. The effect of 4-AP on frog cord synaptic transmission. A & B Ventral root responses to supramaximal stimulation of the dorsal root (A) or lateral column (B). Representative traces are shown before, during, and after 30 minutes superfusion with 4-AP 10 μM. C. The response of DR 8 to supramaximal stimulation of DR 9 was recorded after DC amplification. In the panel on the right, the same response is shown after 27 minutes superfusion with 4-AP 5 μM.

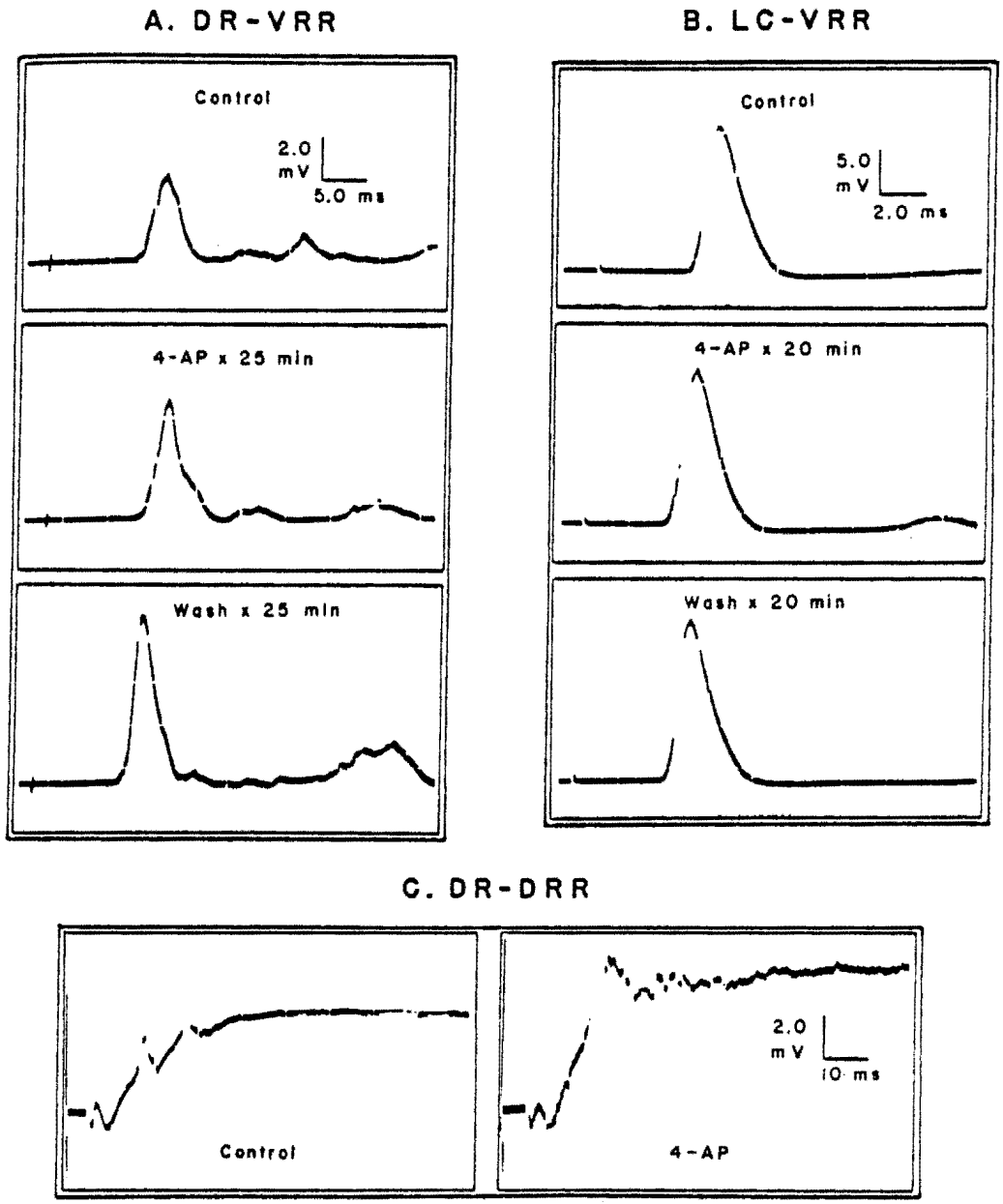
A. DR-VRR
Control
2.0 mV
5.0 ms
4-AP x 25 min
Wash x 25 min
B. LC-VRR
Control
5.0 mV
2.0 ms
4-AP x 20 min
Wash x 20 min
C. DR-DRR
Control
2.0 mV
10 ms
4-AP

amplitude 16.6 mV. During exposure to 4-AP 10.0 μM, DR-VRR amplitude is 36% greater than control and LC-VRR amplitude is 4% greater. Synaptic potentiation by 4-AP was not a reversible effect, in fact, the change in both reflex responses was increased during drug washout. DR-VRR amplitude increased 95% and LC-VRR amplitude increased by 11%. In another experiment, longer exposure to 10.0 μM 4-AP caused depression of the DR-VRR after an initial facilitation at 30 minutes (Fig. 14). In some experiments onset latency of synaptic activity was decreased by 4-AP. This can be seen in Fig. 14, comparing the control DR-VRR (onset latency 12 ms) to the DR-VRR after 30 minutes of 4-AP (onset latency 7 ms).

In Fig. 15 the effects of 4-AP on DR- and LC-evoked VRRs are summarized. These effects depended on drug concentration and length of exposure. The responses of 5 experiments (4 experiments with 4-AP 5.0 μM for 50 minutes and 1 experiment with 4-AP 10.0 μM for 30 minutes) were averaged because of the similarities of the responses. Three time- and stimulation- matched controls were included. The ventral root response area to supramaximal dorsal root or lateral column stimulation was measured and normalized to the response area averaged over a thirty minute control period preceding the test period. Of all groups, the DR-VRR was most affected by 4-AP treatment.

b. Dorsal root potential - effects of 4-AP - In Fig. 13C the response of DR 8 to stimulation of DR 9 is shown. The prolonged depolarization (DR-DRP) with early spike activity (the DR-DR reflex: due to rapid depolarization bringing fibers to action potential threshold)

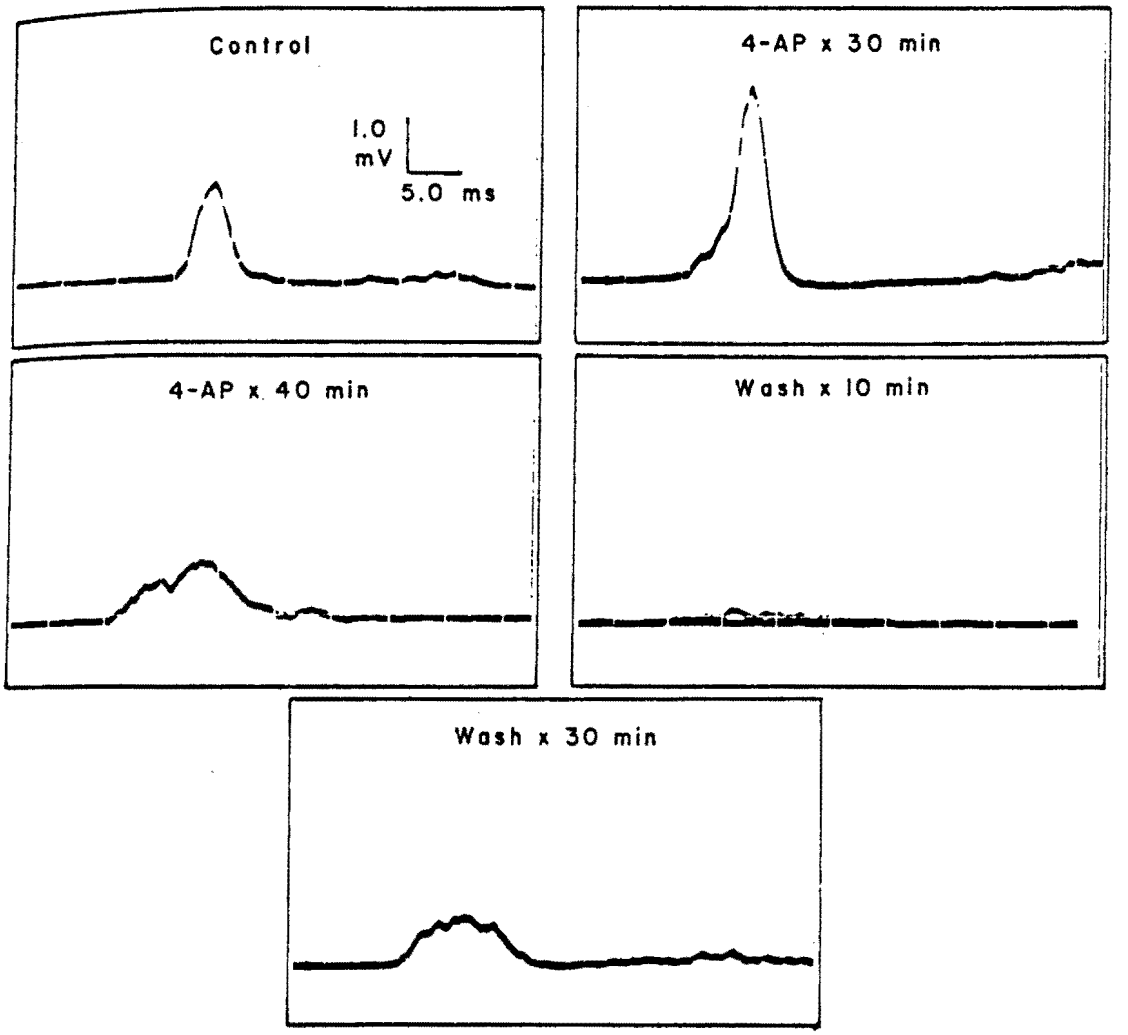

Figure 14. The effect of prolonged 4-AP exposure. The DR-VRR was monitored before, during and after superfusion with 4-AP 10 μM. After 30 minutes with 4-AP, response area and amplitude were increased, at 40 minutes the response appeared decreased. At this time 4-AP was discontinued but depression of transmission continued during the wash. Thirty minutes of washout could only partially restore the response.

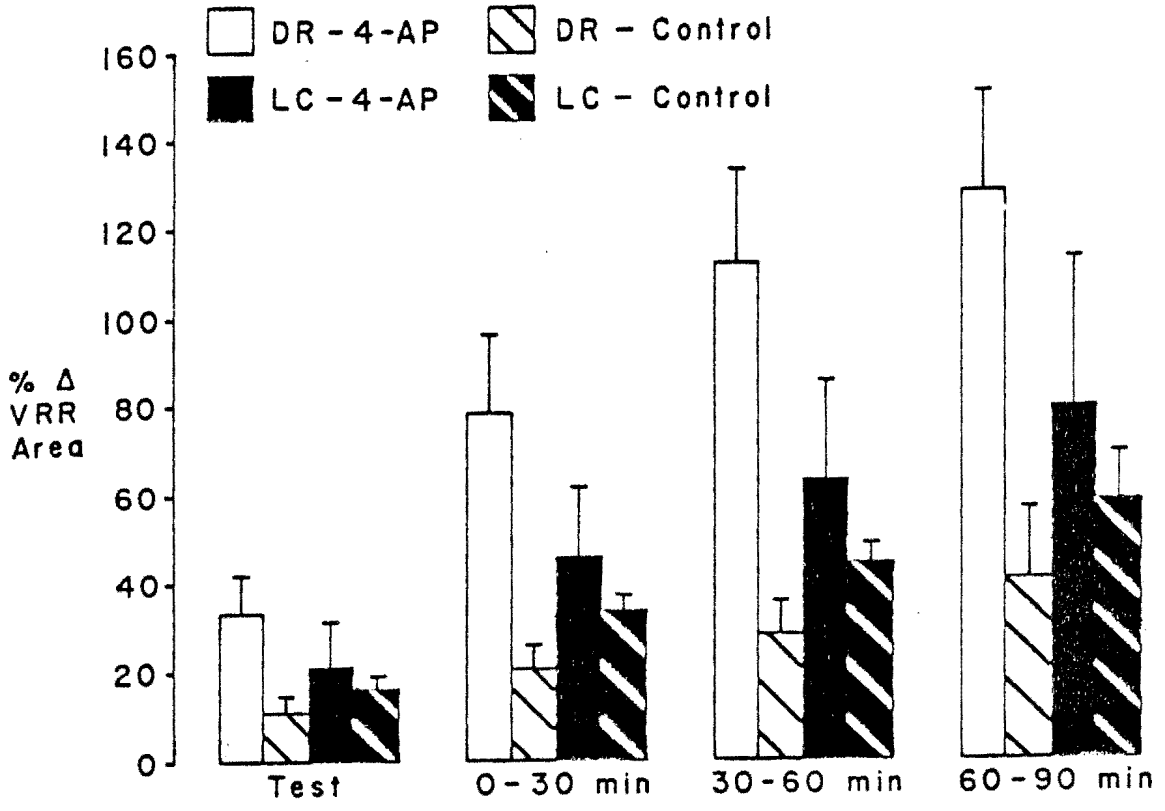

Figure 15. Summary of 4-AP experiments. Bars show mean ± SEM of ventral root response area normalized to values at control. The data were drawn from 5 experiments using 4-AP (5 μM - n=4; 10 μM - n=1) or time- and stimulation-matched controls (n=3). The test period refers to the time of 4-AP superfusion. The responses were also followed for three successive periods of washout.

is consistent with other observations of this response in isolated frog cord (61, 188). At 27 minutes of superfusion with 4-AP 5.0 μM the spike corresponding to the DR-DRR appears to have increased duration. In the 4-AP trace PAD peak amplitude was 38% greater than control.

In experiments measuring the DRP with continuous DC recording, 4-AP caused spontaneous DR spikes resembling the reflex DR-DRP in amplitude and duration. Figure 16, panels A and B show fast traces of spontaneous activity recorded from a dorsal root and associated ventral root activity of a frog spinal cord exposed to 4-AP 5.0 μM for 50 minutes. On a slower time scale, panel C shows a continuous recording from a different experiment where 4-AP superfusion lasted 17 minutes. The arrows indicate delivery of direct stimulation to the DR being recorded from to elicit a DR-DRP. The amplitudes of the spontaneous DRPs were initially much smaller than evoked DR-DRPs. Spontaneous DRP amplitude increased during 4-AP washout.

In 9 out of 12 experiments using various doses of 4-AP (5.0 μM x 30 min or 10.0 μM x 15-20 min or 7.5 μM x 17 min) spontaneous activity was induced. In 3 experiments at the lowest dose (5.0 μM), no spontaneous activity was induced. In the remaining experiments, however, time to onset and peak frequency did not appear to be dose related (Table IV). The activity persisted during washout periods lasting up to 2 hours.

c. Summary of 4-AP experiments - 4-AP in doses of 5.0-10.0 μM increased the area of DR-VRR and DR-DRP greatly, and to a lesser extent the LC-VRR area. It induced spontaneous dorsal root activity, an action which has been shown to depend on enhanced synaptic transmission (165, 182). Prolonged exposure had a deleterious effect on transmission. The

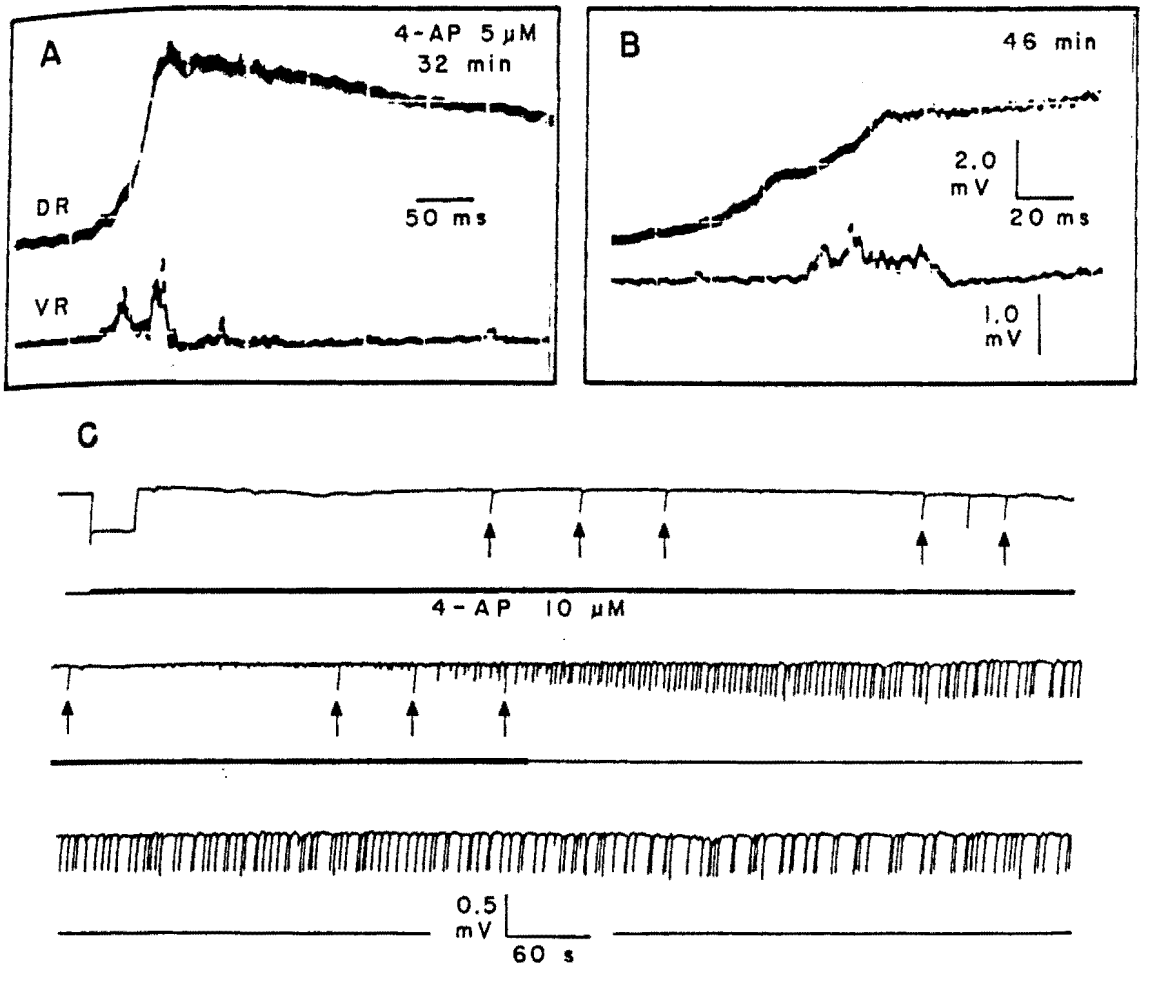

Figure 16. Spontaneous activity during 4-AP treatment. A and B- Spontaneous dorsal root and ventral root activity recorded during 4-AP 10 µM. The onset of DR activity is slower than an evoked DR-DRP but the amplitude is similar (compare to fig. 1C). C. Continuous trace from a different 4-AP experiment. Arrows indicate DR-DRPs induced by direct stimulation to the root used for recording. Spontaneous activity is initially smaller than evoked spikes but increases in frequency and amplitude during washout.

TABLE IV

Summary - 4-AP induced spontaneous activity

Experiment	Dose (μM)	Onset (min)	Peak frequency (spikes/min)
7/16	5	16	15
7/21	5	13	12
8/21	5	12	41
9/15	7.5	16	2
9/18	10	13	19
10/6	10	17	9
10/8	10	14	15
10/19	10	18	18
10/20	10	16	12
mean		14.9	15.9
S.E.M.		0.6	3.6

work of Dubois on potassium channels of peripheral axons would predict effects at this locus at higher doses (K_d= 20 μM)(53). For these reasons, an intermediate dose of 7.5 μM was chosen for the study of nerve terminal refractory period (section C).

2. Tetraethylammonium

In the experiments evaluating 4-AP's effectiveness at enhancing synaptic transmission, the effect on the DR-VRR was more pronounced than the effect on the LC-VRR. This could be related to the relative weakness of this synaptic pathway relative to the LC-VRR (30, 63). Therefore, the effectiveness of TEA to enhance synaptic transmission was only tested on the DR-VRR. Since TEA 0.5 mM has already been shown to enhance synaptic transmission, only one experiment was performed to confirm TEA's effect on frog cord synaptic transmission (117, 119, 166).

The effect of TEA 0.5 mM on the DR-VRR was assessed (Fig. 17). The VRR to submaximal and supramaximal stimulation (6V) during the control period is shown in panel A. The onset latency of the latter response is 14.4 ms. The evoked response appears poorly synchronized and broad, with a duration of 12.2 ms. After 5 minutes of TEA superfusion (panel B), the response to 6V stimulation appears more synchronous (duration is 10.6 ms) and onset latency has decreased to 11.7 ms. After 9 minutes of TEA treatment (panel C), the response is large and synchronous, onset latency is 10.0 ms and duration is 7.8 ms. The change in amplitude was so great that the oscilloscope preamplifier gain was decreased fourfold (see calibration). The response area to supramaximal stimulation (6 V) was 280% of control.

Figure 17. The effect of TEA on frog cord synaptic transmission. A. The DR-VRR to two different stimulation intensities was tested. Stimulation with 6V was supramaximal, so testing continued using this intensity. B. Five minutes after addition of TEA 0.5 mM to the superfusate, the DR-VRR increased rapidly in amplitude. C. At 9 minutes, the response is greatly increased from control (sensitivity is 25% that of panels A, B, and D). At this time less stimulating voltage was required to produce a maximal response. D. After the traces of panel C were recorded the superfusate was changed to a solution containing TEA 0.5 mM and $CdSO_4$ 0.2 mM. The DR-VRR progressively decreased in amplitude and was completely blocked at 15 minutes. At 16 minutes paired-pulses were delivered but this was ineffective at restoring a response.

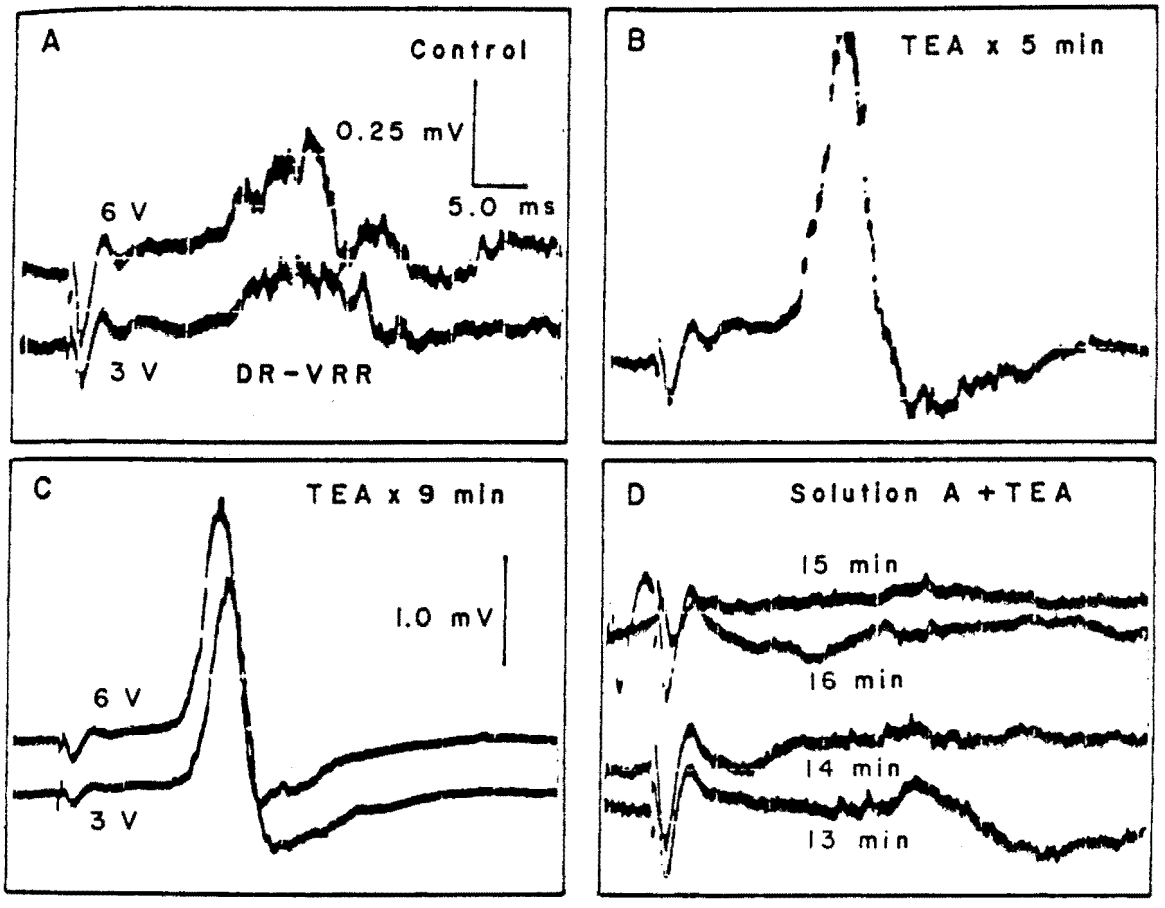
A
Control
0.25 mV
5.0 ms
6 V
3 V
DR-VRR
B
TEA x 5 min
C
TEA x 9 min
1.0 mV
6 V
3 V
D
Solution A + TEA
15 min
16 min
14 min
13 min

This result was taken as confirmation that TEA 0.5 mM could enhance transmission in frog spinal cord as had been shown at many peripheral synapses. The dose of TEA (0.5 mM) was chosen for the study of nerve terminal refractory period (section C).

3. Cadmium

Several experiments evaluated the effectiveness of cadmium to suppress synaptic transmission. The major aim of this dissertation was to study intrinsic properties of nerve terminals within the frog spinal cord. However, these terminals receive synaptic inputs such as those responsible for the DR-DRP (section A2) and VR-DRP. Spinal afferent terminals are, therefore, subject to extrinsic influences when synaptic transmission is not suppressed. Previous studies of afferent terminals in cat spinal cord, in vivo, focused on these extrinsic influences because they could not be eliminated in the intact animal. The in vitro preparation made it possible to focus on intrinsic properties by suppressing release of transmitters which affect afferent terminals. In addition, the effect of suppressing calcium entry into terminals on the early recovery process was also studied (section D).

a. $CdSO_4$ 0.1 mM - Three experiments were done using this concentration of cadmium in standard solution. This dose was effective at suppressing transmission but did not completely block stimulus-evoked responses. A representative experiment is shown in Fig. 18. Again, the striking differences between the LC-VRR and DR-VRRs should be noted. The calibrations for these traces are indicated separately. The DR-VRR was rapidly and completely blocked at this concentration in all three

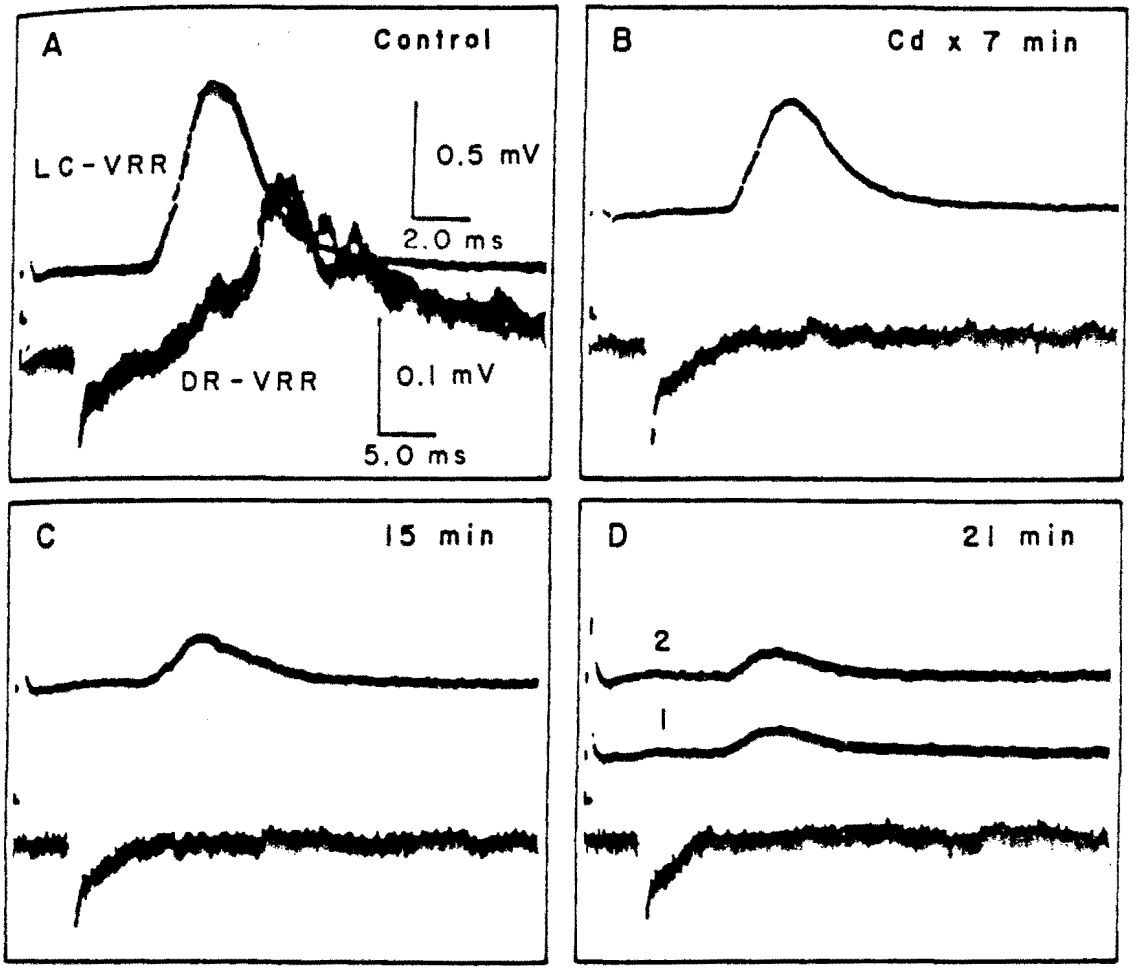

Figure 18. The effect of Cd 0.1 mM on frog cord synaptic transmission. A. Control traces of DR-VRR, LC-VRR have different amplitude and time calibration. B. The DR-VRR was completely blocked after 7 minutes of Cd superfusion. C. The LC-VRR is still not blocked. D. The LC-VRR was decreased but was not abolished after 21 minutes in this solution. In panel D trace 2 was made using a longer stimulus duration but this was no more effective than the stimulus delivered in trace 1.

experiments. The LC-VRR was reduced in two experiments and completely blocked in the third.

b. Solution A - As discussed in section 3a, Cd^{++} 0.1 mM was able to greatly reduce transmission, and in one case, completely blocked the LC-VRR. Doubling this concentration resulted in solution A. This solution blocked the DR-VRR after it was greatly potentiated by TEA (Fig. 17D). Solution A also prevented development of spontaneous DRP's when superfused with TEA and 4-AP (Fig. 19). Figure 20 shows faster traces photographed from the oscilloscope during the experiment shown in Fig. 19. Stimulation at the dorsal root entry zone of DR 8 resulted in the typical DR-DRP recorded from DR 8 in the control period (Fig.20 A). Superfusion of solution A with TEA 1.0 mM and 4-AP 5.0 μM depolarized the root, as seen in the continuous traces of Fig. 19. This is indicated on the oscilloscope trace of Fig. 20B by the decreased distance between the current monitoring trace (upper line) and the DR potential baseline, the very short segment before the onset of stimulus-induced activity. Repolarization of the DRP appears prolonged in panel B. This also corresponds to the widening of the second, third and fourth responses during the treatment period shown in the continuous record, Fig. 19. The three successive sweeps of Fig. 20C demonstrate the progressive block of the DR-DRP which was almost complete by 8 minutes, the lowest trace. Comparison of panel D with the lowest trace of panel C shows no apparent change between 8 minutes and 15 minutes in this solution.

Solution A was effective at blocking the LC-VRR in 13 minutes. In the experiment shown in Fig. 21, solution A was superfused for 18 minutes, followed by 15 minutes of solution A with TEA 0.5 mM and

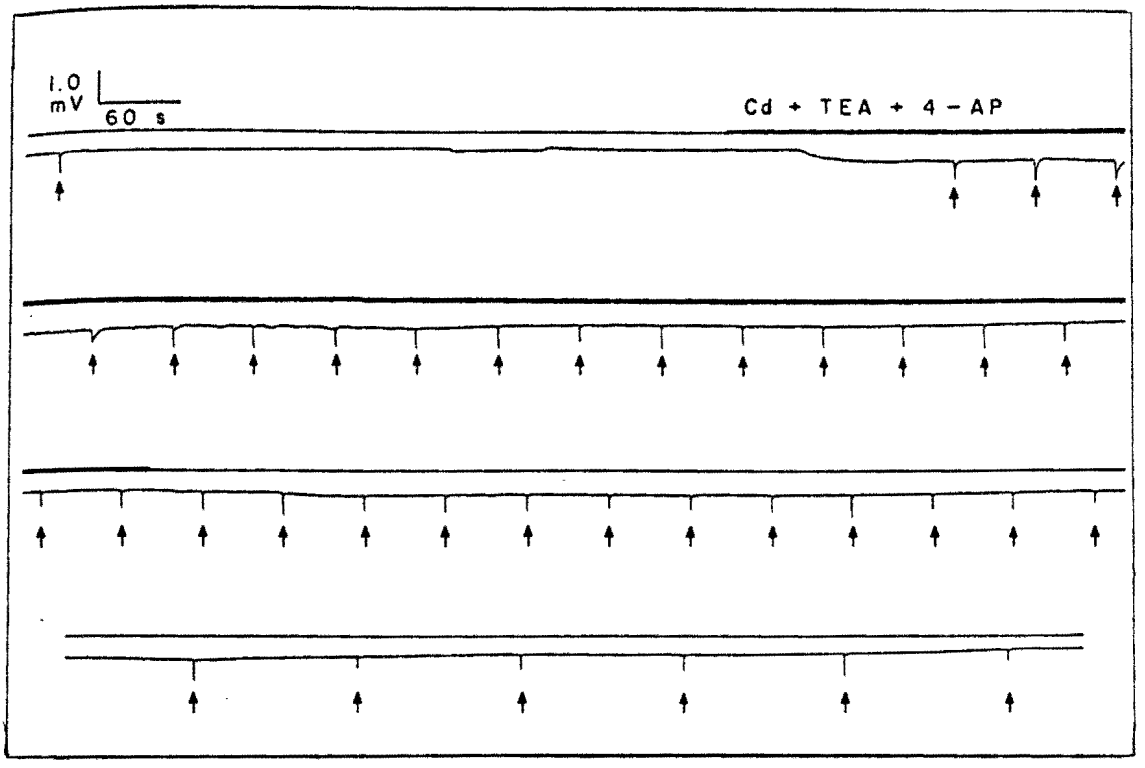

Figure 19. Solution A superfused with K-channel blocking agents suppresses spontaneous activity. Continuous record of DR potential. The response to DR entry zone stimulation was tested every 60 seconds initially, then every 120 seconds (arrows). The evoked responses are shown on a faster time scale in Fig. 20. A test solution which included $CdSO_4$ 0.2 mM, TEA 1.0 mM, and 4-AP 5 μM was superfused for 20 minutes (bold line). The first change observed was depolarization and broadening of the evoked response. The potential slowly returned towards the control value and the response to DH stimulation narrowed. No spontaneous DR spiking activity was observed.

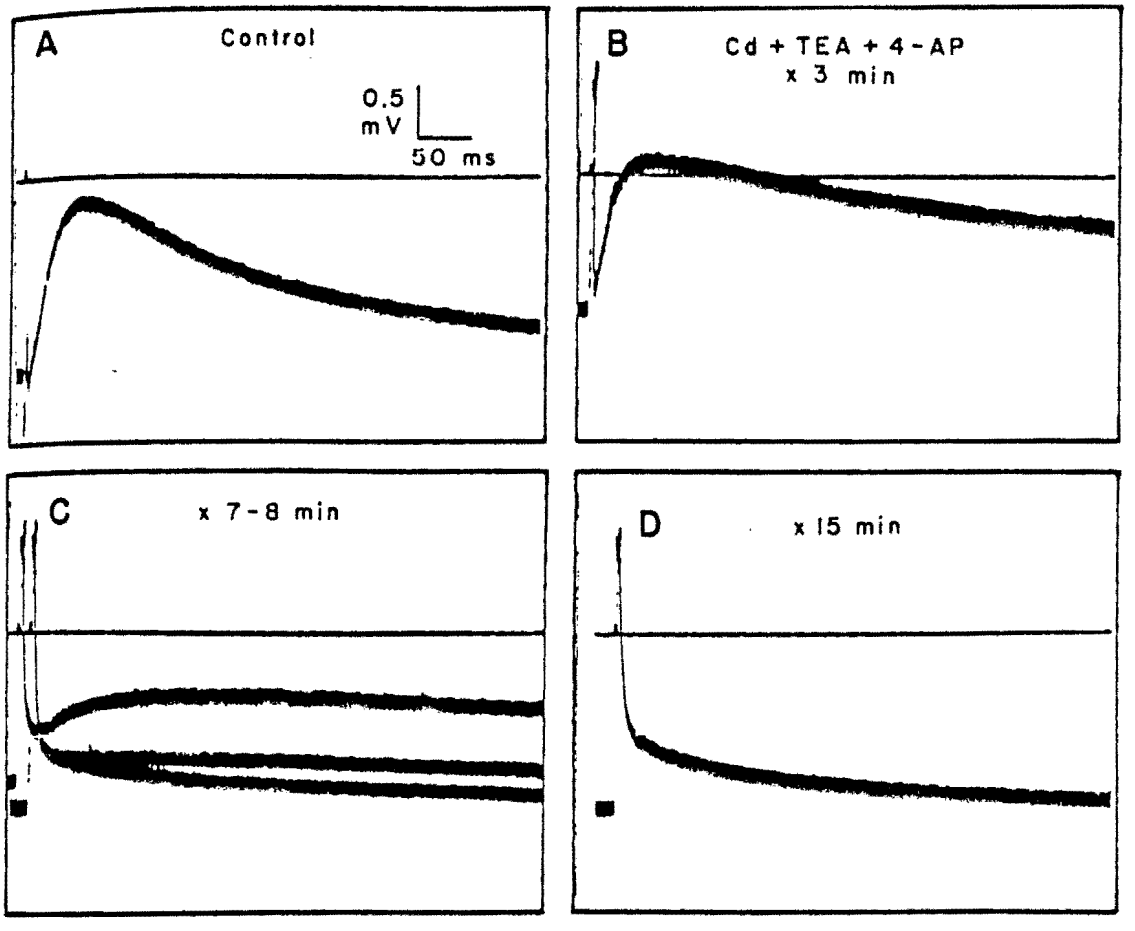

Figure 20. DRPs evoked in DR 8 by stimulation at the DR 8 entry zone. A. Control trace. B. DRP after 3 minutes in Cd 0.2 mM, TEA 1.0 mM, 4-AP 5 μM. C. Top to bottom - three successive DRPs tested at 30 second intervals during minutes 7 and 8 of the treatment period. The DRP is progressively blocked. D. After 15 minutes the usual DRP appears blocked although stimulation is still followed by a prolonged depolarization.

Figure 21. The effect of solution A on the LC-VRR. The VR response to supramaximal stimulation of the lateral column was measured in this experiment. A. Control response B. Superfusion of solution A for 18 minutes blocked the LC-VRR. Addition of TEA 0.5 mM and 4-AP 7.5 μM for 15 minutes did not restore the response to single (1) or paired (2) pulses. C. The viability of the motoneuron pool was confirmed by this response to direct stimulation of the ventral horn.

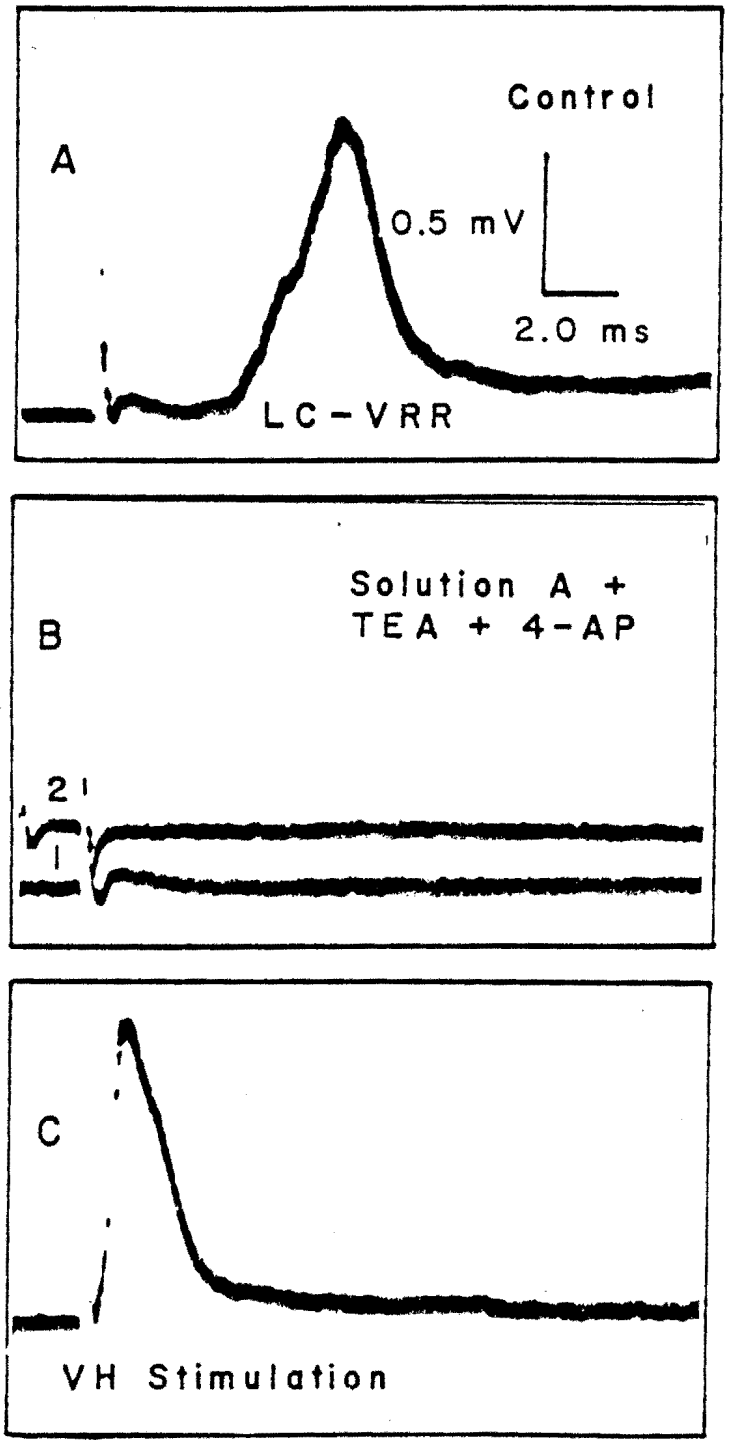
A
Control
0.5 mV
2.0 ms
1
LC-VRR
B
Solution A +
TEA + 4-AP
2
1
C
VH Stimulation

4-AP 7.5 μM. Stimulation with paired pulses did not facilitate a response (panel B, trace 2). Addition of the potassium channel blocking agents did not restore the LC-VRR response (panel B). This reproduces the protocol used to study early recovery of nerve terminals (section C). The ability of the alpha-motoneurons to respond was confirmed by direct ventral horn stimulation (panel C). This stimulation directly depolarizes the motoneurons to threshold, evoking a short-latency ventral root compound action potential. To summarize, this solution blocked the most robust frog cord synaptic pathway in the presence of strong synaptic potentiating agents. Solution A was used in all of the experiments of section C to suppress presynaptic calcium entry and transmitter release.

c. Solution B - Cd^{++} 0.1 mM was effective at blocking synaptic transmission when the Ringer's solution contained Ca^{++} 0.5 mM and Mg^{++} 2.5 mM. In two experiments this combination, solution B, effectively blocked the LC-VRR. In Fig. 22 traces from one of these experiments are shown. Five minutes of solution B superfusion greatly reduced the LC-VRR (note 10x greater gain indicated by calibration in panel B). After ten minutes the block was complete even when stimulus duration was increased (panel C, sweep 1). This block was not reversed by TEA 0.6 mM (panel D).

Solution B also blocked the characteristic DR response to direct stimulation of the dorsal horn or the homologous dorsal root delivered in the same manner as the protocols of sections D and E (Fig. 23). DH stimulation evoked a direct antidromic compound action potential, not distinctly visible on this time scale and amplification. This is

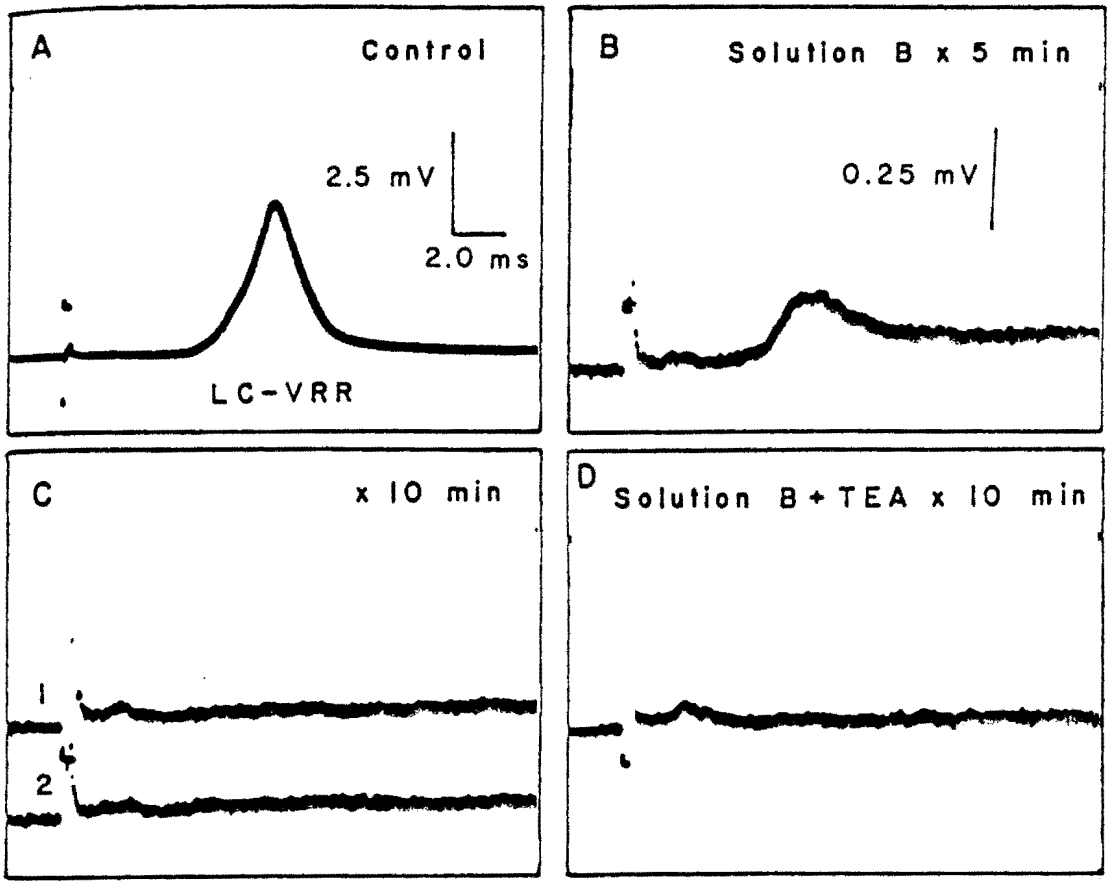

Figure 22. The effect of solution B on frog cord synaptic transmission. A. Control trace. B. Five minutes after beginning solution B the LC-VRR was greatly decreased. C. The response was blocked to the original supramaximal stimulus (trace 2) and to a stimulating pulse of equal amplitude but 40% greater duration (trace 1). D. Addition of TEA 0.6 mM to solution B did not restore the response. Vertical calibration in B also applies to C and D.

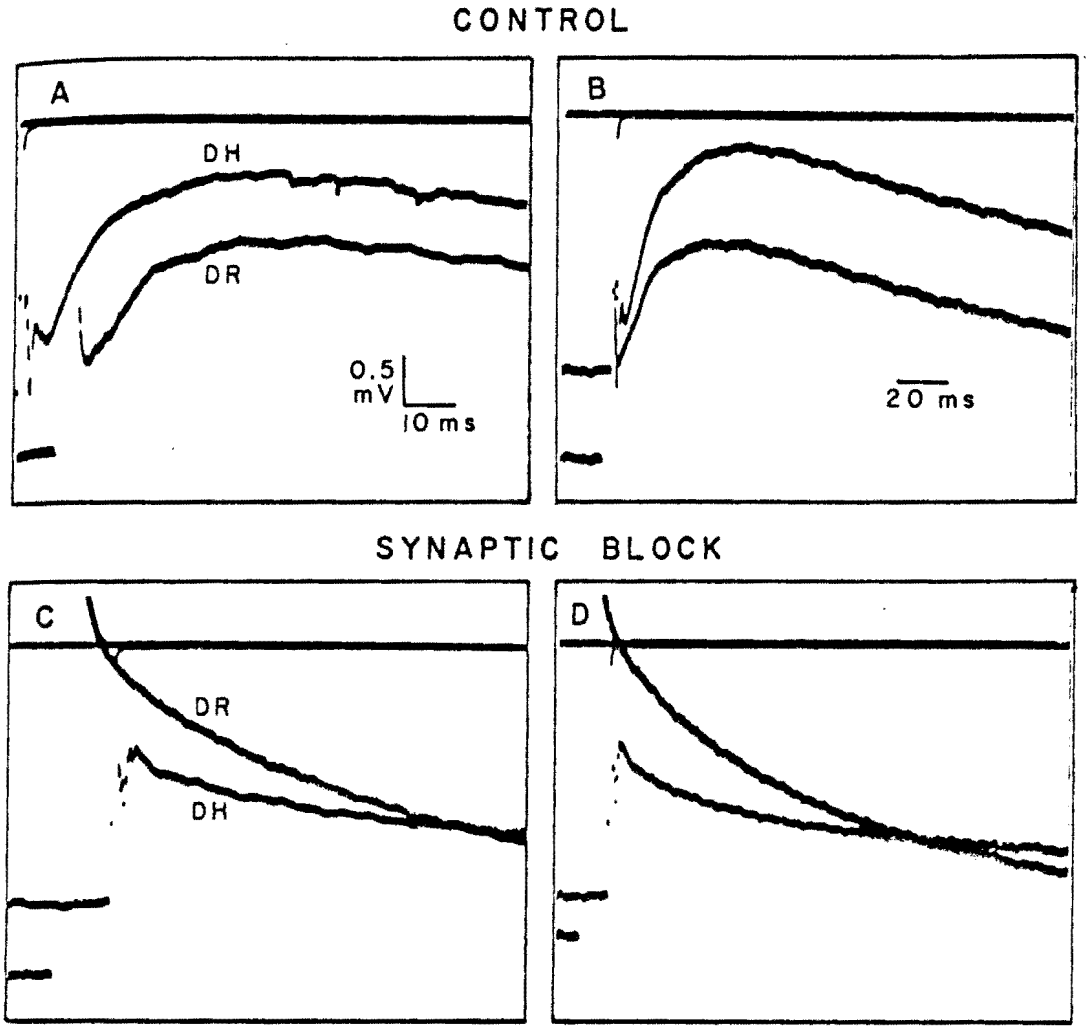

Figure 23. The effect of solution B on the DR-DRP. Traces show responses of DR 8, after DC amplification, to stimulation of the dorsal horn (DH) and DR 8 (DR). Time calibrations are the same for A and C, and for B and D. Panels C and D show responses after 20-22 minutes of superfusion with solution B.

followed by the usual form of the DR-DRP. DR stimulation evokes an orthodromic action potential. This is also not seen in these traces. It is followed by a DR-DRP. Solution B blocked the usual form of the evoked DR-DRP, seen in panels A and B at two different time scales. During solution B, however, stimulation resulted in a very large depolarization particularly when this stimulation was delivered to the whole dorsal root (panels C and D). The depolarization in panels C and D reflects prolonged recovery after the antidromically or orthodromically evoked compound action potential (DH or DR, respectively). This is similar to the effect of solution A as seen in Fig. 20. Solution B was used in some of the experiments of section D and all of the experiments of section E to suppress presynaptic calcium entry and transmitter release.

B. Single Fiber Responses to Extracellular Stimulation of Axon and Terminal Regions

The primary aim of these experiments was to compare values of chronaxie, rheobase, and onset latency of single fiber responses to stimulation of main afferent axons in the dorsal white matter (DW) and terminal regions in the dorsal horn (DH). The onset latency values obtained in these experiments were used to calculate approximate conduction velocity of the axons in these regions. Chronaxie was compared as an index of characteristic membrane differences between these two regions.

Oscilloscope traces from several experiments are shown in

Fig. 24. The upper trace in each panel is the output of the current monitoring circuit. The lower trace shows unit activity. Panel A illustrates the method used to estimate chronaxie. Rheobase determinations were made at a stimulus duration of 500 μs, shown here as the square wave labeled R of the upper trace. The rheobase of the unit shown in panel A was 8 μA. Preamplifier sensitivity for the upper trace was then halved and stimulus intensity was set to achieve the same height of the current monitor trace. The amplitude of the square wave marked C reflects the current intensity of 16 μA. After this level was achieved, duration was varied as described in the methods section to determine the chronaxie (170 μs in the experiment shown here).

Panels B, C and D (Fig. 24) show traces from three separate experiments in which single dorsal root fibers were successfully activated from both stimulation sites. These traces demonstrate the criterion that the action potential of a single fiber should have the same configuration regardless of stimulation site. In each case the onset latency is shorter to stimulation by the DW cathode than to the DH cathode, as indicated by the labels. The unit of panel B responded to DH stimulation 2.9 ms later than to DW stimulation. In panel C the latency difference is 1.5 ms, in panel D this difference is 1.3 ms.

In Fig. 25 current-duration curves for DH and DW stimulation of two different fibers are depicted. At all durations < 500 μs, greater current strength (relative to the rheobase) was required to bring the fiber to threshold when stimulating from the DH than the DW. The chronaxies indicated were 90 and 160 μs for DW and DH, respectively.

Figure 24. Representative traces from single fiber experiments. In each panel the upper trace shows the output of the stimulus current-monitoring circuit, the lower traces show unit activity. A. Chronaxie was measured as illustrated here. Rheobase current was defined as threshold current at 500 μs duration (R). Preamplifier sensitivity was then decreased by half, and current amplitude adjusted visually to the same height as the rheobase trace (C). Maintaining this current intensity, duration was varied until threshold duration was found, as described in the text. B, C, D Single fibers in which action potentials could be evoked at both DH and DW stimulation sites. In each case the later of the responses was elicited from the DH cathode, as shown here. In A, C and D the all-or-none character of these responses can be seen.

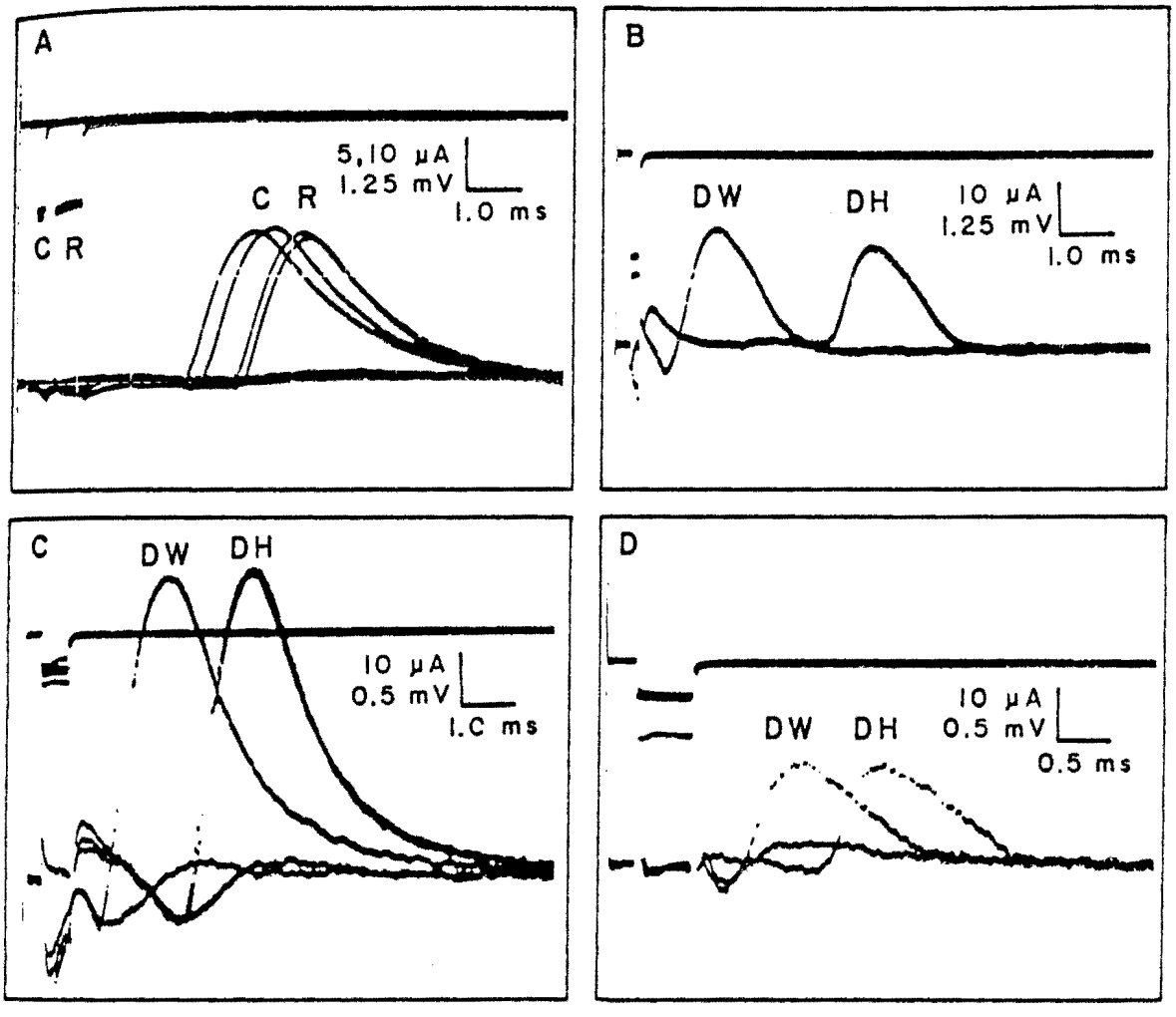
A
5,10 µA
1.25 mV
1.0 ms
C R
C R
B
DW
DH
10 µA
1.25 mV
1.0 ms
C
DW
DH
10 µA
0.5 mV
1.C ms
D
10 µA
0.5 mV
0.5 ms
DW
DH

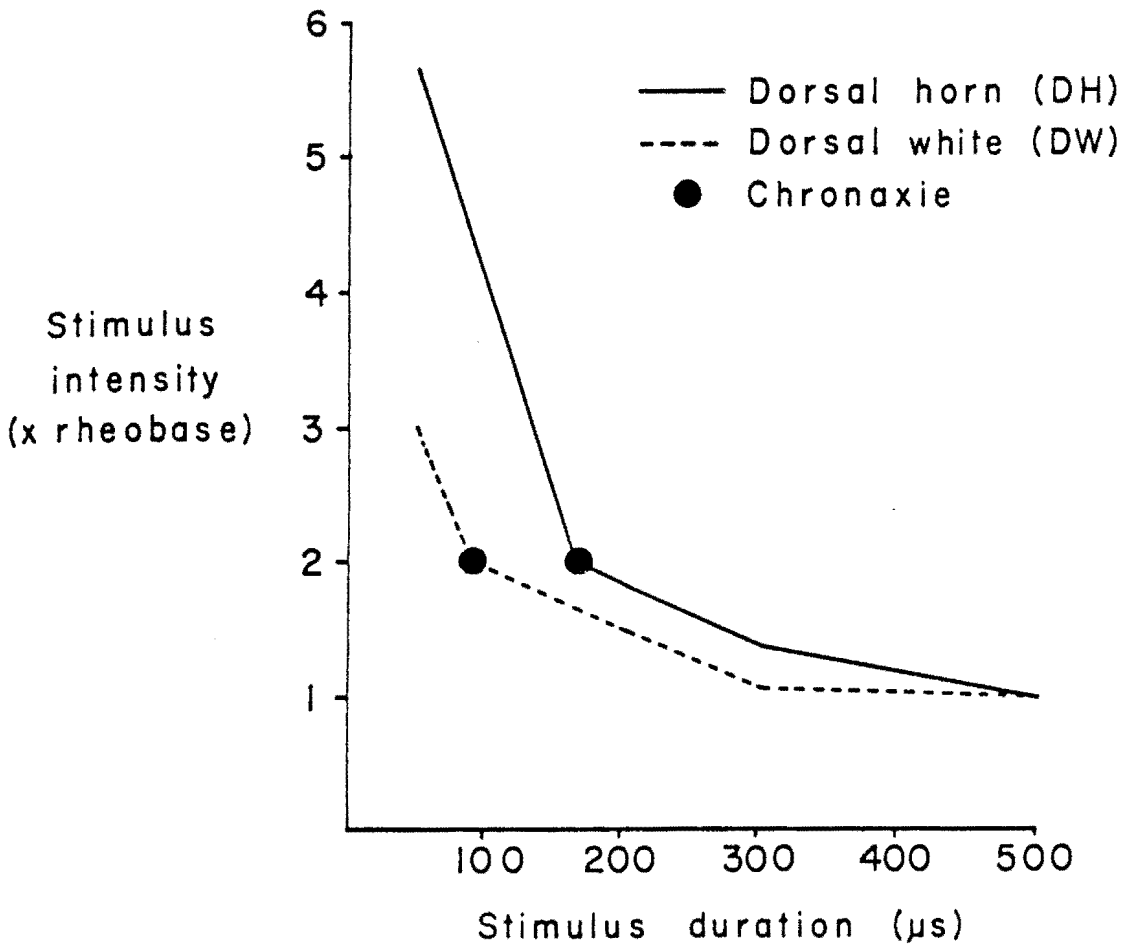

Figure 25. Strength-duration curves. Four-point strength duration curves were obtained in one experiment from each stimulation site. The chronaxie shown here is the threshold duration when stimulus intensity equals 2 x rheobase. Rheobase was defined as threshold current at 500 μs duration. In this example the DW chronaxie is 90 μs, the DH chronaxie is 160 μs.

Latency to onset, rheobase and chronaxie were measured in all experiments. The results include data on 16 fibers from 13 preparations. In 5 experiments the responses were elicited from both dorsal horn (DH) and dorsal white (DW) stimulation sites, 3 of these are shown in Fig. 24 (B, C and D). In the remaining experiments, the responses were elicited from only one site. A two-way analysis of variance was used to compare the data from both types of experiments. No significant difference was found; therefore, the data were pooled and averaged (Table V), and compared using unpaired t-tests. The onset latency and chronaxie measurements were significantly different between the two stimulation sites. Rheobase values were slightly greater to DH stimulation, but this difference was not significant. Chronaxie was significantly longer to dorsal horn stimulation. Chronaxie values ranged from 130 to 210 μs (DH stimulation) and 85 to 130 μs (DW stimulation). The difference between the mean onset latencies at the two sites was 1.91 ms. Onset latency was significantly longer to DH stimulation.

The difference in onset latencies averaged from all the fibers can be used to estimate conduction velocities of the dorsal root and intraspinal portions of these afferent fibers. The distance between the DW cathode and the proximal pole of the recording electrode was usually 1.5-2.0 cm. The estimated conduction velocity of this portion of the afferent fibers is, therefore, 17.5 mm/0.93 ms or 18.8 m/s. This is very close to the conduction velocity expected for the largest diameter myelinated fibers conducting at 14° C. The distance between DW and DH electrodes was < 1.0 mm; therefore, the intraspinal portion of these

TABLE V

Single fiber responses to extracellular stimulation

STIMULATION SITE	LATENCY TO ONSET (ms)	RHEOBASE (μA)	CHRONAXIE (μs)
DH n=10	2.84 ± 0.19 *	9.8 ± 1.0	174 ± 8 *
DW n=11	0.93 ± 0.10	7.7 ± 0.9	111 ± 5

* $p < .001$

fibers had an average conduction velocity of < 1.0 mm/1.91 ms, or < 0.52 m/s.

In order to be certain that rheobase currents were not overestimated leading to an underestimation of chronaxie, these data were analyzed using an approach suggested by Geddes and Bourland (71). The procedure is to reconstruct the linear charge-duration curve from measurements of threshold charge (current x duration) at two durations. The slope of this line is the duration-independent rheobase, and the ratio of the intercept to the slope is the chronaxie.

In Fig. 26 this reconstruction is shown using data from two single fibers, one for each stimulation site. These units had the same threshold current, 7.5 μA, at 500 μs. The initial DW chronaxie was 95 μs; initial chronaxie of the DH-stimulated unit was 170 μs. After converting current to charge by multiplying intensity times duration, these points were used for linear regression. The DH intercept is 1.932×10^{-6} C, with slope 3.636×10^{-6} C/ms. Dividing the intercept by the slope gives the calculated chronaxie, 0.531 ms (531 μs). The same analysis yields a value of 153 μs for the DW chronaxie. Table VI shows the averaged results (mean ± SEM) of all the single-fiber experiments from this analysis. Although considerably longer chronaxie values were obtained, the difference between the two sites was qualitatively the same, with DH chronaxie significantly longer than DW chronaxie.

Recovery of excitability of afferent axons and terminals and pharmacologic sensitivity of these sites were assessed using compound action potential recordings (sections C and D). In single fiber

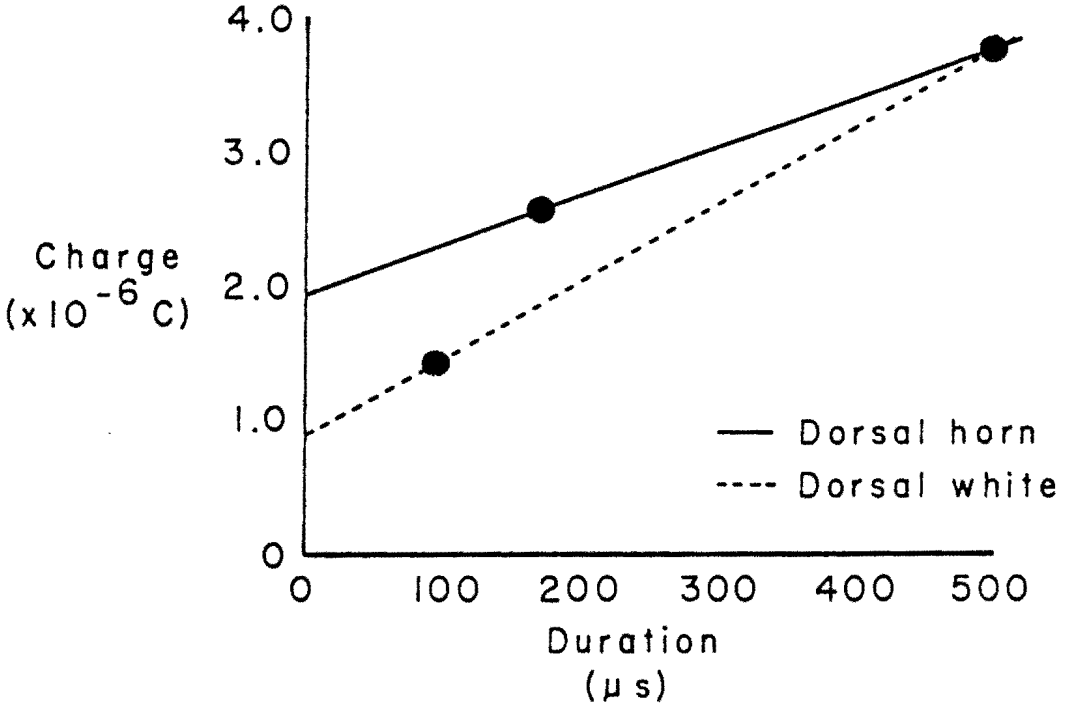

Figure 26. Charge-duration plots. Current-duration data from two experiments is plotted here with stimulating charge (current x duration) vs duration. Based on two points, the slope and intercept for each line is calculated. The slope should approximate the rheobase, and the intercept should be the chronaxie times the rheobase. The chronaxie values from this calculation are: DW=153 μs, DH=531 μs.

TABLE VI

Calculated rheobase and chronaxie of single dorsal root fibers

STIMULATION SITE	RHEOBASE (μA)	CHRONAXIE (μs)
DH	4.3 ± 0.4	670 ± 107 *
DW	5.4 ± 0.6	204 ± 16

* $p < .001$

recordings, relative refractory period is indicated by a period of increased threshold to elicit an action potential following a prior action potential. This was demonstrated in Fig. 27 on a fiber excited from the DH site. When paired pulses were delivered at a 4 ms interstimulus interval, more current was required to bring the membrane to threshold to fire a second action potential. The second action potential was also smaller and appeared at a longer latency than the first action potential.

Summarizing the results of the single fiber experiments, the processes of large diameter afferent axons within the spinal gray matter are characterized by decreased conduction velocity. Chronaxie in this region is longer than at the dorsal root entry zone.

C. The Effect of TEA and 4-AP on Early Recovery of Terminals and Axons

Action potential repolarization in neuronal membranes is generally accomplished by an increase in potassium efflux through voltage-gated potassium channels. Agents which block potassium channels prolong this process. An increase in spike duration should lead to an increase in relative refractory period, prolonging the recovery of excitability measured by paired-stimulation techniques. In these experiments effects of the potassium channel blocking agents TEA and 4-AP on axon and terminal recovery were evaluated.

Forty experiments were included in this study including twenty on isolated dorsal roots and twenty on hemicord preparations. Stimulating currents used in dorsal horn stimulation were low

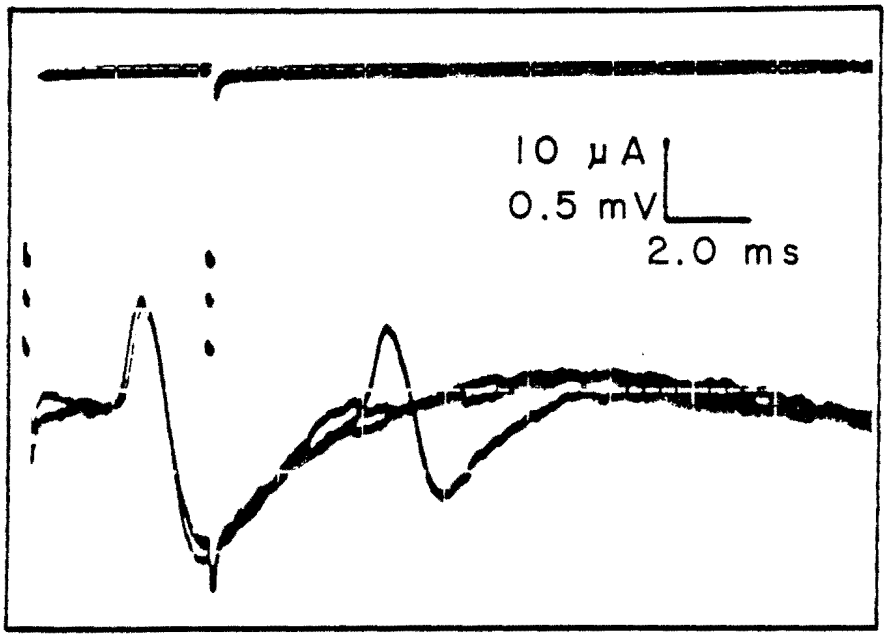

Figure 27. Single fiber relative refractory period. Paired pulses of equal amplitudes were delivered with a 4 ms interstimulus interval. In each case the current was suprathreshold for the first response but only the highest current (150 % of threshold) achieved threshold for a second action potential. The later evoked potential had a lower amplitude and greater latency to onset than did the first three.

(16.9 ± 2.0 μA). Mean onset latencies of responses to unconditioned test stimuli during the cadmium control period were 0.63 ± 0.03 ms and 1.78 ± 0.07 ms (mean ± SEM) for DR and DH experiments, respectively.

To demonstrate the stimulation site in the dorsal horn, electrolytic lesions were created via the DH stimulating electrode. Inspection of the lesion sites shows that the stimulating electrodes were placed deep in the intermediate gray matter in the region of large diameter afferent terminations. Representative sections from two experiments are shown in color photographs (Fig. 28). The relationship between the lesion sites and the motoneuron pool in the ventral horn in both cases indicates correct electrode placement. The tip was deep in the intermediate gray, far from the dorsal root entry zone. Figures 29 and 30 show the appearance of the lesions in several alternate sections from these tissues, reproduced from camera lucida projections.

Figures 31 and 32 show oscilloscope traces from representative experiments on DR and DH recovery, respectively. Responses to test stimuli are shown at indicated delays (ms, indicated to left of panel) after the conditioning stimulus. Responses evoked by the same strength stimulus but without a prior conditioning stimulus were tested twice in each series (unconditioned responses - designated "un"). The area of these two unconditioned test responses were averaged and recovery at each interstimulus interval was expressed relative to unconditioned area (%). Measurements made from these representative traces are given in Table VII.

Data points from table VII showing recovery $\leq$ 100% were fitted to a linear regression equation and the x coordinate (time in ms)

Figure 28. Color photographs of sections from lesioned cords. The Klüver-Barrera stain was used to visualize myelin (blue) and cell bodies (violet). Note the position of the lesion relative to the large motoneurons in the ventral horn.

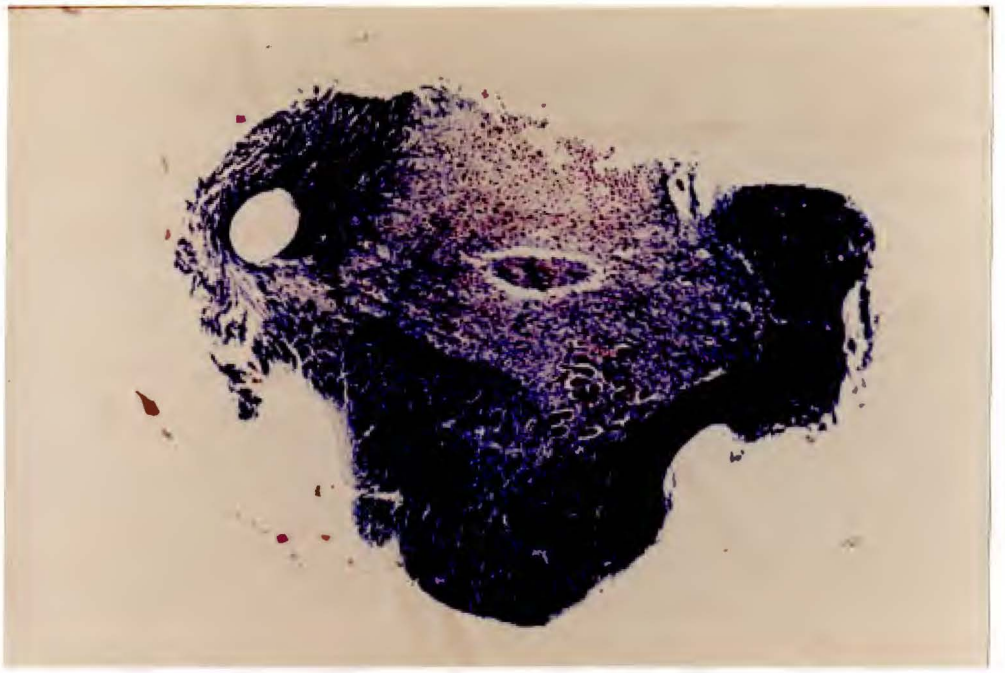

Figure 29. Lesion site in frog spinal cord. Camera lucida reproductions of several alternate sections from one hemicord lesioned and fixed after an experiment. The lesion site has been blackened. Filled circles indicate the locations of motoneuron cell bodies in the ventral horn. The inner line marks the approximate boundary between white and gray matter. The position of the stimulating cathode appears to be deep in the intermediate gray, well separated from the dorsal root entry zone.

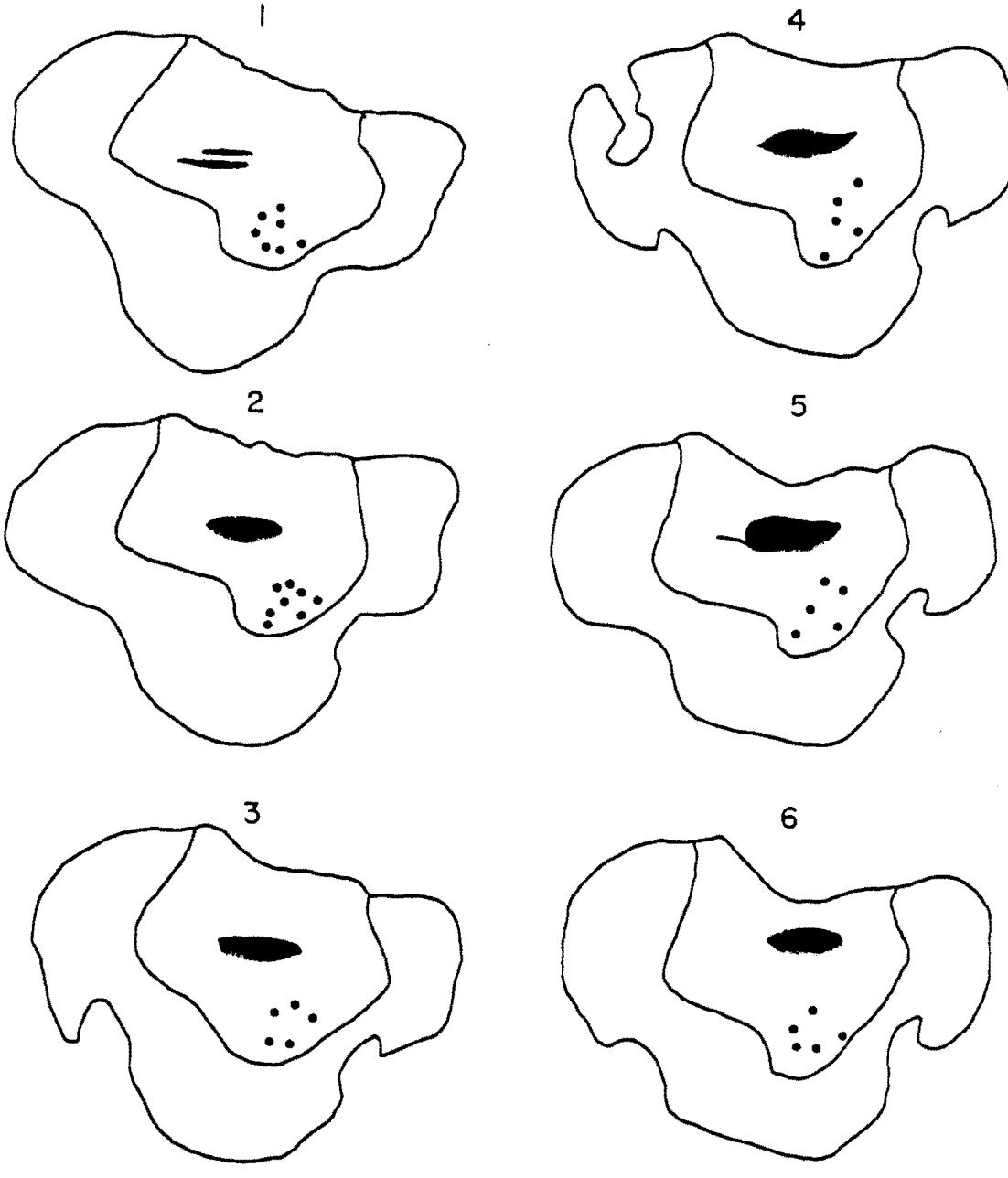
1
4
2
5
3
6
500 µm

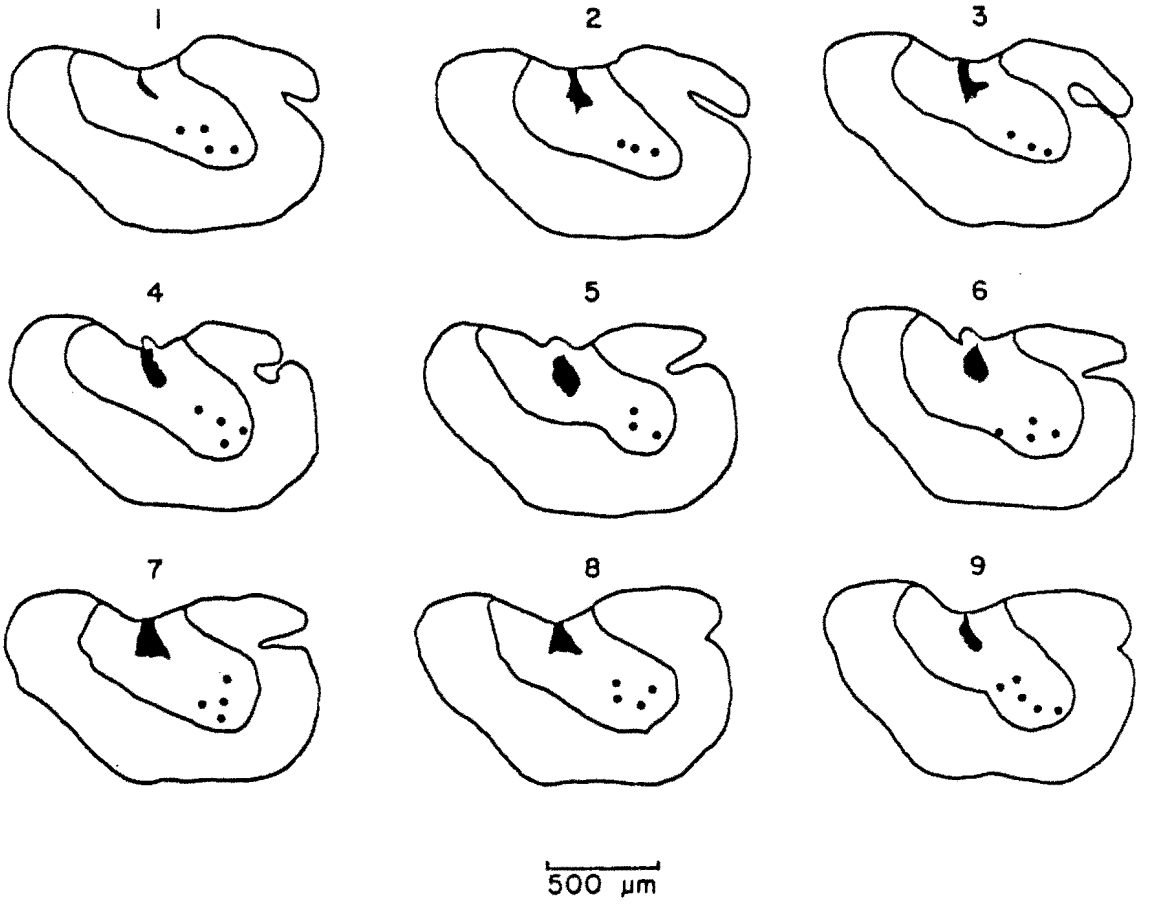

Figure 30. Lesion site in frog spinal cord. Histology was done on a different hemicord after an experiment. Camera lucida reproductions of alternate 10 µm sections through the longitudinal extent of the lesion (black) made by passage of DC current through the DH cathode. Filled circles denote positions of motoneurons in the ventral horn.

Figure 31. Traces of early recovery to DR stimulation. The upper traces show the output of the current monitoring circuit. The response to the unconditioned test stimulus (un) shows the characteristic short onset latency of these responses (0.8 ms). The delay between conditioning and test stimuli is given to the left of each trace. Recovery values at each time point are given in Table VII.

Cadmium

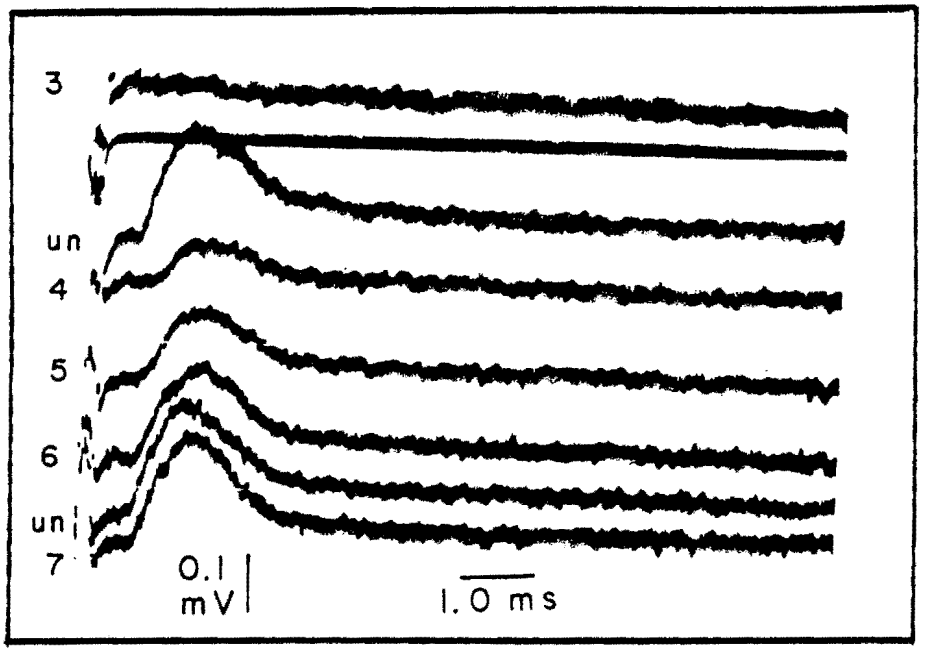

Cadmium + TEA

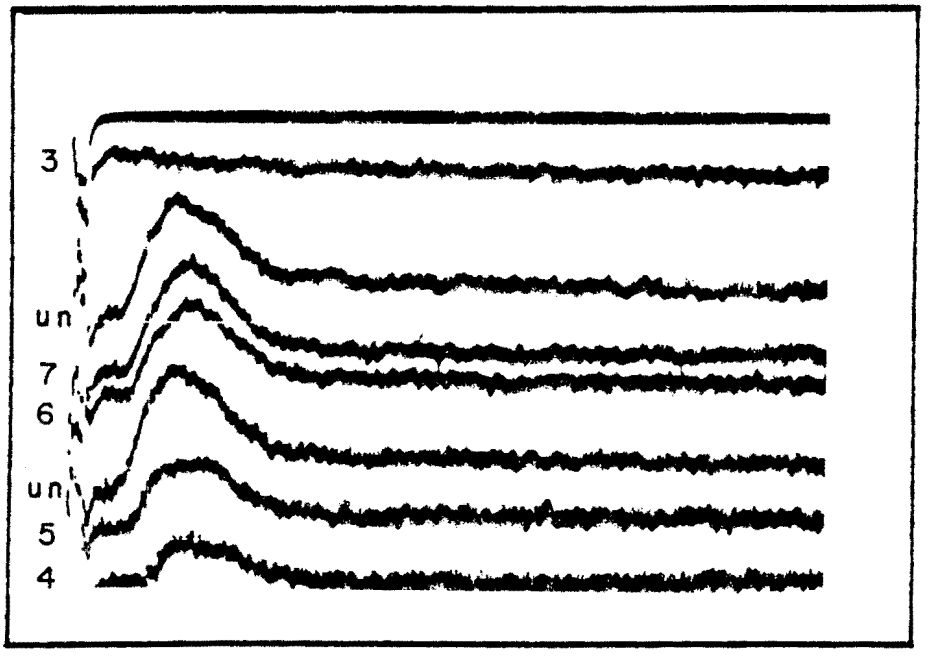

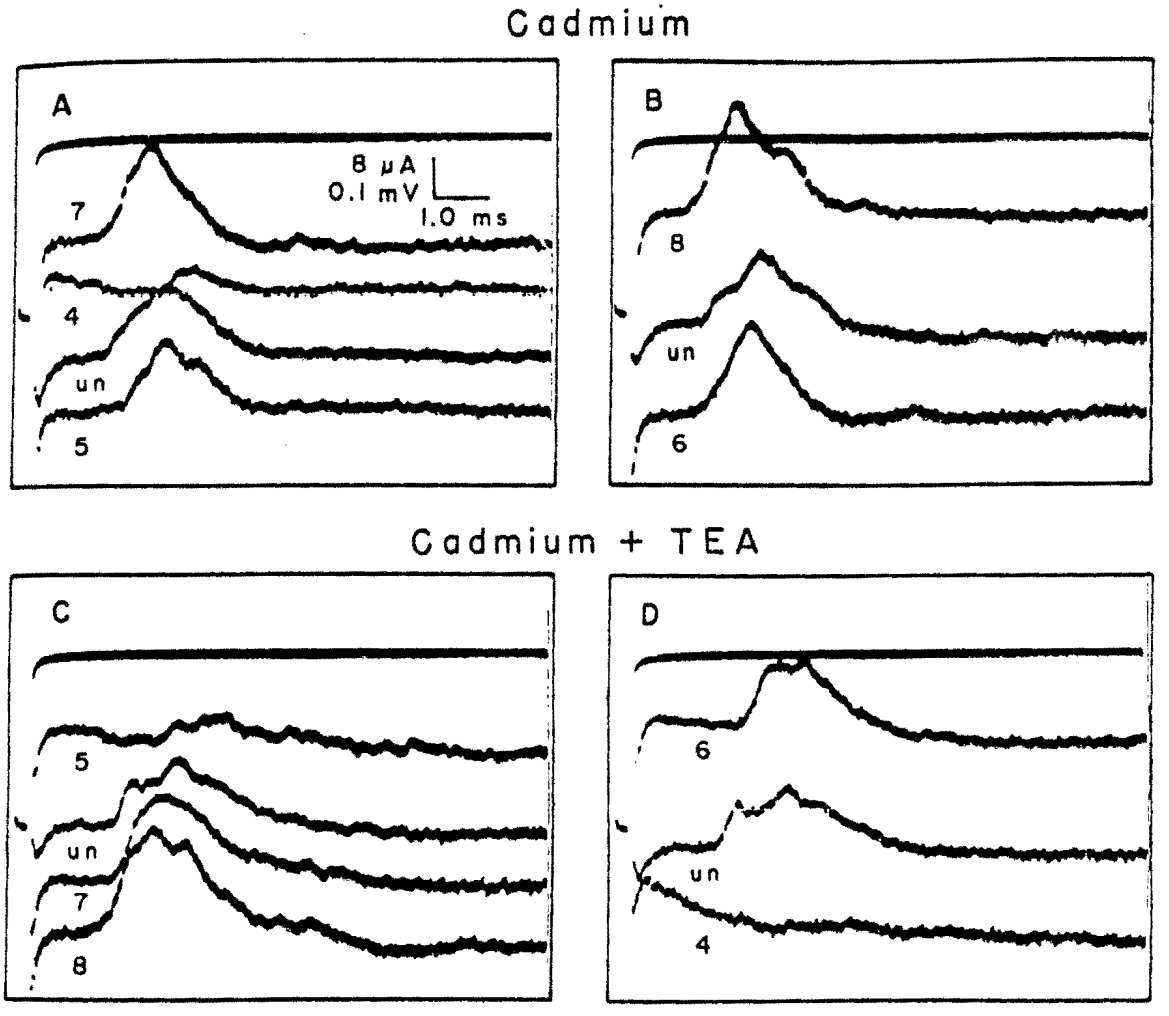

Figure 32. Traces of early recovery to DH stimulation. The upper trace indicates the output of the current monitoring circuit. Onset latency to the unconditioned test response is 1.7 ms. Condition-test delay is shown beneath each trace. Recovery values at each time point are given in Table VII.

TABLE VII

Early recovery to DH and DR stimulation
Results in two representative experiments

Recovery (% unconditioned area)

Dorsal root - delay (ms)	3	4	5	6	7
Cd	0	37	63	89	89
Cd+TEA	0	40	63	91	97

Dorsal horn - delay (ms)	4	5	6	7	8
Cd	16	72	92	100	136
Cd+TEA	0	40	84	124	153

corresponding to 50% recovery was calculated (t_{50}). Control t_{50} was subtracted from test t_{50} to yield a Δt_{50} for that experiment. In the above example TEA had little effect on DR recovery with Δt_{50}=-0.04 ms. TEA's effect on the DH was to prolong recovery with Δt_{50}=+0.47 ms.

Test period recovery values at each delay were averaged for each tissue and treatment group. These averaged recovery curves (unpaired data) are shown in Figs. 33 and 34. One treatment group for each tissue consisted of a test period of continued cadmium superfusion with no added potassium channel blocker (Cd). This is the control to which the other groups should be compared. The dorsal horn data (Fig. 33) for the 4-AP group is shifted to the right of the Cd curve at the earliest two time points. TEA, on the other hand, reduced the recovery at all interstimulus intervals tested. The addition of 4-AP to TEA shifted the curve more dramatically than either drug did individually. The dorsal root curves (Fig. 34) were less affected by all drugs tested. 4-AP tended to shift the curve slightly to the left from the Cd control. TEA reduced the response area at each time point. From the appearance of this unpaired data, the TEA effect on DR recovery was not greatly changed by the addition of 4-AP. However, the paired data shown below does indicate a difference between the effect of TEA alone and TEA+4-AP on DR recovery.

The Δt_{50} values (mean ± S.E.M.) from these experiments are summarized in Table VIII and displayed graphically in Fig. 35. The Δt_{50} was negative for the DH cadmium control. This indicates that recovery during the test period (the final 20 minutes of cadmium

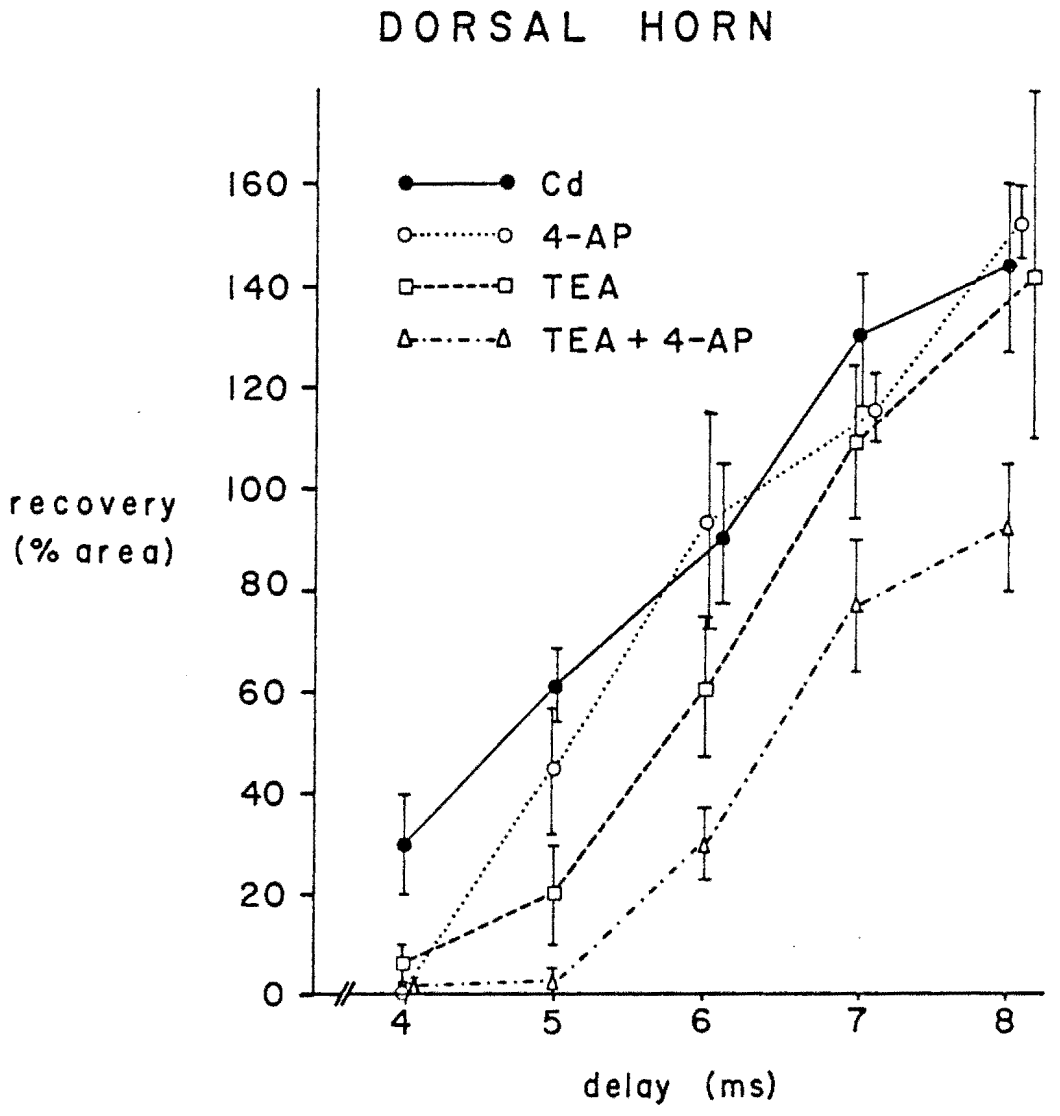

Figure 33. Dorsal horn - pharmacology of early recovery. Averaged recovery curves for 20 dorsal horn experiments. Each line represents data from five experiments. In each experiment recovery was tested at the same interstimulus intervals.

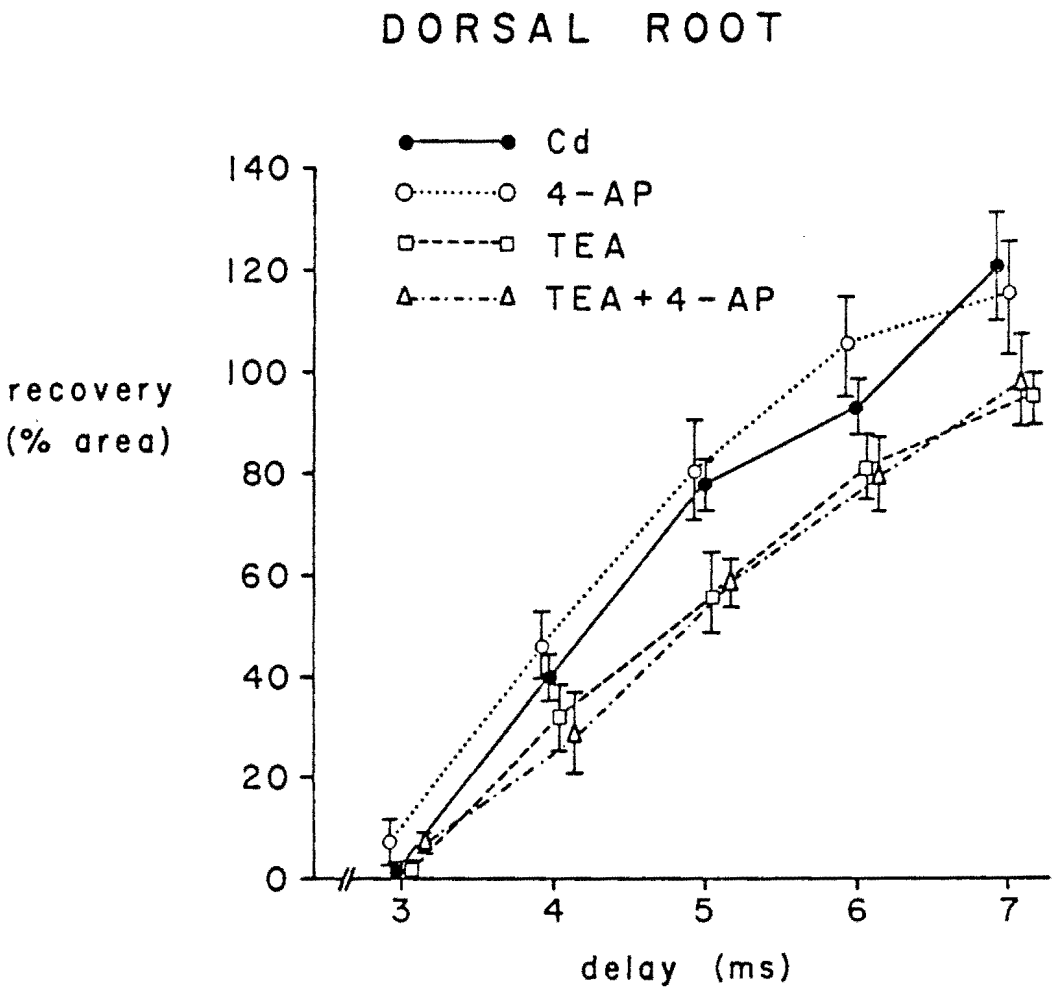

Figure 34. Dorsal root - pharmacology of early recovery. Averaged recovery curves for 20 dorsal root experiments. Each line represents data from 5 experiments.

TABLE VIII

Pharmacology of early recovery to dorsal horn and dorsal root stimulation

Δt_{50} (ms)

STIMULATION SITE	Cd	TEA	4-AP	TEA + 4-AP
DH	-0.28 ± 0.10	+0.77 ± 0.12 *#	+0.51 ± 0.14 *#	+1.53 ± 0.20 *#
DR	+0.09 ± 0.17	+0.15 ± 0.09	-0.23 ± 0.15	+0.59 ± 0.24

* Significantly different from DH - Cd
# Significantly different from DR

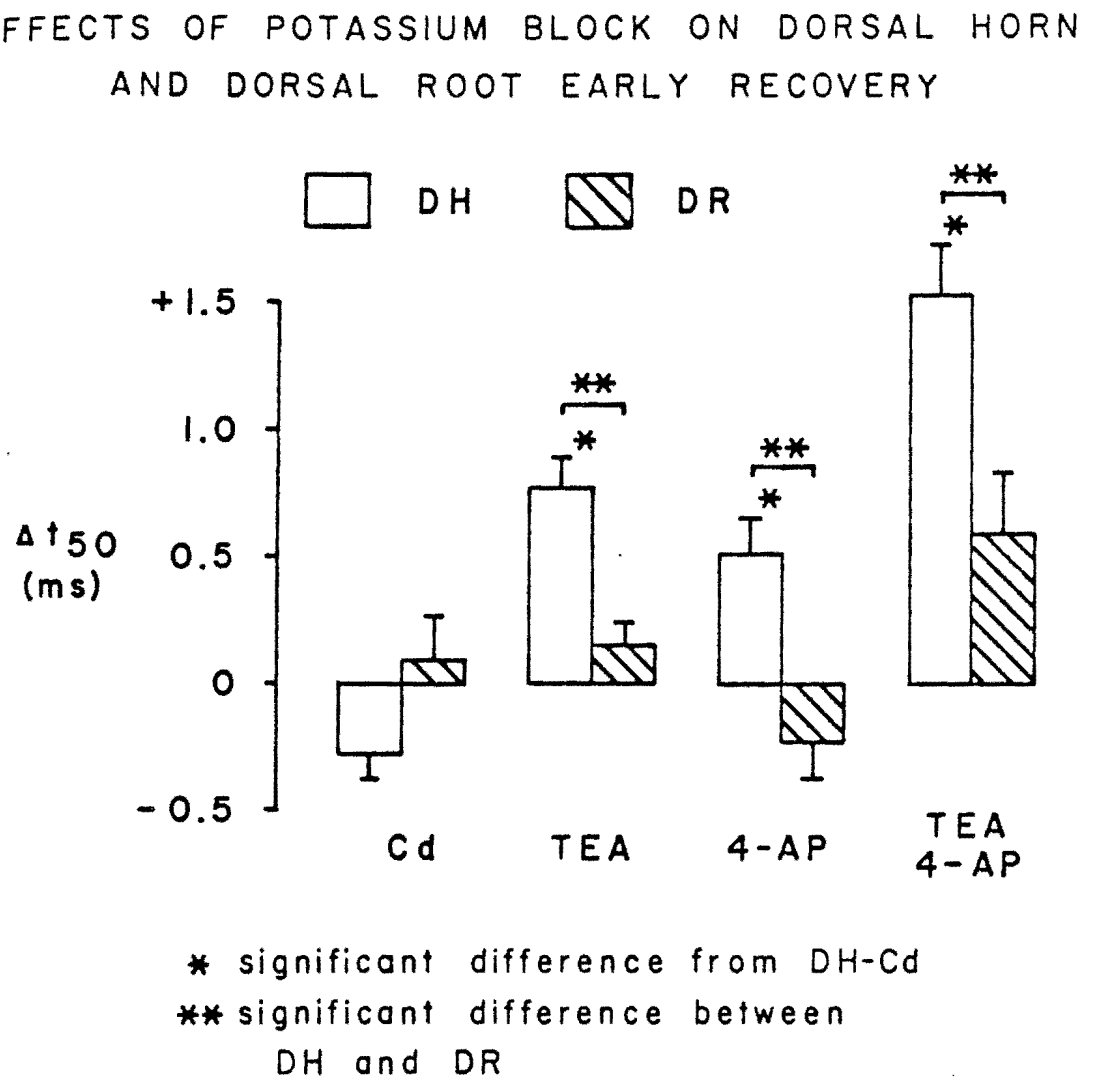

Figure 35. Pharmacological modifications of dorsal horn and dorsal root early recovery. Summary graph from 40 experiments. Twenty experiments were done on each tissue. Each bar shows mean ± SEM of 5 experiments.

superfusion) was slightly faster than during the control period (the initial 20 minutes of cadmium). Slower recovery in the presence of TEA, 4-AP and TEA+4-AP is indicated by the positive Δt_{50} values. This change probably reflects prolongation of the relative refractory period in the region of afferent fiber terminals caused by these agents relative to the cadmium control. The effect of combined TEA and 4-AP on DH recovery was greater prolongation than the sum of the individual effects.

DR recovery was altered much less by potassium channel blocking agents. This could indicate less prolongation of the relative refractory period in the large axonal regions of afferent fibers. A two-way analysis of variance was performed, with post hoc analysis by the Newman-Keuls procedure. The Δt_{50} was significantly increased by all three potassium channel-blocking treatments only for the DH groups, relative to the time-matched DH-Cd control. Each treatment produced a significantly greater effect in the DH groups relative to similarly treated DRs. Although there was an increase in Δt_{50} in the DR TEA+4-AP group, this was not significantly different from the DR-Cd control.

D. Early Recovery to Dorsal Horn Stimulation Before and During Synaptic Block

Nerve terminals have ion channels permeable to calcium which open on membrane depolarization. Calcium influx is the step linking excitation to transmitter release. Another effect of increased

intracellular calcium in many neuronal systems is to increase potassium efflux via calcium-activated potasssium channels. The contribution of these channels to terminal action potential repolarization was evaluated in these experiments by measuring early recovery before and after synaptic block.

The effect of blocking nerve terminal calcium influx on relative refractory period was studied in two ways. First, in 14 of the experiments included in the previous study (section C), the effect of solution A was measured. Using dorsal horn stimulation at interstimulus intervals of 4, 5, 6, 7 and 8 ms, t_{50} values were calculated during the initial part of the experiment and compared to values during the final 5 minutes of superfusion with solution A. In 4 additional experiments using solution B, interstimulus intervals used were from 4 to 7 ms at 0.5 ms increments. Averaged curves from the solution B experiments are shown in Fig. 36. Solution B slightly decreased the recovery at each time point. The results of these experiments are summarized in Table IX (mean ± SEM).

Comparison of initial and test means with paired t-tests led to the conclusion of no significant differences in both sets of experiments. These results do not support a role for calcium-activated potassium channels in repolarization of terminal regions of spinal afferent fibers.

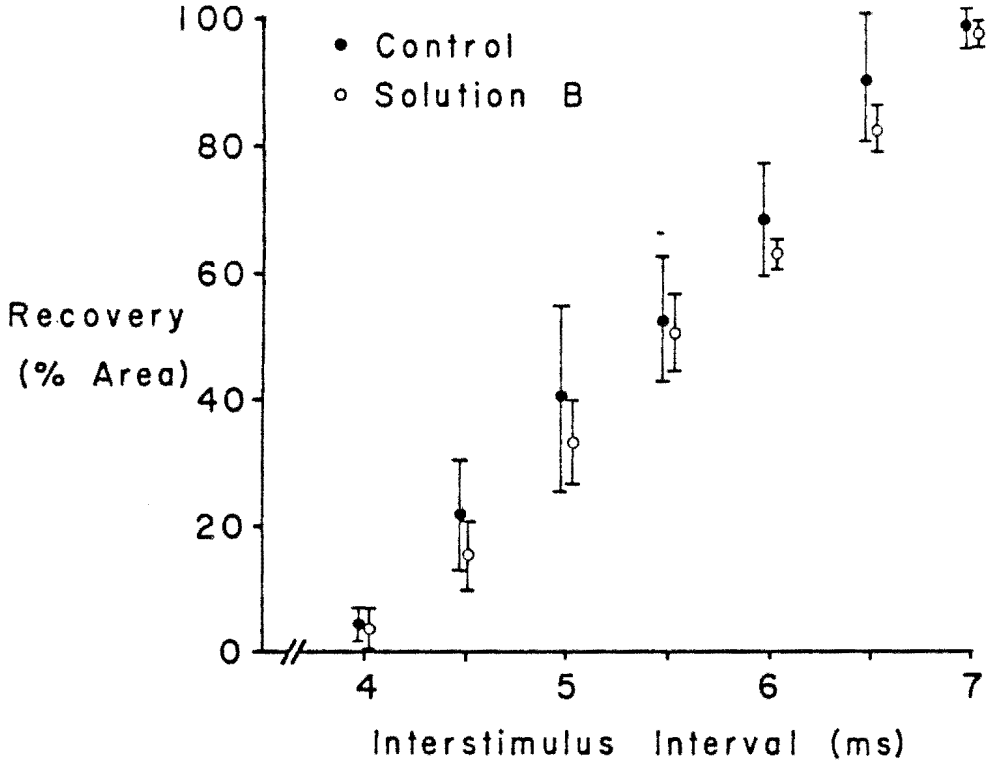

Figure 36. The effect of solution B on DH early recovery. Summary of 4 experiments on early recovery to DH stimulation before and after synaptic block with solution B.

TABLE IX

Dorsal horn early recovery
Effect of two calcium blocking solutions

Solution	n	Initial t_{50}	Test t_{50}	Δt_{50}
A	14	4.93 ± 0.2	5.00 ± 0.15	+ 0.07
B	4	5.36 ± 0.3	5.56 ± 0.11	+ 0.20

E. Supernormal Period

Increased excitability of afferent terminals following a conditioning DR stimulus has generally been attributed to synaptically mediated PAD (36, 60, 192). However, the same property, when observed in peripheral axons, is termed the supernormal period (SNP). This characteristic may be due to a passive depolarizing afterpotential (11, 27, 75). In this study the excitability changes of terminals and axons were monitored at intervals up to 150 ms following a conditioning stimulus. Supernormality of excitability and conduction velocity of terminals were markedly greater than that of peripheral axons. Terminal SNP was only slightly altered by synaptic block, which indicates that a strong tendency to supernormality is intrinsic in this region of afferent fibers.

This study included five isolated dorsal root preparations and five hemicord preparations for a total of ten experiments. Paired-pulse stimulation was used at interstimulus intervals of 10, 20, 30, 40, 60, 80, 100, and 150 ms. The responses to the test (conditioned) stimulus were compared to the unconditioned response to the same stimulus. Mean onset latencies of the unconditioned responses were characteristic for each tissue and were not changed by superfusion with solution B as indicated by Table X.

Traces from representative experiments are shown in Figs. 37 and 38. The interstimulus interval is marked next to each trace and the unconditioned test response is identified (un). The traces of DR-SNP (Fig. 37) were taken during solution B superfusion. The DH-SNP

TABLE X

Onset latencies to dorsal horn and dorsal root stimulation before and during solution B

STIMULATION SITE	ONSET LATENCY INITIAL (ms)	ONSET LATENCY SOLUTION B (ms)
DH	2.19 ± 0.05	2.20 ± 0.06
DR	0.47 ± 0.02	0.44 ± 0.01

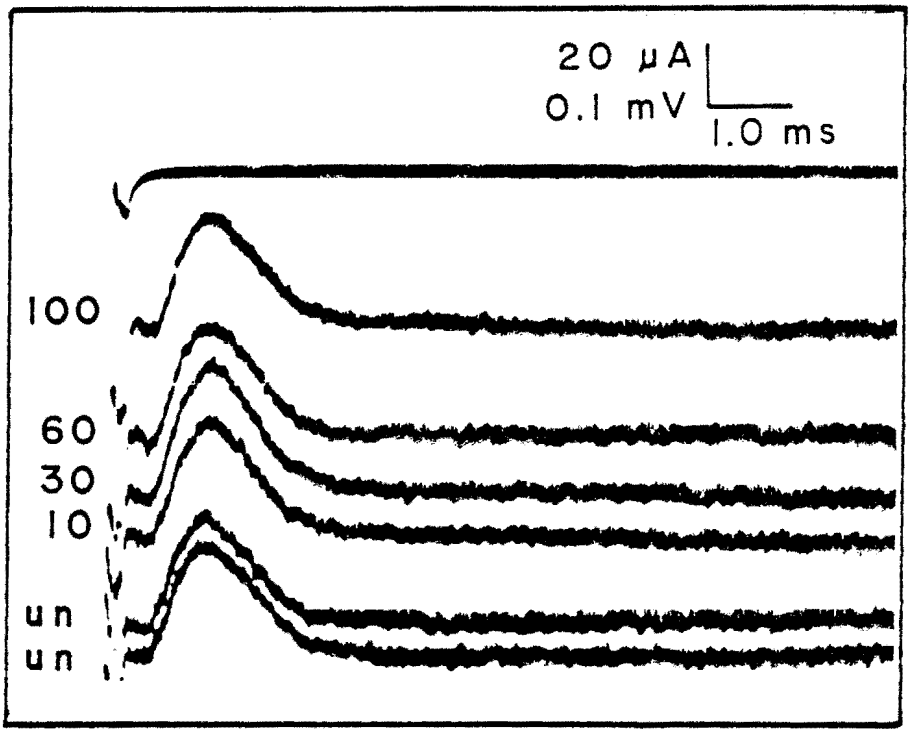

Figure 37. Dorsal root - supernormal period. Traces from a representative experiment on supernormal period of an isolated dorsal root after superfusion with solution B for 18 minutes. Onset latency of the unconditioned test stimulus is 0.5 ms. Interstimulus intervals are indicated to the left of each conditioned response. Unconditioned responses are marked "un". Output of the current monitoring circuit is shown above indicating that the same stimulating current was delivered with each sweep.

Figure 38. Dorsal horn - supernormal period. Traces from a representative experiment on supernormal period to dorsal horn stimulation. Onset latency to the unconditioned test stimulus is 2.4 ms. Panel B shows responses tested after 18 - 20 minutes of superfusion with solution B. Interstimulus intervals are indicated to the left of each conditioned response. Unconditioned responses are marked "un". Output of the current monitoring circuit is shown in the upper trace of each panel. Stimulating current did not vary between sweeps.

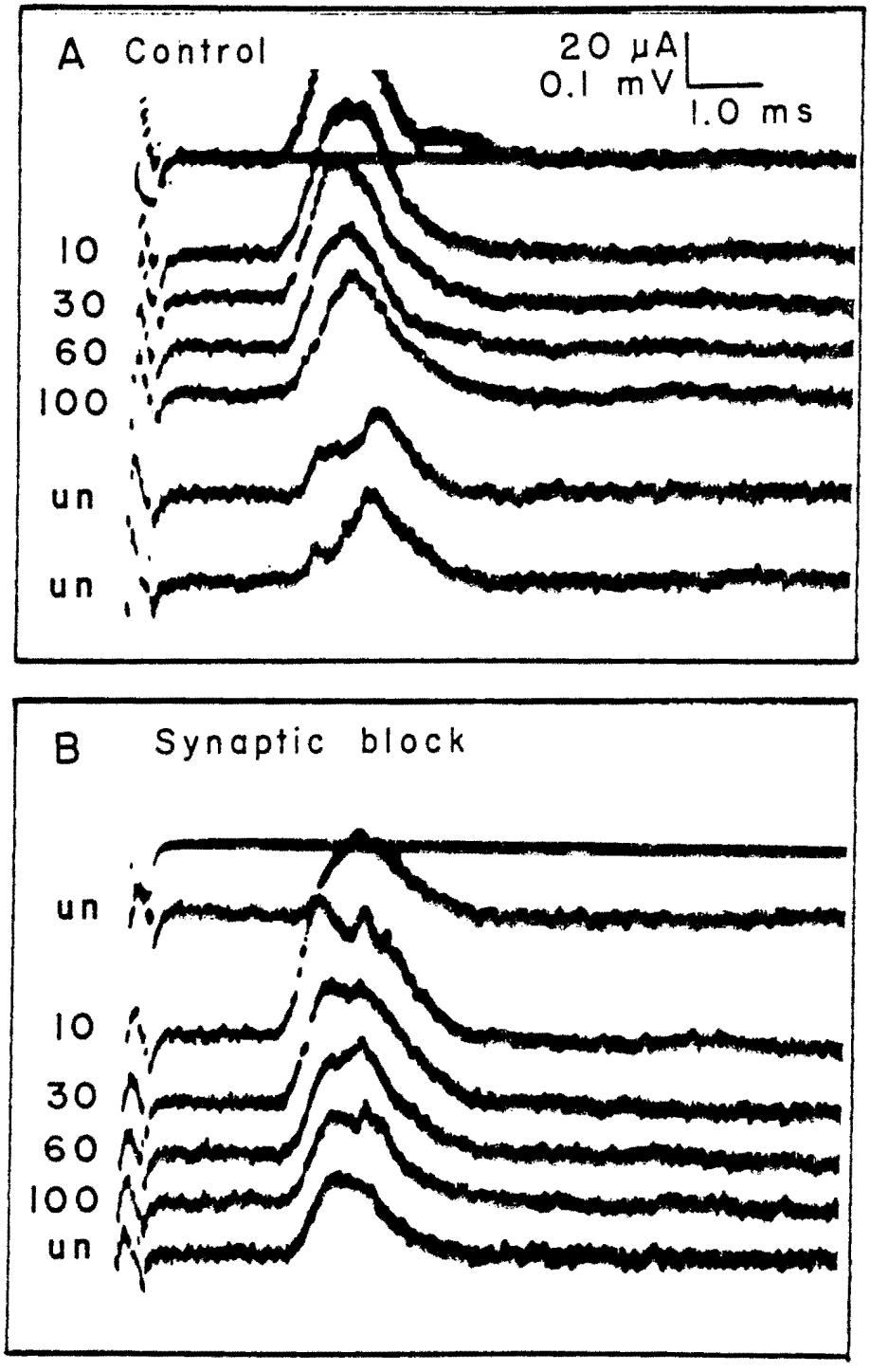

Dorsal horn - Supernormal period

(Fig. 38) traces clearly show the effect of a prior conditioning stimulus to increase the area and decrease the onset latency of the test response. There is little change visible between panel A and panel B, implicating some nonsynaptically-mediated event contributing to the SNP in the terminal region.

Summarizing the data of all the SNP experiments, at all time points tested, the average response area was greater to the conditioned test stimulus than to the unconditioned test stimulus. This was true for both tissues as shown in Figs. 39 and 40. However, the magnitude of supernormal excitability was much greater in the DH region as can be seen by comparing the ordinates of the graphs in Figs. 39 and 40.

Overall responses were analyzed by taking the mean of all 8 time points in each experiment. A two way analysis of variance was performed to analyze the effect of tissue differences (DH vs DR) and condition difference (control vs Solution B) and any possible interaction. The results are summarized in table XI.

Based on this analysis, the responses to DH stimulation showed a significantly greater response area following a conditioning stimulus than DR responses. Linear regression analysis was also performed on both sets of data. Only the DH data could be fit well with this method (r values averaged 0.87 and 0.85 for initial and solution B, respectively). The slopes were negative, averaging:

-0.82 ± 0.23 % area/ms delay (control)

and

-1.05 ± 0.25 % area/ms delay (solution B).

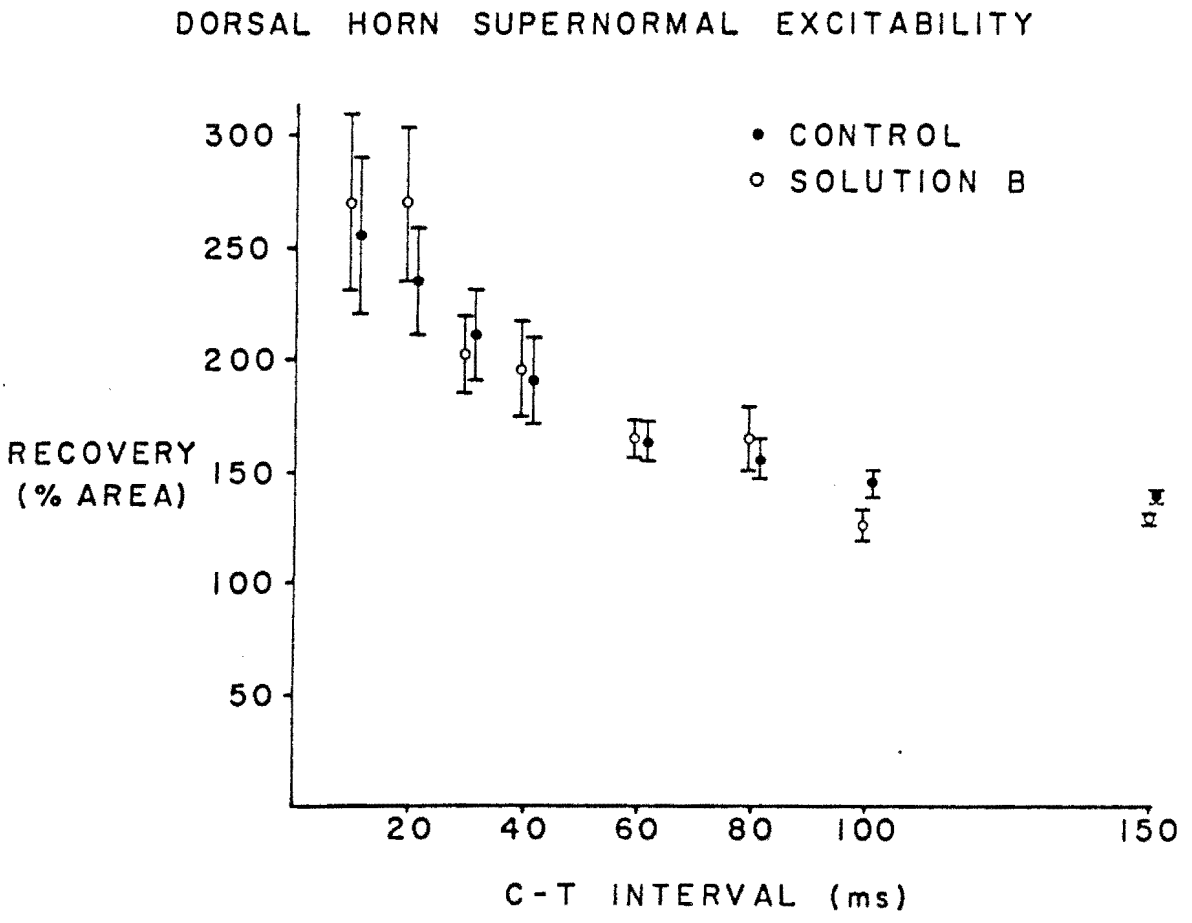

Figure 39. Dorsal horn - supernormal excitability . Data on dorsal horn supernormal excitability summarized from 5 experiments on isolated hemicord preparations. C - T intervals used were identical in all experiments.

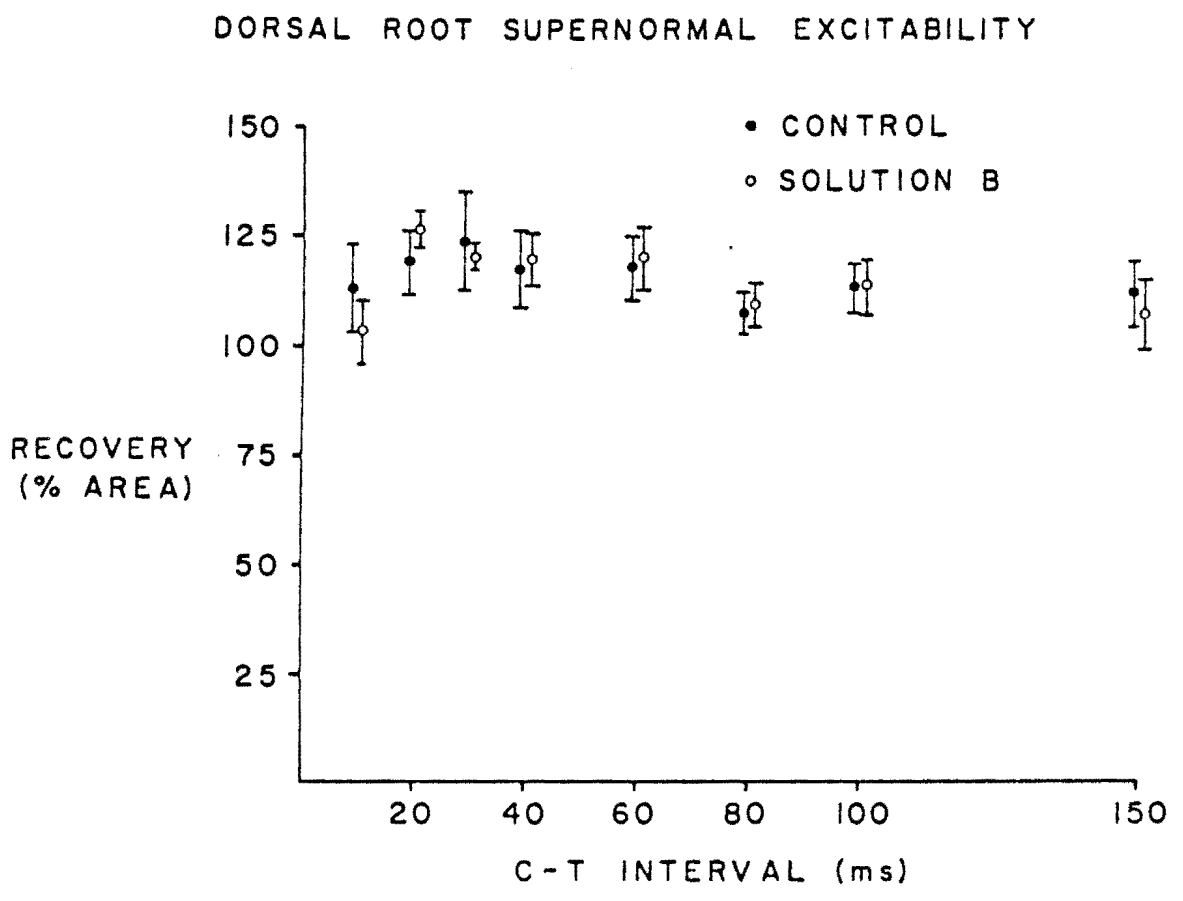

Figure 40. Dorsal root - supernormal excitability. Data on dorsal root supernormal excitability summarized from 5 experiments on isolated dorsal roots. C - T intervals were identical in all experiments.

TABLE XI

Supernormal period - dorsal horn and dorsal root excitability changes

Conditioned response areas (% of unconditioned)

TISSUE	CONTROL	SOLUTION B
DH *	187 ± 13	190 ± 16
DR	115 ± 8	115 ± 5

* $p < .005$

The slope was significantly steeper after synaptic block ($p < .005$, paired t-test).

In addition to the change in excitability indicated by the increased response area, the supernormal period was associated with decreased onset latency of the evoked potentials. The latency changes were very small in the DR-SNP responses and were not seen in some cases. The DH responses, on the other hand, showed marked latency shifts throughout the supernormal period, as plotted in Fig. 41. These data were analyzed in the same manner as the area data described above (table XII). The analysis of variance indicates that the change in onset latency was significantly greater at the dorsal horn region than for the isolated dorsal roots. In addition, latency changes were significantly decreased by synaptic blockade.

As before, the data were also subjected to linear regression analysis and a good correlation was found only for the DH data (average $r = 0.770$ and 0.826 for control and solution B, respectively). Unlike the results described for the area data, the control (2.4 μs/ms delay) and solution B (2.2 μs/ms delay) slopes were not significantly different (paired t-test).

In conclusion, supernormal excitability and conduction velocity of the terminal region, before or after synaptic block were greater than supernormality of the roots alone. The areas of conditioned test responses during the supernormal period, which should reflect excitability changes in the terminals, were not different after PAD was blocked, but the decay of area changes over the first 150 ms was steeper. Onset latency shifts to terminal stimulation during

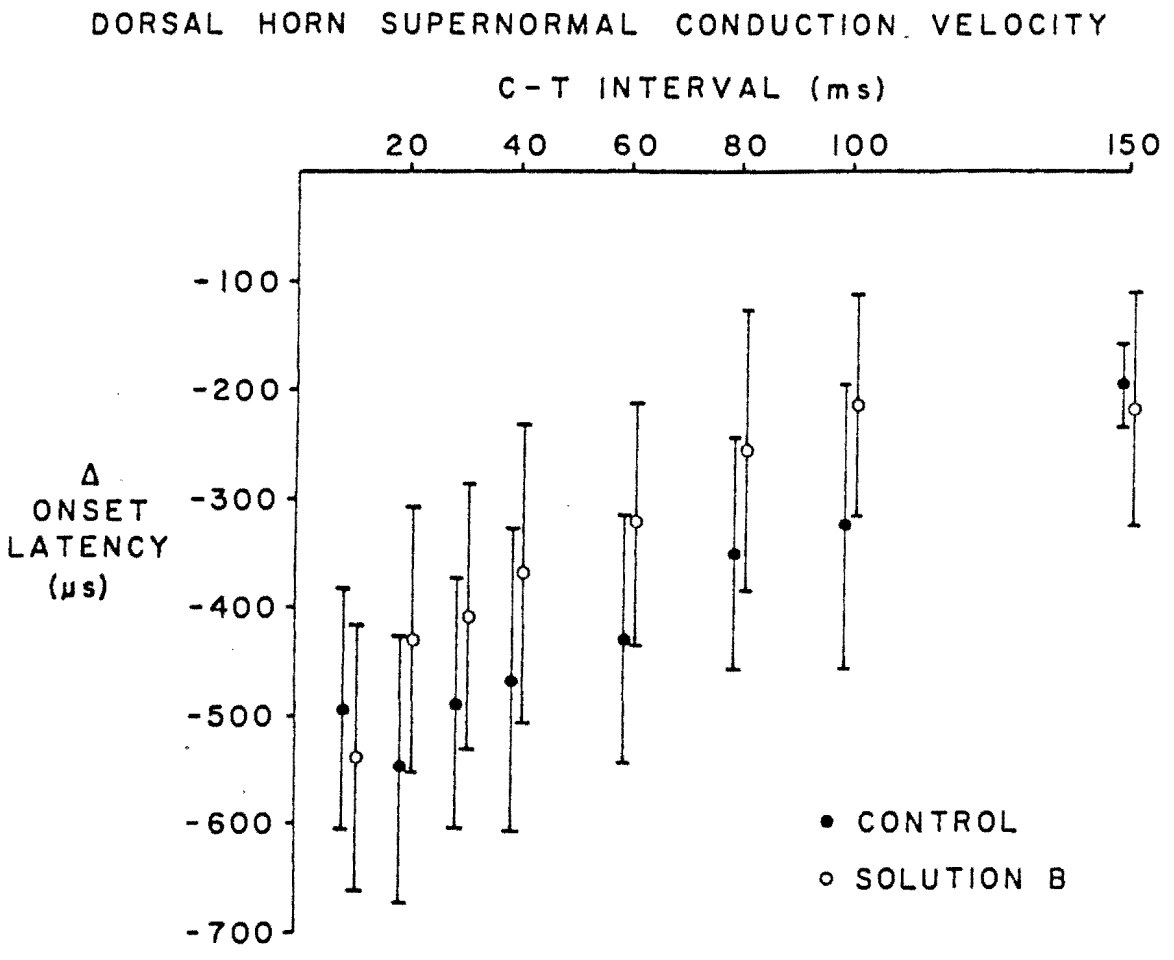

Figure 41. Dorsal horn - supernormal conduction velocity. Data on latency shifts during DH supernormal period from 5 hemicord experiments.

TABLE XII

Supernormal period - dorsal horn and dorsal root onset latency changes

Latency to onset, μs (Δ from unconditioned)

TISSUE	CONTROL	**	SOLUTION B
DH *	-412 ± 103		-344 ± 116
DR	-13 ± 8		-7 ± 6

* $p < .01$
** $p < .05$

the supernormal period were decreased by synaptic block. The profile of latency changes over the delays tested, up to 150 ms, was not affected by synaptic block.

CHAPTER VI

DISCUSSION

A. Introduction

The aim of this dissertation was to identify physiological properties of neuronal terminal arborizations within the vertebrate central nervous system. The small diameter and tortuosity of these processes made it necessary to use indirect techniques rather than intracellular recording methods. Test solutions were developed from the literature on synaptic transmission and effects were tested on reflex responses in frog cords. Single fiber experiments were performed to study onset latency of stimulus-evoked responses from sites close to afferent terminals, or in main axonal regions. Threshold electrical stimulation responses were measured to determine rheobase and chronaxie. Paired pulse testing with compound action potential measurement evaluated relative refractory period and it's sensitivity to potassium and calcium channel block. Other paired pulse studies compared supernormality of afferent axons in dorsal roots to terminals within the spinal gray matter.

Some of these techniques and pharmacologic agents have been used in studies of a peripheral neuron terminal, the neuromuscular junction. Peripheral studies have the advantage that the terminal region can be visualized for correct electrode placement. There are, however,

structural and functional differences between neuromuscular transmission and central neuron-neuronal transmission. The frog neuromuscular junction is characterized by an abrupt change from the large myelinated motoneuron axon to a 200 μm long terminal region closely applied to the muscle with calcium sensitive release sites all along the terminal (107, 132). In comparison, sensory axons entering the spinal cord arborize progressively with narrow axon branches stringing together enlargements of < 5 μm diameter, the synaptic boutons. These boutons are thought to be the localized sites of calcium-dependent transmitter release (31, 157, 184). Transmitter release failure at the neuromuscular junction is only seen under artificial conditions such as high magnesium/low calcium solutions (49). Failures may be the normal condition at some central synapses (86, 99, 144). These differences between peripheral and central synaptic structure and function reinforce the importance of the present neurophysiological studies of central terminal arborizations.

B. Modulation of Synaptic Transmission in Frog Spinal Cord

1. Synaptic facilitation

a. General considerations - Ventral root reflex areas evoked by supramaximal DR or LC stimulation were not stable over a two hour recording period. Rather, transmission was continually potentiated (results, Fig. 15, control). This may indicate gradual calcium accumulation in axon terminals at the low experimental temperatures

(14°C). This would be expected if terminal calcium extrusion depended on Na-Ca exchange, thus, ultimately, on Na-K ATPase activity (141, 142, 167, 190). Calcium accumulation at low temperature is also consistent with a role of Ca-ATPase in terminal calcium extrusion (174).

However, this temperature is within the range routinely used in frog spinal cord experiments to maintain optimum viability (46, 145, 188). This instability should be considered in designing experiments on frog cord synaptic transmission. The effect of drugs having a prolonged time course of action must be compared with appropriate time-matched controls.

b. 4-AP - Potentiation of reflex transmission by 4-AP was characterized by slow onset (30-50 min) and irreversibility for several hours after 4-AP exposure was stopped. This is consistent with the hypothesis that 4-AP acts by diffusing through the membrane in its nonprotonated, uncharged form, then is trapped by protonation at the lower intracellular pH (136). The slow onset of action and apparent increase in effectiveness during the wash period complicates the interpretation of drug effects. The action of 4-AP is less dramatic when compared to the time-matched control (see above, 1a).

c. TEA - TEA 0.5 mM potentiated DR-VRR area. TEA's onset of action was much more rapid than 4-AP's, with a plateau reached after 9 minutes of TEA treatment. Qualitatively, the action of TEA appeared to be similar to 4-AP's in increasing reflex amplitude and area, decreasing onset latency, and increasing synchronization of the evoked response. More experiments should be done to determine the effective dose range of TEA in this model. The frog cord could be more useful in

studying TEA's effects on transmission than either the neuromuscular junction (117, 166) or the sympathetic ganglion (119). This is because higher doses of TEA, which may be most effective in enhancing transmission, also block cholinergic receptors in these tissues, ultimately causing transmission failure at the postsynaptic site.

d. Summary of potentiation experiments - The potassium-channel blocking agents 4-AP and TEA potentiate frog cord synaptic transmission, particularly in the DR-VRR pathway. This effect is consistent with 4-AP and TEA actions in peripheral tissues (17, 74, 100, 117, 119, 136, 166). Many of the previous experiments demonstrating synaptic potentiation by 4-AP and TEA used high Mg^{++}/low Ca^{++} solutions to initially suppress transmission. The facilitation by potassium-channel blockers is more accurately quantitated against this background.

The present work demonstrates a similar contrast. Single supramaximal shocks to the frog cord dorsal root apparently do not maximally excite the motoneuron pool, during superfusion with physiological Ringer's solution (30, 93). Against this background, it may be easier to demonstrate synaptic facilitation. One disadvantage with this pathway is its disynaptic nature. It is, therefore, a fairly indirect measure of synaptic activity. An additional difficulty is the apparent change in synchronization of the evoked response after exposure to potentiating agents (above, results section; 93). The area of the reflex response should be measured, rather than the (usually reported) amplitude (cf. 145, 183). Greater synchronization of the response could result in larger response amplitude even if no additional motoneurons are responding (62).

2. Synaptic depression

a. DR-VRR vs LC-VRR - A variety of solutions were evaluated for effectiveness at blocking these two synaptic pathways in frog spinal cord. Each solution (Ringer's + 0.1 mM Cd, solution A, solution B) rapidly and completely blocked the DR-VRR. Block of the DR-VRR was complete while the LC-VRR was still present (albeit reduced). Therefore, a more stringent evaluation of a synaptic blocking agent's effectiveness may be to study the agent's effect on the LC-VRR. This point should be noted in experiments using frog cord as a "bioassay" of synaptic blocking effectiveness. For example, several studies have reported suppression of frog cord synaptic transmission during exposure to serum from multiple sclerosis patients (37, 169, 170). Only one of these studies evaluated the serum's effects on both pathways and discussed the implications of these differences (37).

b. Cadmium as a synaptic blocking agent - Cadmium's effectiveness at blocking synaptic transmission depended on the other divalent cations in the medium. In the standard solution (Ca^{++} - 1.5 mM, Mg^{++} - 1.5 mM), addition of Cd^{++} 0.2 mM resulted in an effective block (solution A). Cd^{++} 0.1 mM was effective when Ca^{++} was reduced to 0.5 mM and Mg^{++} was increased to 2.5 mM (solution B). This is consistent with reports of other divalent cation synaptic blocking agents which seem to act by competing with calcium (7, 49, 50).

Solution B was more stable than solution A, the latter of which tended to precipitate at the pH used in these experiments. Manganese

and cobalt were also tested for their stability in this bicarbonate buffered solution, but concentrations sufficient to block transmission were not achieved without precipitation. Intracellular recording studies from mammalian central neurons frequently use cadmium (usual concentration - 0.2 mM) as a calcium channel-blocking agent (38, 121, 122, 160). In many cases, it is used with synthetic buffers or omitting phosphate to prevent precipitation.

In the present studies solution B was the most satisfactory synaptic blocking solution. Solution B did not change onset latency of DH and DR evoked activity (results, table X). This may indicate that this solution does not substantially raise threshold. However, most substitutions of divalent cations alter active and passive membrane properties (5, 29, 65, 73, 139). Therefore, further physiological and biophysical studies of solution B are warranted. The aim would be to determine the effect of solution B on membrane responses to other ionic changes and on Na and K channel gating characteristics.

C. Single Fiber Studies

1. Conduction velocity

Stimulation at the two sites compared in these studies evoked responses with different onset latencies. If activation time is the same at two different points on a fiber, conduction velocity can be estimated by dividing the distance between the stimulating electrodes by the difference in onset latency of the evoked spike. The assumption of similar activation time at the DH site and at the DW site was made in

this study. This assumption was based on the finding that activation time does not differ between stimulation of main axons and axon branches of spinal interneurons. Activation time at these sites was < 0.2 ms (102).

The average conduction velocity of the peripheral portion of these fibers was calculated to be 18.8 m/s. This is similar to values other investigators have calculated for large-diameter, fast-conducting fibers (when temperature differences are considered) (62, 148, 156).

The calculated intraspinal conduction velocity of single dorsal root fibers was <0.52 m/s. Correcting for the cold temperature (using 1.8, the Q_{10} value of Tasaki & Fujita (187)), the conduction velocity at room temperature would be 0.75 m/s. This is very close to the conduction velocity reported for frog C fibers at room temperature, which was 0.7 m/s (62).

Conduction velocity of the intraspinal region of frog afferent fibers is much slower than in the parent fibers. This confirms similar findings for other central and peripheral nerve terminals (107, 140, 194).

2. Chronaxie

Chronaxie values were longer at the DH stimulation site than at the DW site. Chronaxie was measured in two different ways. In the course of the single fiber experiments, threshold current intensity at 500 μs stimulus duration was determined. This was termed the rheobase. After this level was measured, stimulus intensity was increased to twice this value, and duration was varied until threshold was achieved. This

was the experimentally measured chronaxie. After all experiments were completed, the data were reanalyzed using a mathematical formula of Geddes and Bourland (71), resulting in a calculated rheobase and chronaxie. Regardless of how chronaxie was determined, the values were greater for DH stimulation than for DW stimulation.

The experimental chronaxie (averaged) to DW stimulation was 111 μs. This is higher than the chronaxie of 77 μs measured from dorsal column fibers in cats (16). The latter study, as the present one, defined rheobase as threshold intensity with a 500 μs duration pulse. This difference may be related to the experimental temperatures used or the species difference. Central unmyelinated fibers in cats had longer chronaxies of 180-310 μs (134). The longest duration pulses used in this last study was 5000 μs, considerably longer than the above two studies.

The experimental chronaxie (averaged) to DH stimulation was 174 μs. The only comparable studies in the literature, based on electrode type and experimental procedures, are the two cited in the last paragraph. Of these, DH chronaxie appears to be closer to the values of central unmyelinated fibers (134).

The calculated chronaxies to both DH and DW stimulation were considerably longer than the experimentally determined values. This discrepancy indicates the difficulty of using this measurement to quantitate membrane properties. However, the qualitative relationship is preserved, with DH chronaxie considerably longer than DW chronaxie. This may be due to a longer time constant of the membrane in the terminal region, compared to the main axonal membrane (16, 72, 155).

Increased membrane capacitance or resistance could contribute to a greater time constant at the terminal region. The calculated terminal conduction velocity (see above) would be characteristic for unmyelinated or very thinly myelinated axons. Capacitance of either type of axon is much greater than the large parent axons of these sensory fibers (22). Input resistance of these fibers also would be expected to be greater than in parent axons, due to decreased diameter in the terminal regions.

D. Pharmacology of Axon and Terminal Early Recovery

1. Stimulation site

Correct electrode placement within the afferent terminal region was important in each study included in this dissertation. Verification of electrode placement is evident in two ways. First, electrolytic lesions were created with the DH cathode to provide anatomical confirmation of correct electrode placement. Microscopic inspection of the lesion sites indicated that the stimulating electrode was correctly placed. Lesion sites were far from the main axonal region of large sensory fibers at the dorsal root entry zone and appeared to be centered at the muscle afferent terminal region in the intermediate gray matter (103, 184).

The other observation supporting appropriate electrode positioning was the data on evoked response latency. In the experiments included in this study, the average onset latency of the compound action potential response to DH stimulation was 1.78 ms. This is 1.15 ms longer than the average onset latency to DR stimulation. The distance

between the usual DR stimulating site on the transected dorsal root and the DH site in the cord was approximately 2.0 mm. Therefore, the DH electrode was positioned in a slowly conducting fiber region, as in the single fiber study.

2. 4-AP

Superfusion with 4-AP 7.5 μM prolonged recovery at the DH, but not the DR stimulation site. This would be expected if K channels sensitive to 4-AP were contributing to spike repolarization at the terminals or in the conducting pathway to the terminals. This effect of 4-AP is not consistent with the hypothesis that "A" type potassium channels are present on presynaptic terminals regulating terminal excitability (74, 173). The effect of 4-AP was seen during calcium channel block, therefore, it is unlikely that it is due to a direct effect on presynaptic calcium current (74, 161).

This result is consistent with Dolly's hypothesis of a novel K channel, which is particularly sensitive to 4-AP, localized to presynaptic nerve terminals (52). The prolongation of recovery of the compound action potential by 4-AP supports the hypothesis that the 4-AP sensitive channel contributes to action potential repolarization in the terminal regions. Thus, action potential repolarization in terminal regions may involve a different mechanism than repolarization in main axons.

3. TEA

The potassium channel-blocking agent, TEA, also prolonged

terminal recovery. Axon recovery was not changed by TEA, although the dose given would be predicted to decrease nodal potassium conductance (89). Cadmium was used to block calcium channels throughout the test period. Therefore, this action of TEA is not due to an effect on potassium conductances activated by presynaptic calcium influx. At frog neuromuscular junction, low doses of TEA (0.1-1.0 mM) potentiated synaptic transmission. The same doses produced very little change in axonal spike duration (117). As with the 4-AP effects, the TEA results may indicate that action potential repolarization at terminals involves a different mechanism than repolarization in main axons.

4. TEA + 4-AP

The Δt_{50} values listed in table VIII can be used to estimate prolongation of terminal relative refractory period by each treatment. Relative to the cadmium control group, the average prolongation by 4-AP was 0.79 ms. Prolongation by TEA was 1.05 ms. The combination of TEA and 4-AP prolonged relative refractory period by 1.81 ms. Thus, the effect of combining 4-AP and TEA was essentially additive; there did not appear to be any occlusion of the actions of TEA and 4-AP to prolong recovery. However, the combination also appeared to have an effect on recovery of the conducting pathway (DR). This also could have contributed to the prolongation evaluated from the DH site. Therefore, this cannot be taken as evidence supporting the hypothesis that 4-AP and TEA block two different types of K channels at nerve terminals (74, 166). Further experiments are indicated to test this hypothesis. A dose-response curve could be done using 4-AP. The aim

would be to find a dose which is maximally effective at prolonging terminal recovery, without altering axon recovery. This dose could then be combined with a small dose of TEA to determine if TEA's effect was still additive (similar to a protocol used at neuromuscular junction (166)).

5. Calcium block

Dorsal horn recovery of excitability was not prolonged during calcium channel block by either synaptic blocking solution. This contradicts findings at rat and lizard neuromuscular junctions, indicating terminal calcium-activated potassium currents (133, 138). Potassium efflux from synaptosomes also has a calcium-activated component (13).

Three explanations may resolve this discrepancy. First, the time course of some calcium-activated potassium currents indicates that they are not involved in action potential repolarization. Rather, these currents influence membrane potential and excitability through afterhyperpolarizations (10, 38, 121). Nerve terminal studies with limited time resolution (13) or extracellular recordings (133) would be unable to distinguish the contribution of these currents to action potential repolarization.

Second, inward calcium current may be an important component contributing to the action potential in presynaptic terminals (108, 125). Thus, blocking this current could shorten the terminal action potential. This effect would counteract the prolongation due to block of calcium-activated potassium currents.

The third explanation proposed for the failure of calcium block to alter terminal recovery is based on the structure of Ia terminal arborizations and boutons. Anatomical studies show profuse intraspinal branching of Ia axons with enlargements of < 5 μm diameter irregularly spaced along thin axon branches (31, 184). If calcium-activated potassium currents do contribute to action potential repolarization, their contribution would be limited to those small regions where calcium entry occurs, i.e. at the boutons. The bulk of the terminal arborization consists of fine axon branches where repolarization is sensitive to 4-AP and TEA (see above), but perhaps not to calcium block. Since the boutons are small structures, continuous with these axon branches, they will probably be isopotential with the branches (157, 158). At the boutons, therefore, action potential repolarization will be influenced by the characteristics of the adjacent axon branch membranes as well as the currents characteristic of the boutons.

6. Functional implications

Repolarization of the action potential in nerve terminal regions is more sensitive to potassium channel blocking agents than the same process in main axons. This could be due to a greater number of potassium channels or a different type of potassium channel distribution in the terminal region. The potassium channels of boutons or terminal axons may be similar to those present, though normally inactive, in the paranode and internode region. Demyelination of large fibers exposes these regions, greatly increasing fiber sensitivity to potassium channel block by TEA and 4-AP (25, 26, 168).

The effective dose of 4-AP found in this study may implicate a different type of potassium channel contributing to action potential repolarization in terminal regions. Evidence for a presynaptic, 4-AP sensitive potassium channel possibly involved in spike repolarization was given in the literature review.

Is there any functional significance of increased potassium permeability or novel potassium currents localized to nerve terminal regions? The importance of brevity of presynaptic action potentials may be inferred from the consequences of blocking presynaptic potassium currents. Regenerative calcium responses induced in squid presynaptic terminals by TTX and TEA treatment were reduced in duration after repetitive pulses. The postsynaptic response elicited under these conditions was greatly decreased during repetitive stimulation, returning to normal after recovery. It was, therefore, concluded that prolonged increases in presynaptic $[Ca^{++}]_i$ lead to exhaustion or inactivation of the transmitter release mechanism (108). A similar fatigue process was observed during recordings of frog muscle endplate potentials during maximal potentiation with 4-AP or TEA (109). The present work showed an example of potentiation of reflex activity during 4-AP, changing to failure after longer exposure. Inactivation of calcium currents during prolonged repetitive activation has been observed in neuron somas (131, 144).

It has been proposed that synaptic boutons have limited calcium buffering capabilities. This is due to their small size, high surface area/volume ratio, and limited volume for mitochondria. This could predispose terminals to greater calcium inactivation, leading to

synaptic depression on repetitive activation (104, 144).

To summarize, the results of the present study indicate prolongation of relative refractory period at terminals at low doses of 4-AP and TEA that do not alter axonal recovery. Greater sensitivity to 4-AP and TEA at terminals than at axons could be due to greater exposure of axonal potassium channels, or could be due to specific potassium channel types present mainly at terminals. Both of these factors may be involved in terminal potassium permeability. Rapid action potential repolarization may be important in the terminal regions to limit calcium influx. Conditions which maximize calcium entry may lead to calcium overload with subsequent inactivation of calcium currents or to failure of the transmitter release mechanism.

E. Supernormal Period

In the previous section anatomical and physiological evidence was presented that the DH stimulation sites were located in the terminal regions. In the SNP experiments average onset latency to DH stimulation was 1.7 ms longer than onset latency to DR stimulation. This indicates that the DH cathode position was in a slowly conducting fiber region, as in the previous studies.

Afferent terminals within the frog spinal cord were much more excitable, and had increased conduction velocity, following the passage of a single orthodromic conditioning stimulus. The excitability change would be expected due to the presence of synaptically mediated PAD (36, 60, 192). The surprising finding in this study was that there was

little change in these post-conditioning terminal excitability changes under conditions of synaptic block. This could indicate an intrinsic tendency to supernormality in afferent terminals. This same property is also seen in frog peripheral axons, shown in the dorsal root data here, as well as in several other studies (3, 11, 27, 75, 156). However, the degree of supernormality was significantly greater in the terminal region.

A correlation between supernormal excitability and a depolarizing afterpotential has been made with intracellular recording studies (11, 23, 27). Extracellular recordings of the same event show the opposite polarity, a negative afterpotential (77). Evidence is shown here (results, Figs. 20 and 23) of a pronounced negative afterpotential following antidromic stimulation from the dorsal horn or orthodromic stimulation of the dorsal root. This potential was seen after block of synaptic transmission by solution A or solution B. A similar depolarization has been observed during magnesium block of transmission (191). Thus, terminal regions of frog primary afferent fibers may have a large intracellular depolarizing afterpotential.

1. Terminal SNP: Is the DAP larger?

The extreme degree of supernormal excitability and conduction velocity seen in terminals, relative to the parent axons, could be due to a larger depolarizing afterpotential in this region. This difference could be due to passive properties (11) or potassium accumulation (77, 200).

The contribution of potassium accumulation to SNP is more likely

for unmyelinated axons. These axons have greater potassium efflux after a single impulse than myelinated axons (110, 147). If terminal properties resemble unmyelinated axons (which also have large SNP's), they might also be expected to develop elevated extracellular potassium after a single impulse.

Further studies are required to elucidate the mechanism of terminal SNP. A distinction between potassium-induced and passive SNP could possibly be made with TEA. TEA increases amplitude and duration of the passive DAP of large myelinated axons (11). It would, therefore, be expected to increase terminal SNP, if this SNP is due to passive membrane properties. Alternatively, TEA would be expected to reduce potassium efflux from terminals, therefore, it should reduce SNP if due to potassium accumulation.

2. Does the degree of SNP reflect DAP amplitude?

Another proposal is that the extreme SNP found in terminals may not necessarily reflect a proportionately larger DAP at this location. A slight depolarization may have greater impact on threshold and conduction velocity in unmyelinated and thinly myelinated regions than in thickly myelinated axons. The basis for this proposal is as follows: Action potential propagation proceeds from active to adjacent inactive regions by means of local circuit currents preceding the active zone. These depolarizing currents are almost entirely capacitative. The low level of resting membrane conductance allows very little resistive current to flow (97). It is reasonable to consider that a slight depolarization would cause a greater increase of conduction velocity in

unmyelinated and thinly myelinated fibers than in thickly myelinated fibers. The increased capacitance associated with decreased or absent myelin, would require proportionately larger and longer local circuit currents to support propagation. Partial depolarization of the membrane capacitance would greatly speed this process. This hypothesis could be tested using peripheral nerves of different composition. One possible experiment would be to measure conduction velocity changes during varying degrees of potassium-induced depolarization.

Onset latency of DH-evoked activity decreased by 25% at the peak of supernormality, both before and after synaptic block. This was a surprising finding and is difficult to reconcile with the presumed ionic mechanism of PAD. Prolonged depolarization of axons might be expected to result in increased threshold due to sodium inactivation and increased potassium conductance (90). Padjen and Hashiguchi observed increases in membrane conductance to applied depolarization, with additional increases during PAD. They even proposed that the greatly increased conductance could be responsible for presynaptic inhibition by inducing branch point failure (148). The increased conduction velocity found in this study seems to conflict with that hypothesis. However, one model of propagation predicts little decrease in conduction velocity with increased membrane conductance. This would be seen if the conductance changes during PAD are small relative to the conductance changes during the action potential (146).

The changes in onset latency during the DH-SNP could be explained on the basis of a shift in the site bringing the afferent fibers to threshold. Perhaps after conditioning, excitation occurs at

branches closer to the periphery, in the more rapidly conducting fiber regions. Two observations are proposed to counter this suggestion. First, the shift in latency at the 10 and 20 ms C-T delays averaged more than 500 μs. At the calculated terminal conduction velocity of < 0.5 m/s, this represents a shift in effective stimulation site of 250 μm. It is doubtful that the current density at that distance would be sufficient to excite these axons. Second, studies of the supernormal period in central unmyelinated fibers have documented similar increases in conduction velocity paralleling increases in excitability, independent of changes in stimulation site.

3. Is the SNP after synaptic block an artifact?

Possibly, the large terminal supernormal period is an artifact of the synaptic blocking solution used. Elevated divalent cation concentrations increase the DAP of large peripheral axons. This is thought to be caused by screening of surface charges, producing an effective hyperpolarization of the membrane electric field. Hyperpolarization increases DAP amplitude (11). However, if this were the mechanism, a similar effect of solution B on DR-SNP should have been evident. The results presented here indicate that solution B did not alter DR-SNP.

This finding clearly has implications for afferent depolarization studies. An orthodromic conditioning stimulus in a dorsal root is followed by an intrinsic SNP of the terminals. Antidromic excitability testing after a conditioning stimulus to the homologous root may reflect both passive and synaptically mediated

supernormality (60, 192).

4. Functional implications

The physiological significance of nerve terminal supernormality is twofold. First, this finding underscores results of the single fiber study. The degree of nerve terminal supernormality most closely resembles that reported for central unmyelinated and thinly myelinated axons (68, 134, 179, 180). In addition to increased axial resistance as axons narrow, another factor impacting on propagation through the axonal arbor could be an increase in membrane capacitance in the terminal region.

Second, the supernormal period of nerve terminals may have functional implications in the transmission process. As mentioned previously, transmission failure by some boutons is the normal condition in the Ia-motoneuron system. This may be the result of branch point failure, particularly if the branches present a large capacitative load. However, transmission can be facilitated by paired pulses, particularly at interstimulus intervals of 10-20 ms (43, 93, 120). In the present studies this corresponds to the time of maximum supernormality of response area and conduction velocity. It is possible that the facilitation of transmission at these intervals is related to more effective action potential invasion of the superexcitable terminals.

CHAPTER VII

CONCLUSIONS

The results obtained in the experiments making up this dissertation allow a profile of axon and terminal characteristics to be made. In each study differences were found between afferent terminals in the spinal cord dorsal horn and main axons in the dorsal root. Thus, it is concluded that the following changes occur as the axon approaches the terminal:

1. Conduction velocity decreases.
2. Chronaxie is longer.
3. The relative refractory period is more sensitive to K-channel blocking agents.
4. Supernormal excitability and conduction velocity following a single impulse are greater.

Of these nerve terminal characteristics, three of them (1, 2, and 4) most closely resemble properties ascribed to central unmyelinated and thinly myelinated fibers (68, 134, 179, 180). These changes in properties should be considered in studies of transmission in the Ia-motoneuron pathway. Synaptic effectiveness of the second of two impulses in a single Ia fiber may be altered by that fiber's SNP interacting with synaptically mediated PAD. In addition, changes in membrane homogeneity should be considered in studies modeling conduction

through branching axons.

Prolongation of terminal refractory period was achieved at low doses of 4-AP and TEA that did not affect main axons. Terminal spike duration cannot be measured with intracellular recording, as indicated elsewhere in this dissertation. These relative refractory period measurements, therefore, are an indirect reflection of intracellular events. However, this is the first study based on measurements evoked directly from the terminals, which supports the hypothesis of presynaptic spike broadening by low concentrations of K-channel blocking drugs. This finding may indicate that action potential repolarization in terminal regions occurs by a different mechanism than action potential repolarization in main axons.

CHAPTER VIII

REFERENCES

1. Adams, P.R. and Galvan, M. Voltage-dependent currents of vertebrate neurons and their role in membrane excitability. In: Advances in Neurology 44:137-170. New York: Raven Press, 1986.

2. Adrian, E.D. The recovery process of excitable tissues. Part I. J. Physiol. Lond. 54:1-31, 1920.

3. Adrian, E.D. and Lucas, K. On the summation of propagated disturbances in nerve and muscle. J. Physiol. Lond. 44:68-124, 1912.

4. Alsen, C. Biological significance of peptides from Anemonia sulcata . Federation Proc. 42:101-108, 1983.

5. Armstrong, C.M. and Lopez-Barneo, J. External calcium ions are required for potassium channel gating in squid neurons. Science 236:712-714, 1987.

6. Bagust, J., Forsythe, I.D., and Kerkut, G.A. Demonstration of the synaptic origin of primary afferent depolarization (PAD) in the isolated spinal cord of the hamster. Brain Res. 341:385-389, 1985.

7. Bagust, J. and Kerkut, G.A. Some effects of magnesium ions upon conduction and synaptic activity in the isolated spinal cord of the mouse. Brain Res. 177:410-413, 1979.

8. Barker, J.L., Nicoll, R.A., and Padjen, A. Studies on convulsants in the isolated frog spinal cord. I. Antagonism of amino acid responses. J. Physiol. Lond. 245:521-536, 1975.

9. Barker, J.L., Nicoll, R.A., and Padjen, A. Studies on convulsants in the isolated frog spinal cord. II. Effects on root potentials. J. Physiol. Lond. 245:537-548, 1975.

10. Barrett, E.F. and Barrett, J.N. Separation of two voltage-sensitive potassium currents, and demonstration of a tetrodotoxin-resistant calcium current in frog motoneurones. J. Physiol. Lond. 255:737-774, 1976.

11. Barrett, E.F. and Barrett, J.N. Intracellular recording from vertebrate myelinated axons: Mechanism of the depolarizing afterpotential. J. Physiol. Lond. 323:117-144, 1982.

12. Barron, D.H. and Matthews, B.H.C. The interpretation of potential changes in the spinal cord. J. Physiol. Lond. 92:276-321, 1938.

13. Bartschat, D.K. and Blaustein, M.P. Calcium-activated potassium channels in isolated presynaptic nerve terminals from rat brain. J. Physiol. Lond. 361:441-457, 1985a.

14. Bartschat, D.K. and Blaustein, M.P. Potassium channels in isolated presynaptic nerve terminals from rat brain. J. Physiol. Lond. 361:419-440, 1985b.

15. Baylor, D.A. and Nicholls, J.G. After-effects of nerve impulses on signalling in the central nervous system of the leech. J. Physiol. Lond. 203:571-589, 1969.

16. BeMent, S.L. and Ranck, J.B., Jr. A quantitative study of electrical stimulation of central myelinated fibers. Exp. Neurol. 24:147-170, 1969.

17. Benoit, P.R. and Mambrini, J. Modification of transmitter release by ions which prolong the presynaptic action potential. J. Physiol. Lond. 210:681-695, 1970.

18. Black, A.R., Breeze, A.L., Othman, I.B., and Dolly, J.O. Involvement of neuronal acceptors for dendrotoxin in its convulsive action in rat brain. Biochem. J. 237:397-404, 1986.

19. Black, A.R. and Dolly, J.O. Two acceptor sub-types for dendrotoxin in chick synaptic membranes distinguishable by Beta-bungarotoxin. Eur. J. Biochem. 156:609-617, 1986.

20. Blatz, A.L. and Magleby, K.L. Calcium-activated potassium channels. Trends in Neurosci. 10:463-467, 1987.

21. Blaustein, M.P. and Goldring, J.M. Membrane potentials in pinched-off presynaptic nerve terminals monitored with a fluorescent probe: Evidence that synaptosomes have potassium diffusion potentials. J. Physiol. Lond. 247:589-615, 1975.

22. Blight, A.R. Computer simulation of action potentials and afterpotentials in mammalian myelinated axons: The case for a lower resistance myelin sheath. Neuroscience 15:13-31, 1985.

23. Blight, A.R. and Someya, S. Depolarizing afterpotentials in myelinated axons of mammalian spinal cord. Neuroscience 15:1-12, 1985.

24. Bostock, H. and Grafe, P. Activity-dependent excitability changes in normal and demyelinated rat spinal root axons. J. Physiol. Lond. 365:239-257, 1985.

25. Bostock, H., Sears, T.A., and Sherratt, R.M. The effects of 4-aminopyridine and tetraethylammonium ions on normal and demyelinated nerve fibres. J. Physiol. Lond. 313:301-315, 1981.

26. Bowe, C.M., Kocsis, J.D., Targ, E.F., and Waxman, S.G. Physiological effects of 4-aminopyridine on demyelinated mammalian motor and sensory fibers. Ann. Neurol. 22:264-268, 1987.

27. Bowe, C.M., Kocsis, J.D., and Waxman, S.G. The association of the supernormal period and the depolarizing afterpotential in myelinated frog and rat sciatic nerve. Neuroscience 21:585-593, 1987.

28. Braga, P.C., Dall'Oglio, G., and Fraschini, F. Microelectrode tip in five seconds. A new simple, rapid, inexpensive method. Electroencephalog. and Clin. Neurophysiol. 42:840-842, 1977.

29. Brodie, M.S., Shefner, S.A., and Levy, R.A. Elevated divalent cation concentration decreases potassium-induced depolarization of bullfrog primary afferent fibers. Brain Res. 240:181-185, 1982.

30. Brookhart, J.M., Machne, X., and Fadiga, E. Patterns of motor neuron discharge in the frog. Arch. ital. Biol. 97:53-67, 1959.

31. Brown, A.G. and Fyffe, R.E.W. The morphology of group Ia afferent fibre collaterals in the spinal cord of the cat. J. Physiol. Lond. 274:111-127, 1978.

32. Brown, D. M-currents: an update. Trends in Neurosci. 11:294-299, 1988.

33. Buckle, P.J. and Haas, H.L. Enhancement of synaptic transmission by 4-aminopyridine in hippocampal slices of the rat. J. Physiol. Lond. 326:109-122, 1982.

34. Bullock, T.H. Facilitation of conduction rate in nerve fibres. J. Physiol. Lond. 114:89-97, 1951.

35. Burke, R.E. and Rudomin, P. Chapter 24: Spinal neurons and synapses. In: Handbook of Physiology, Sect. 1: The Nervous System. Vol. 1 Part 2. Edited by J.M. Brookhart and V.M. Mountcastle, Bethesda: American Physiol. Soc., 1977.

36. Carpenter, D.O. and Rudomin, P. The organization of primary afferent depolarization in the isolated spinal cord of the frog. J. Physiol. Lond. 229:471-493, 1973.

37. Cerf, J.A. and Carels, G. Multiple sclerosis: Serum factor producing reversible alterations in bioelectric responses. Science 152:1066-1068, 1966.

38. Constanti, A. and Sim, J.A. Calcium-dependent potassium conductance in guinea-pig olfactory cortex neurones in vitro . J. Physiol. Lond. 387:173-194, 1987.

39. Conway, E.J. The nature and significance of concentration relations of potassium in skeletal muscle. Physiol. Rev. 37:84-132, 1957.

40. Cook, N.S. The pharmacology of potassium channels and their therapeutic potential. Trends in Pharmacol. Sci. 9:21-28, 1988.

41. Cooper, G.P. and Manalis, R.S. Cadmium: effects on transmitter release at the frog neuromuscular junction. Eur. J. Pharmacol. 99:251-256, 1984.

42. Cruce, W.L.R. A supraspinal monosynaptic input to hindlimb motoneurons in lumbar spinal cord of the frog, Rana catesbeiana . J. Neurophysiol. 37:691-704, 1974.

43. Curtis, D.R. and Eccles, J.C. Synaptic action during and after repetitive stimulation. J. Physiol. Lond. 150:374-398, 1960.

44. Czeh, G. The role of dendritic events in the initiation of monosynaptic spikes in frog motoneurons. Brain Res. 39:505-509, 1972.

45. Czeh, G., Kriz, N., and Sykova, E. Extracellular potassium accumulation in the frog spinal cord induced by stimulation of the skin and ventrolateral columns. J. Physiol. Lond. 320:57-72, 1981.

46. Davidoff, R.A. Gamma-aminobutyric acid antagonism and presynaptic inhibition in the frog spinal cord. Science 175:331-333, 1972.

47. Davidoff, R.A., Hackman, J.C., Holohean, A.M., Vega, J.L., and Zhang, D.X. Primary afferent activity, putative excitatory transmitters and extracellular potassium levels in frog spinal cord. J. Physiol. Lond. 397:291-306, 1988.

48. Davis, H. The relationship of the "chronaxie" of muscle to the size of the stimulating electrode. J. Physiol. Lond. 57:81-82P, 1923.

49. Del Castillo, J. and Engbaek, L. The nature of the neuromuscular block produced by magnesium. J. Physiol. Lond. 124:370-384, 1954.

50. Del Castillo, J. and Katz, B. The effect of magnesium on the activity of motor nerve endings. J. Physiol. Lond. 124:553-559, 1954.

51. Dolly, J.O. Potassium channels - what can the protein chemistry contribute? Trends in Neurosci. 11:186-188, 1988.

52. Dolly, J.O., Stansfeld, C.E., Breeze, A., Pelchen-Matthews, A., Marsh, S.J., and Brown, D.A. Neuronal acceptor sub-types for dendrotoxin and their relation to K^+ channels. In: Neurotoxins and their Pharmacological Implications . Edited by P. Jenner, New York: Raven Press, 1987.

53. Dubois, J.M. Evidence for the existence of three types of potassium channels in the frog Ranvier node membrane. J. Physiol. Lond. 318:297-316, 1981.

54. Dun, F.T. The delay and blockage of sensory impulses in the dorsal root ganglion. J. Physiol. Lond. 127:252-264, 1955.

55. Eccles, J.C. The Physiology of Synapses . Berlin, Springer-Verlag, 1964, pp. 122-137.

56. Eccles, J.C., Fatt, P., Landgren, S., and Winsbury, G.J. Spinal cord potentials generated by volleys in the large muscle afferents. J. Physiol. Lond. 125:590-606, 1954.

57. Eccles, J.C., Kostyuk, P.G., and Schmidt, R.F. The effect of electric polarization of the spinal cord on central afferent fibres and on their excitatory synaptic action. J. Physiol. Lond. 162:138-150, 1962.

58. Eccles, J.C. and Krnjevic, K. Potential changes recorded inside primary afferent fibres within the spinal cord. J. Physiol. Lond. 149:250-273, 1959a.

59. Eccles, J.C. and Krnjevic, K. Presynaptic changes associated with post-tetanic potentiation in the spinal cord. J. Physiol. Lond. 149:274-287, 1959b.

60. Eccles, J.C., Magni, F., and Willis, W.D. Depolarization of central terminals of group I afferents from muscle. J. Physiol. Lond. 160:62-93, 1962.

61. Eccles, J.C. and Malcolm, J.L. Dorsal root potentials of the spinal cord. J. Neurophysiol. 9:139-160, 1946.

62. Erlanger, J. and Gasser, H.S. Electrical Signs of Nervous Activity . Philadelphia, PA: Univ. of Pennsylvania Press, 1937.

63. Fadiga, E. and Brookhart, J.M. Monosynaptic activation of different portions of the motor neuron membrane. Am. J. Physiol. 198:693-703, 1960.

64. Frankenhaeuser, B. and Hodgkin, A.L. The after-effects of impulses in the giant nerve fibres of Loligo . J. Physiol. Lond. 131:341-376, 1956.

65. Frankenhaeuser, B. and Meves, H. The effect of magnesium and calcium on the frog myelinated nerve fibre. J. Physiol. Lond. 142:360-365, 1958.

66. Fu, T.C. and Schomburg, E.D. Electrophysiological investigation of the projection of secondary muscle spindle afferents in the cat spinal cord. Acta Physiol. Scand. 91:314-329, 1974.

67. Galindo, J. and Rudomin, P. Facilitation of synaptic activity in the frog spinal cord produced by 4-aminopyridine. Neurosci. Lett. 10:299-304, 1978.

68. Gardner-Medwin, A.R. An extreme supernormal period in cerebellar parallel fibers. J. Physiol. Lond. 222:357-371, 1972.

69. Gasser, H.S. and Grundfest, H. Action and excitability in mammalian A fibers. Am. J. Physiol. 117:113-133, 1936.

70. Gasser, H.S., Richards, C.H., and Grundfest, H. Properties of the nerve fibers of slowest conduction in the frog. Am. J. Physiol. 123:299-306, 1938.

71. Geddes, L.A. and Bourland, J.D. The strength-duration curve. IEEE Trans. Biomed. Eng. BME-32:458-459, 1985a.

72. Geddes, L.A. and Bourland, J.D. Tissue stimulation: theoretical considerations and practical applications. Med. & Biol. Eng. & Computing 23:131-137, 1985b.

73. Gilbert, D.L. and Ehrenstein, G. Effect of divalent cations on potassium conductance of squid axons: determination of surface charge. Biophysical J. 9:447-463, 1969.

74. Glavinovic, M.I. Differences in presynaptic action of 4-aminopyridine and tetraethylammonium at frog neuromuscular junction. Canad. J. Physiol. Pharmacol. 65:747-752, 1987.

75. Graham, H.T. Supernormality, a modification of the recovery process in nerve. Am. J. Physiol. 110:225-242, 1934.

76. Graham, H.T. and Lorente de No, R. Recovery of blood-perfused mammalian nerves. Am. J. Physiol. 123:326-340, 1938.

77. Greengard, P. and Straub, R.W. After-potentials in mammalian non-myelinated nerve fibres. J. Physiol. Lond. 144:442-462, 1958.

78. Grinnell, A.D. Electrical interaction between antidromically stimulated frog motoneurones and dorsal root afferents: Enhancement by gallamine and TEA. J. Physiol. Lond. 210:17-43, 1970.

79. Grossman, Y., Spira, M.E., and Parnas, I. Differential flow of information into branches of a single axon. Brain Res. 64:379-386, 1973.

80. Grundfest, H. Excitability of the single fibre nerve-muscle complex. J. Physiol. Lond. 76:95-115, 1932.

81. Grundfest, H. and Gasser, H.S. Properties of mammalian nerve fibers of slowest conduction. Am. J. Physiol. 123:307-318, 1938.

82. Hagiwara, S. and Tasaki, I. A study on the mechanism of impulse transmission across the giant synapse of the squid. J. Physiol. Lond. 143:114-137, 1958.

83. Halliwell, J.V., Othman, J.B., Pelchen-Matthews, A., and Dolly, J.O. Central action of dendrotoxin: Selective reduction of a transient K conductance in hippocampus and binding to localized acceptors. Proc. Natl. Acad. Sci. USA 83:493-497, 1986.

84. Hampson, D.R. and Poduslo, S.E. Comparisons of proteins and glycoproteins in neuronal plasma membranes, axolemma, synaptic membranes, and oligodendroglial plasma membranes. J. Neurosci. Res. 17:277-284, 1987.

85. Harvey, A.L. and Karlsson, E. Protease inhibitor homologues from mamba venoms: Facilitation of acetylcholine release and interactions with prejunctional blocking toxins. Br. J. Pharmacol. 77:153-161, 1982.

86. Henneman, E., Luscher, H.-R., and Mathis, J. Simultaneously active and inactive synapses of single Ia fibres on cat spinal motoneurones. J. Physiol. Lond. 352:147-161, 1984.

87. Hermann, A. and Gorman, A.L.F. Effects of 4-aminopyridine on potassium currents in a molluscan neuron. J. Gen. Physiol. 78:63-86, 1981a.

88. Hermann, A. and Gorman, A.L.F. Effects of tetraethylammonium on potassium currents in a molluscan neuron. J. Gen. Physiol. 78:87-110, 1981b.

89. Hille, B. The selective inhibition of delayed potassium currents in nerve by tetraethylammonium ion. J. Gen. Physiol. 50:1287-1302, 1967.

90. Hille, B. Chapter 4. Ionic basis of resting and action potentials. Handbook of Physiology. Section I: The Nervous System. Volume 1. Cellular biology of neurons, Part 1. Volume Editor: E.R. Kandel. Bethesda, MD: American Physiological Society, 1977.

91. Hille, B. Ionic Channels of Excitable Membranes . Sunderland, MA: Sinauer, 1984.

92. Hirst, G.D.S., Redman, S.J., and Wong, K. Post-tetanic potentiation and facilitation of synaptic potentials evoked in cat spinal motoneurones. J. Physiol. Lond. 321:97-109, 1981.

93. Holemans, K.C., Meij, H.S., and Meyer, B.J. The existence of a monosynaptic reflex arc in the spinal cord of the frog. Exp. Neurol. 14:175-186, 1966.

94. Howell, B.J., Baumgardner, F.W., Bondi, K., and Rahn, H. Acid-base balance in cold-blooded vertebrates as a function of body temperature. Am. J. Physiol. 218:600-606, 1970.

95. Hubbard, J.I. and Schmidt, R.F. Stimulation of motor nerve terminals. Nature 191:1103-1104, 1961.

96. Hubbard, J.I. and Schmidt, R.F. An electrophysiological investigation of mammalian motor nerve terminals. J. Physiol. Lond. 166:145-167, 1963.

97. Jack, J.J.B., Noble, D., and Tsien, R.W. Electric Current Flow in Excitable Cells . Oxford: Clarendon Press, 1975.

98. Jack, J.J.B., Redman, S.J., and Wong, K. Modifications to synaptic transmission at group Ia synapses on cat spinal motoneurones by 4-aminopyridine. J. Physiol. Lond. 321:111-126, 1981a.

99. Jack, J.J.B., Redman, S.J., and Wong, K. The components of synaptic potentials evoked in cat spinal motoneurones by impulses in single group Ia afferents. J. Physiol. Lond. 321:65-96, 1981b.

100. Jacobs, R.S. and Burley, E.S. Nerve terminal facilitatory action of 4-aminopyridine: an analysis of the rising phase of the endplate potential. Neuropharmacol. 17:439-444, 1978.

101. Jankowska, E., Lundberg, A., Rudomin, P., and Sykova, E. Effects of 4-aminopyridine on transmission in excitatory and inhibitory synapses in the spinal cord. Brain Res. 136:387-392, 1977.

102. Jankowska, E., and Roberts, W.J. An electrophysiological demonstration of the axonal projections of single spinal interneurons in the cat. J. Physiol. Lond. 222:597-622, 1972.

103. Jhaveri, S. and Frank, E. Central projections of the brachial nerve in bullfrogs: muscle and cutaneous afferents project to different regions of the spinal cord. J. Comp. Neurol. 221:304-312, 1983.

104. Jia, M. and Nelson, P.G. Calcium currents and transmitter output in cultured spinal cord and dorsal root ganglion neurons. J. Neurophysiol. 56:1257-1267, 1986.

105. Jinnaka, S. and Azuma, R. Electric current as a stimulus, with respect to its duration and strength. Proc. R. Soc. Lond. B 94:49-70, 1923.

106. Katz, B. and Miledi, R. A study of spontaneous miniature potentials in spinal motoneurones. J. Physiol. Lond. 168:389-422, 1963.

107. Katz, B. and Miledi, R. Propagation of electric activity in motor nerve terminals. Proc. R. Soc. Lond. B 161:453-482, 1965.

108. Katz, B. and Miledi, R. Tetrodotoxin-resistant electric activity in presynaptic terminals. J. Physiol. Lond. 203:459-487, 1969.

109. Katz, B. and Miledi, R. Estimates of quantal content during "chemical potentiation" of transmitter release. Proc. R. Soc. Lond. B 205:369-378, 1979.

110. Keynes, R.D. and Ritchie, J.M. The movements of labelled ions in mammalian non-myelinated nerve fibres. J. Physiol. Lond. 179:333-367, 1965.

111. Klüver, H. and Barrera, E. A method for the combined staining of cells and fibers in the nervous system. J. Neuropathol. Exp. Neurol. 12:400-403, 1953.

112. Kocsis, J.D., Malenka, R.C., and Waxman, S.G. Effects of extracellular potassium concentration on the excitability of the parallel fibres of the rat cerebellum. J. Physiol. Lond. 334:225-244, 1983.

113. Kocsis, J.D., Ruiz, J.A., and Waxman, S.G. Maturation of mammalian myelinated fibers: Changes in action-potential characteristics following 4-aminopyridine application. J. Neurophysiol. 50:449-463, 1983.

114. Kocsis, J.D. and VanderMaelen, C.P. A supernormal period in central axons following single cell stimulation. Exp. Brain Res. 36:381-386, 1979.

115. Koketsu, K. Intracellular potential changes of primary afferent nerve fibers in spinal cords of cats. J. Neurophysiol. 19:375-392, 1956a.

116. Koketsu, K. Intracellular slow potential of dorsal root fibers. Am. J. Physiol. 184:338-344, 1956b.

117. Koketsu, K. Action of tetraethylammonium chloride on neuromuscular transmission in frogs. Am. J. Physiol. 193:213-218, 1958.

118. Kudo, N. and Yamada, T. Morphological and physiological studies of development of the monosynaptic reflex pathway in the rat lumbar spinal cord. J. Physiol. Lond. 389:441-459, 1987.

119. Kumamoto, E. and Kuba, K. Effects of K^+-channel blockers on transmitter release in bullfrog sympathetic ganglia. J. Pharmacol. Exp. Ther. 235:241-247, 1985.

120. Kuno, M. Mechanism of facilitation and depression of the excitatory synaptic potential in spinal motoneurones. J. Physiol. Lond. 175:100-112, 1964.

121. Lancaster, B. and Adams, P.R. Calcium-dependent current generating the afterhyperpolarization of hippocampal neurons. J. Neurophysiol. 55:1268-1282, 1986.

122. Lancaster, B. and Nicoll, R.A. Properties of two calcium-activated hyperpolarizations in rat hippocampal neurones. J. Physiol. Lond. 389:187-203, 1987.

123. Lemeignan, M. Analysis of the action of 4-aminopyridine on the cat lumbar spinal cord. 1. Modification of the afferent volley, the monosynaptic discharge amplitude and the polysynaptic evoked responses. Neuropharmacol. 11:551-558, 1972.

124. Lipski, J. Antidromic activation of neurones as an analytical tool in the study of the central nervous system. J. Neurosci. Methods 4:1-32, 1981.

125. Llinas, R., Steinberg, I.Z., and Walton, K. Presynaptic calcium currents in squid giant synapse. Biophys. J. 33:289-322, 1981.

126. Llinas, R., Sugimori, M., and Simon, S.M. Transmission by presynaptic spike-like depolarization in the squid giant synapse. Proc. Natl. Acad. Sci. USA 79:2415-2419, 1982.

127. Llinas, R., Walton, K., and Bohr, V. Synaptic transmission in squid giant synapse after potassium conductance blockage with external 3- and 4-aminopyridine. Biophys. J. 16:83-86, 1976.

128. Lundberg, A. Differences in afterpotentials of frog motor and sensory A fibers. Acta. physiol. Scand. 23:279-282, 1951.

129. Lüscher, H.-R., Ruenzel, P.W. and Henneman, E. Composite EPSPs in motoneurons of different sizes before and during PTP: Implications for transmission failure and its relief in Ia projections. J. Neurophysiol. 49:269-289, 1983.

130. Macagno, E.R., Muller, K.J., and Pitman, R.M. Conduction block silences parts of a chemical synapse in the leech central nervous system. J. Physiol. Lond. 387:649-664, 1987.

131. MacDonald, J.F. and Schneiderman, J.H. Frequency-dependent decay of calcium spikes in cultured spinal cord neurons. Neurosci. 19:1335-1347, 1986.

132. Mallart, A. Presynaptic currents in frog motor endings. Pflügers Arch. 400:8-13, 1984.

133. Mallart, A. A calcium-activated potassium current in motor nerve terminals of the mouse. J. Physiol. Lond. 368:577-591, 1985.

134. Merrill, E.G., Wall, P.D., and Yaksh, T.L. Properties of two unmyelinated fibre tracts of the central nervous system: lateral Lissauer tract, and parallel fibres of the cerebellum. J. Physiol. Lond. 284:127-145, 1978.

135. Miller, R.J. Multiple calcium channels and neuronal function. Science 235:46-52, 1987.

136. Molgo, J., Lundh, H., and Thesleff, S. Potency of 3,4-diaminopyridine and 4-aminopyridine on mammalian neuromuscular transmission and the effect of pH changes. Eur. J. Pharmacol. 61:25-34, 1980.

137. Molgo,J. and Mallart, A. Effects of Anemonia sulcata toxin II on presynaptic currents and evoked transmitter release at neuromuscular junctions of the mouse. Pflügers Arch. 405:349-353, 1985.

138. Morita, K. and Barrett, E.F. Lizard motor nerve terminals have two calcium-dependent potassium conductances. Soc. Neurosci. Abstr. 14:70, 1988.

139. Mozhayeva, G.N. and Naumov, A.P. Effect of surface charge on the steady-state potassium conductance of the nodal membrane. Nature 228:164-165, 1970.

140. Munson, J.B. and Sypert, G.W. Properties of single central Ia afferent fibres projecting to motoneurones. J. Physiol. Lond. 296:315-327, 1979.

141. Nachshen, D.A. Regulation of cytosolic calcium concentration in presynaptic nerve endings isolated from rat brain. J. Physiol. Lond. 363:87-101, 1985.

142. Nachshen, D.A., Sanchez-Armass, S., and Weinstein, A.M. The regulation of cytosolic calcium in rat brain synaptosomes by sodium-dependent calcium efflux. J. Physiol. Lond. 381:17-28, 1986.

143. Neafsey, E.J. A simple method for glass insulating tungsten microelectrodes. Brain Res. Bull. 6:95-96, 1981.

144. Nelson, P.G., Jia, M., and Neale, E.A. Regulation of calcium currents and synaptic transmitter release. In: Calcium Electrogenesis and Neuronal Functioning Exp. Brain Res. Ser. 14. Edited by U. Heinemann, M. Klee, E. Neher and W. Singer. Berlin: Springer-Verlag, 1986, pp. 196-206.

145. Nicoll, R.A. Dorsal root potentials and changes in extracellular potassium in the spinal cord of the frog. J. Physiol. Lond. 290:113-127, 1979.

146. Offner, F., Weinberg, A., and Young, G. Nerve conduction theory: Some mathematical consequences of Bernstein's model. Bull. Math. Biophys. 2:89-103, 1940.

147. Orkand, R.K., Nicholls, J.G., and Kuffler, S.W. Effect of nerve impulses on the membrane potential of glial cells in the central nervous system of amphibia. J. Neurophysiol. 29:788-806, 1966.

148. Padjen, A. and Hashiguchi, T. Primary afferent depolarization in frog spinal cord is associated with an increase in membrane conductance. Can. J. Physiol. Pharmacol. 61:626-631, 1983.

149. Paintal, A.S. The influence of diameter of medullated nerve fibres of cats on the rising and falling phases of the spike and its recovery. J. Physiol. Lond. 184:791-811, 1966.

150. Paintal, A.S. A comparison of the nerve impulses of mammalian non-medullated nerve fibres with those of the smallest diameter medullated fibres. J. Physiol. Lond. 193:523-533, 1967.

151. Paintal, A.S. Conduction properties of normal peripheral myelinated axons. In: Physiology and Pathobiology of Axons . Edited by S.G. Waxman. New York: Raven, 1978.

152. Parnas, H. and Parnas, I. Influence of depolarizing pulse duration on the time course of transmitter release in lobster. J. Physiol. Lond. 388:487-494, 1987.

153. Penner, R., Petersen, M., Pierau, F.-K., and Dreyer, F. Dendrotoxin: A selective blocker of a non-inactivating potassium current in guinea-pig dorsal root ganglion neurones. Pflügers Arch. 407:365-369, 1986.

154. Perney, T.M., Hirning, L.D., Leeman, S.E., and Miller, R.J. Multiple calcium channels mediate neurotransmitter release from peripheral neurons. Proc. Natl. Acad. Sci. USA 83:6656-6659, 1986.

155. Ranck, J.B., Jr. Which elements are excited in electrical stimulation of mammalian central nervous system: A review. Brain Res. 98:417-440, 1975.

156. Raymond, S.A. Effects of nerve impulses on threshold of frog sciatic nerve fibres. J. Physiol. Lond. 290:273-303, 1979.

157. Redman, S. and Walmsley, B. Amplitude fluctuations in synaptic potentials evoked in cat spinal motoneurones at identified group Ia synapses. J. Physiol. Lond. 343:135-145, 1983a.

158. Redman, S. and Walmsley, B. The time course of synaptic potentials evoked in cat spinal motoneurones at identified group Ia synapses. J. Physiol. Lond. 343:117-133, 1983b.

159. Rogawski, M.A. The A-current: how ubiquitous a feature of excitable cells is it? Trends in Neurosci. 8:214-219,1985.

160. Rogawski, M.A. Single voltage-dependent potassium channels in cultured rat hippocampal neurones. J. Neurophysiol. 56:481-493, 1986.

161. Rogawski, M.A. and Barker, J.L. Effects of 4-aminopyridine on calcium action potentials and calcium current under voltage clamp in spinal neurons. Brain Res. 280:180-185, 1983.

162. Rudin, D.O. and Eisenman, G. The action potential of spinal axons in vitro. J. Gen. Physiol. 37:505-538, 1954.

163. Rushton, W.A.H. The effect upon the threshold for nervous excitation of the length of nerve exposed, and the angle between current and nerve. J. Physiol. Lond. 63:357-377, 1927.

164. Rutecki, P.A., Lebeda, F.J., and Johnston, D. 4-aminopyridine produces epileptiform activity in hippocampus and enhances synaptic excitation and inhibition. J. Neurophysiol. 57:1911-1924, 1987.

165. Ryan, G.P., Hackman, J.C., Wohlberg, C.J., and Davidoff, R.A. Spontaneous dorsal root potentials arise from interneuronal activity in the isolated frog spinal cord. Brain Res. 301:331-341, 1984.

166. Saint, D.A., Quastel, D.M.J., and Guan, Y.-Y. Multiple potassium conductances at the mammalian motor nerve terminal. Pflügers Arch. 410:408-412, 1987.

167. Sanchez-Armass, S. and Blaustein, M.P. Role of sodium-calcium exchange in regulation of intracellular calcium in nerve terminals. Am. J. Physiol. 252:C595-C603, 1987.

168. Schauf, C.L. Differential sensitivity of amphibian nodal and paranodal K + channels to 4-aminopyridine and TEA. Experientia 43:405-408, 1987.

169. Schauf, C.L., Davis, F.A., Sack, D.A., Reed, B.J., and Kesler, R.L. Neuroelectric blocking factors in human and animal sera evaluated using the isolated frog spinal cord. J. Neurol. Neurosurg. and Psychiat. 39:680-685, 1976.

170. Schmutz, M., von Hahn, H.P., and Honegger, C.G. Effect of multiple sclerosis serum on ventral root responses in isolated frog spinal cord. Eur. Neurol. 15:345-351, 1977.

171. Segal, M., Rogawski, M.A., and Barker, J.L. A transient potassium conductance regulates the excitability of cultured hippocampal and spinal neurons. J. Neurosci. 4:604-609, 1984.

172. Shefner, S.A. and Levy, R.A. The contribution of increases in extracellular potassium to primary afferent depolarization in the bullfrog spinal cord. Brain Res. 205:321-335, 1981.

173. Shimahara, T. Presynaptic modulation of transmitter release by the early outward potassium current in Aplysia . Brain Res. 263:51-56, 1983.

174. Snelling, R. and Nicholls, D. Calcium efflux and cycling across the synaptosomal plasma membrane. Biochem. J. 226:225-231, 1985.

175. Sokolove, P.G. and Cooke, I.M. Inhibition of impulse activity in a sensory neuron by an electrogenic pump. J. Gen. Physiol. 57:125-163, 1971.

176. Stansfeld, C.E., Marsh, S.J., Halliwell, J.V., and Brown, D.A. 4-aminopyridine and dendrotoxin induce repetitive firing in rat visceral sensory neurones by blocking a slowly inactivating outward current. Neurosci. Lett. 64:299-304, 1986.

177. Stockbridge, N. Differential conduction at axonal bifurcations. II. Theoretical basis. J. Neurophysiol. 59:1286-1295, 1988.

178. Stockbridge, N. and Stockbridge, L.L. Differential conduction at axonal bifurcations. I. Effect of electrotonic length. J. Neurophysiol. 59:1277-1285, 1988.

179. Swadlow, H.A. Systematic variations in the conduction velocity of slowly conducting axons in the rabbit corpus callosum. Exp. Neurol. 43:445-451, 1974.

180. Swadlow, H.A. and Waxman, S.G. Activity-dependent variations in the conduction properties of central axons. In: Physiology and Pathobiology of Axons Edited by S.G. Waxman, New York: Raven Press, 1978.

181. Sykova, E., Hajek, I., Chvatal, A., Kriz, N. and Diatchkova, G.I. Changes in extracellular potassium accumulation produced by opioids and naloxone in frog spinal cord: relation to changes of Na-K pump activity. Neurosci. Lett. 59:285-290, 1985.

182. Sykova, E., Kriz, N., and Preis, P. Elevated extracellular potassium concentration in unstimulated spinal dorsal horns of frogs. Neurosci. Lett. 43:293-298, 1983.

183. Sykova, E. and Orkand, R.K. Extracellular potassium accumulation and transmission in frog spinal cord. Neuroscience 5:1421-1428, 1980.

184. Szekely, G. The morphology of motoneurons and dorsal root fibers in the frog's spinal cord. Brain Res. 103:275-290, 1976.

185. Szekely, G. and Kosaras, B. Electron microscopic identification of postsynaptic dorsal root terminals: A possible substrate of dorsal root potentials in the frog spinal cord. Exp. Brain Res. 29:531-539, 1977.

186. Takeuchi, A. and Takeuchi, N. Electrical changes in pre- and postsynaptic axons of the giant synapse of Loligo . J. Gen. Physiol. 45:1181-1193, 1962.

187. Tasaki, I. and Fujita, M. Action currents of single nerve fibers as modified by temperature changes. J. Neurophysiol. 11:311-315, 1948.

188. Tebecis, A.K. and Phillis, J.W. The pharmacology of the isolated toad spinal cord. Exp. in Physiol. and Biochem. Edited by G.A. Kerkut. London: Academic Press, 1969, pp. 361-395.

189. Thompson, S.H. Three pharmacologically distinct potassium channels in molluscan neurones. J. Physiol. Lond. 265:465-488, 1977.

190. Thompson, S.M. and Prince, D.A. Activation of electrogenic sodium pump in hippocampal CA1 neurons following glutamate-induced depolarization. J. Neurophysiol. 56:507-522, 1986.

191. Vyklicky, L., Sykova, E., and Mellerova, B. Depolarization of primary afferents in the frog spinal cord under high Mg^{2+} concentrations. Brain Res. 117:153-156, 1976.

192. Wall, P.D. Excitability changes in afferent fiber terminations and their relation to slow potentials. J. Physiol. Lond. 142:1-21, 1958.

193. Wall, P.D. and Johnson, A. Changes associated with post-tetanic potentiation of a monosynaptic reflex. J. Neurophysiol. 21:148-158, 1958.

194. Wall, P.D. and Werman, R. The physiology and anatomy of long ranging afferent fibres within the spinal cord. J. Physiol. Lond. 255:321-334, 1976.

195. Wallenstein, S., Zucker, C.L., and Fleiss, J.L. Some statistical methods useful in circulation research. Circ. Res. 47:1-9, 1980.

196. Waxman, S.G. Regional differentiation of the axon: A review with special reference to the concept of the multiplex neuron. Brain Res. 47:269-288, 1972.

197. Waxman, S.G. and Swadlow, H.A. Morphology and physiology of visual callosal axons: evidence for a supernormal period in central myelinated axons. Brain Res. 113:179-187, 1976.

198. Woolsey, C.N. and Larrabee, M.G. Potential changes and prolonged reflex facilitation following stimulation of dorsal spinal roots. Am. J. Physiol. 129:501-502P, 1940.

199. Zbicz, K.L. and Weight, F.F. Transient voltage and calcium-dependent outward currents in hippocampal CA3 pyramidal neurons. J. Neurophysiol. 53:1038-1058, 1985.

200. Zucker, R.S. Excitability changes in crayfish motor neurone terminals. J. Physiol. Lond. 241:111-126, 1974.

APPROVAL SHEET

The dissertation submitted by Nancy C. Tkacs has been read and approved by the following committee:

Dr. Robert D. Wurster, Director
Professor, Physiology, Loyola

Dr. Charles L. Webber, Jr.
Associate Professor, Physiology, Loyola

Dr. David E. Euler
Associate Professor, Medicine (Physiology), Loyola

Dr. David O. Carpenter
Dean, School of Public Health Sciences
New York State Department of Health

Dr. Sarah A. Shefner
Assistant Professor, Physiology and Biophysics
University of Illinois College of Medicine at Chicago

The final copies have been examined by the director of the dissertation and the signature which appears below verifies the fact that any necessary changes have been incorporated and that the dissertation is now given final approval by the Committee with reference to content and form.

The dissertation is therefore accepted in partial fulfillment of the requirements for the degree of Doctor of Philosophy.

May 10, 1989
Date

Robert D Wurster
Director's Signature